A SIMPLIFIED LOW HEAD PROPELLER TURBINE FOR MICRO HYDROELECTRIC POWER

A thesis

submitted in fulfilment

of the requirements for the Degree

of

Master of Engineering

in the

University of Canterbury

by

Simon A. Faulkner

University of Canterbury

1991

CONTENTS

CHAPTER PAGE

continued...

CHAPTER PAGE

continued...

CHAPTER PAGE

LIST OF FIGURES

LIST OF TABLES

ABSTRACT

This thesis describes the development of a simplified propeller turbine unit to produce power in a low head micro hydroelectric power installation.

To be appropriate for remote areas and developing countries, a micro hydro system needs to be simple in design. There are good turbine designs for medium to high heads but traditional designs for heads under about 10m, ie, the crossflow turbine and waterwheel, are slow running, requiring substantial speed increase to drive an AC generator. Propeller turbines have a higher running speed but are normally too complicated for micro hydro installations.

In this thesis a suitable propeller turbine was developed. The effect of flat blades and optimum turbine blade and guide vane angles has been determined, as has the effect of various cones attached to the downstream end of the hub. The large hub diameter is an important compromise.

A prototype turbine for installation on a New Zealand farm was developed from model tests. The turbine has a hub diameter to blade tip diameter ratio of 0.66 and 8 flat blades set at 30° to tangential (60° from axial). The best efficiency of the model turbine was 62%, with an efficiency of 57% at the best power point. Using scaling laws it is predicted that the prototype, with a blade tip diameter of 0.410m, will produce 6.0kW at 612 RPM from a head of 2.7m and a flow rate of 0.41m^3/s. This gives 4.3kW output from the 50Hz 2-pole generator. This prediction is for no cone fitted on the downstream end of the hub, but model tests indicate that the power could be improved by about 5% with the addition of a straight sided cone on the hub.

SYMBOLS

SYMBOL	MEANING	UNITS
D	turbine blade tip diameter (characteristic turbine dimension)	m
H	total head acting on turbine	m
N	rotational speed	RPM
Q	flow rate	m^3/s
P	power	kW
F	ratio of hub diameter to D	1
A	cross-sectional area	m^2
V	fluid flow velocity	m/s
r	radius	m
ω	rotational speed	rad/s
η	efficiency	%
p	pressure	Pa
ρ	density	kg/m^3
μ	viscosity	kg/ms
g	acceleration of gravity	m/s^2
Re	Reynold's number	1
S	dynamometer scale reading	-
σ	Thoma's cavitation coefficient	1
N_S	specific speed[1]	"RPM"
k_S	characteristic number	1
n_S	"specific speed" (fully non-dimensional)	1

Note 1 : The value of N_S depends on the units used for power and head (see Appendix I.2).

ACKNOWLEDGEMENTS

I wish to thank the following people, without whose willing help this project would not have been possible:

Supervisor G.J. Parker,
Advisor E.P. Giddens,
Technicians I. Sheppard,
A. Poynter,
K. Brown,
C.S. Amies,
O. Bolt,
P. Smith,
B. Sparks,
the owners of the farm, I. and A. Price,
and my friends and family.

The use of the Civil Engineering Fluid Mechanics Laboratory is gratefully acknowledged.

CHAPTER 1

INTRODUCTION

1.1 MICRO HYDROELECTRIC POWER

Electricity generation from water in a stream or river is virtually pollution free and fully renewable.

The energy in falling water is normally lost through turbulence as heat, equivalent to raising the temperature of the water by a quarter of a degree per 100m dropped. A water turbine and generator transforms part of this energy to electricity, which eventually ends up as heat elsewhere in the environment.

The term "micro" indicates the size of the generating system, ie that the power produced is a few kilowatts, usually under 10kW. But more importantly the term also refers to concepts in the design, which are different from those of larger systems.

Micro hydro systems are simple, cheap, and robust. They must be "appropriate" to the society in which they are to be used. They can be found supplying a house, farm, small village, or small factory with power in areas too remote to have power from a national grid, in developing countries and in some areas of countries such as New Zealand.

The important requirements are safety, reliability, and low cost. The micro hydro system should be as safe and reliable as a large system, and it must be easy to maintain and repair. The design must be appropriate for manufacture in a small workshop, on a one-off basis. The cost, which is almost entirely initial capital, needs to be minimised, because the ownership is usually private. If a suitable water resource is available then a well designed micro hydro system will be cheaper and more convenient than other renewable energy sources, a diesel powered generator, or the national grid, even if the distance is only a few kilometres from the nearest power lines.

To satisfy these requirements the system must be simple. This means there is less to go wrong, less to maintain, and the equipment and structures can be

designed, manufactured and maintained by non-specialists. This should ensure that the cost is minimised. Costs can be reduced by using readily available equipment, for instance, centrifugal pumps can be used in reverse as turbines. The simplicity of the system may be at the expense of efficiency, but while efficiency is important it is usually of secondary importance to the overall requirement of low cost.

An important advance in micro hydro power is the development of the electronic controller. Conventionally turbines are controlled mechanically with guide vanes or valves to adjust the power produced by the turbine to match the changing load, and so keep the speed constant. With an electronic controller the turbine runs continuously at full power. The electronic controller varies the additional "dump" load to match the total load to the power being produced by the turbine, and hence keep the speed constant. Although an electronic controller is in itself complicated it is not expensive and it makes the turbine far simpler, as the complicated adjustable guide vanes or valves are not needed.

The major environmental impacts caused by a micro hydro installation are the site works and disruption to the river or stream. When the system is small these effects should not be significant. With a large river only a small part of the flow is diverted, though a small stream may have its entire flow diverted through the turbine. The environmental effects of the site works (channels, weir, concrete structures) should be less significant than other construction found on a farm, eg, roads, fords, ditches, and buildings.

1.2 OBJECTIVES

There is a large potential for micro hydro power in New Zealand, since many areas do not have sufficient population density to support reticulation of the national grid (Blakely, 1981). There is also a large potential for micro hydro power in developing countries, and many systems have already been installed (Inversin, 1986).

There are a number of suitable turbine designs for medium to high heads. For example pelton wheels can be used for high heads, centrifugal pumps running backwards as turbines are suitable for heads of about 200m down to 30m, and crossflow turbines are suitable for heads down to about 10m with some speed increase (Section 1.3). With substantial speed increasing transmission waterwheels or crossflow turbines can be used with heads lower than 10m but there is a need for an appropriate higher speed turbine design for these low heads.

The objective of this study is to address the problem of low head power generation by:

i. testing various model turbines to find a simple design with reasonable performance

ii. building a full size prototype turbine and testing it in a typical installation.

The simple construction of the turbine makes the flow more complicated, since the simple geometry does not match the flow geometry correctly. Hence the flow can not be predicted accurately with theoretical calculations and an understanding of the flow and the way it is affected by the turbine geometry must be obtained from observation, so that better configurations can be designed.

Testing of a scaled down model was necessary because the smaller size reduces the cost of building different designs for testing and because there was a limit to the flow rate available in the laboratory where the testing was to be done.

A real life application existed where the prototype could be installed and tested. This was on a farm near Springs Junction, South Island, New Zealand. The farm is about 10km from the national grid so reticulation is not viable. A diesel driven AC generator was previously used, with high fuel costs, some noise and pollution, and the inconvenience of not having continuously available power (the diesel generator was only turned on for short periods due to the high fuel cost). There is a large river running through the property which can be utilised. The head, made available by

dropping diverted flow from one terrace level to another, was estimated by surveying to be 2.7m.

A high head can only be obtained from a river that falls rapidly in height. There are many areas where the land is too flat and so only a low head can be obtained. Hence a successful low head turbine design would increase the range of viable sites for micro hydro power.

1.3 LOW HEAD TURBINES

At low heads the main problem is the low speed of the turbine. Although mechanical power can sometimes be utilised directly, usually AC electricity is required and the generator must be driven fast enough to produce a standard frequency, so that readily available appliances can be used. As the head reduces the fluid velocity decreases and so the speed of the moving parts decrease. Also as the head reduces, the flow rate must increase to get the same power, and so the diameter of the turbine must increase, which further reduces its rotational speed. A waterwheel is a suitably simple solution for heads of around 1m to 4m. It is simple and easy to build, but it runs very slowly. The torque is therefore large requiring strong transmission components. The theoretical maximum speed is given by $\mathbf{D^{-½}\ 42.2\ RPM}$ where D is the wheel outside diameter. The operating point for best power is at slightly under half this speed, so,

$$\mathbf{N \approx D^{-½}\ 19\ RPM} \qquad \text{(D in metres)}$$

(Chapman, 1986). For an available head of 2.7m the wheel diameter would be about 2.5m, giving a speed of 12 RPM. Hence a two stage speed increase is required, which can make the overall system expensive. To produce 4.0kW of electricity the wheel width would be 0.90m.

Crossflow turbines are also suitable in terms of simplicity of construction, but their speed is also low at low heads. The running speed of a typical design is given by

$$\mathbf{N = H^{½}D^{-1}\ 40.4\ RPM}$$
(H, D in metres)

(VITA, 1980). For a head of say H = 10m and a typical turbine diameter of D = 0.30m, the speed would be N = 430 RPM. An available head of H = 2.7m, and a likely

diameter of 0.50m would give N=130 RPM, and to give 4kW of electricity the turbine width would be at least 1.0m.

A turbine with a large specific speed is required, and the type of turbine with the highest specific speed is the propeller turbine. This is because the blades move across the flow, at a speed greater than the flow velocity (Figure 1.1). Propeller turbines are usually only used for larger systems since their complex curved blades and guide vanes make them expensive to design and manufacture. There is therefore a need for a simple propeller turbine design, to enable economic utilisation of micro hydro power at sites that only have a low head available.

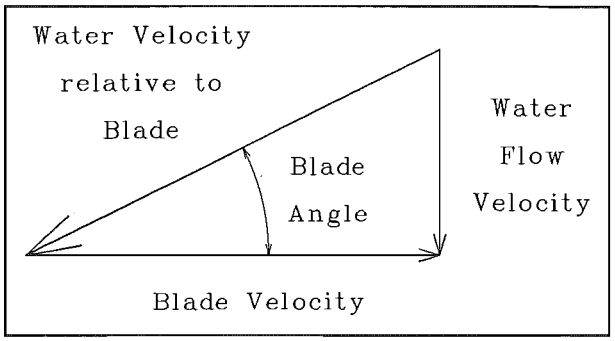

Figure 1.1 Velocity Diagram for Propeller Turbine.

1.4 PREVIOUS WORK ON SIMPLIFIED PROPELLER TURBINES

There has been a small amount of research done on simplified designs, suitable for micro hydro applications. There is very little information on how aspects of the design such as blade angle, shape, hub size, etc, affect the performance.

Rao (1988) has tested a turbine with eight helical blades which produces 5kW from a head of 5m. It would be a suitable design for lower heads but it was thought that further simplifications to the design would be worth testing, particularly using flat rather than helical blades. A comparison of performance is made in Section 6.4).

A turbine with moulded fibreglass blades, hub, and housing designed to produce 5kW from a head of 10m was tested at M.I.T. This is described by Ho, L.W in *Manufacture and Evaluation of a Five-Kilowatt Axial-Flow Water Turbine*, Master of Science Thesis, (Massachusetts Institute of Technology, Cambridge, MA02139, USA), 1976 (not sighted by this author).

Susanto (1983) describes a 200mm diameter turbine with four cast iron blades, designed to produce 2.5kW from a head of 2m. Its design speed was 1000 RPM, giving a specific speed of N_S=665 RPM (kW,m) or 174 RPM (hp,ft) (Susanto

gives N_S=236, with no units). However the turbine had not been tested so the actual performance was not known.

The "Metaz" turbine manufactured in various sizes in Czeckoslovakia, is briefly described by Nechleba and Kopecky (1986). This turbine is built in a syphon configuration (Figure 2.1 E), which enables it to be installed on existing weirs and dams. It was designed with an emphasis on economical mass production and simple operation, with few parts. Most of the parts, including the blades, are iron castings and only a few parts require machining. A graph indicates a head range from 1m to 6m, and a flow rate of up to 0.5m^3/s at 1m head and up to 1.1m^3/s at 6m head. The efficiency indicated is approximately 70%-80%, with the higher efficiencies occurring as the power (ie, size and head) increases. A turbine with a diameter D=300mm and head H=2.6m was tested and the efficiency found to be 76% (including mechanical losses from seals, etc.).

There are a few other simplified propeller turbines that have been manufactured, for example the French "Hydrolec" described briefly by Monition (1984), and an "8-inch, fixed-blade propeller turbine, which generates 1-10kW under a head of 2-8m", described briefly by Inversin (1986). This turbine, and the one described by Susanto (1983), have the shaft mounted in a right angle pipe bend (Figure 2.1 D), so that the shaft can be positioned horizontally, and the hub can be positioned low down near the outlet water level, which allows a higher head before cavitation occurs. Some authors mention that boat propellers etc. can be used in turbines, but no record of their actual use was found.

CHAPTER 2

DESIGN

2.1 MAIN PARAMETERS (PROTOTYPE)

After developing a suitable design by model testing, a prototype turbine is to be built and installed on a farm. The main parameters required for the prototype give an idea of the scaling between the model and the prototype, and the general performance that is required.

The comments on power and speed apply to most micro hydro installations, and only those on head and flow rate are specific to the prototype designed for this thesis. A good design would be useful for a wide range of low head applications.

2.1.1 Power

The instantaneous demand in a typical New Zealand residence supplied by the national grid may reach 15kW but the average use is only about 1kW to 2kW. It is not viable to try to provide for the maximum demand so the users must organise their activities so that the load is spread out. High demand appliances such as washing machines and workshop tools must be used when there is little other demand. There will be many times when very little power is being used, and the spare power can be automatically fed to lower priority uses such as water heating, drying clothes, and heating of a swimming pool or greenhouse.

A power supply of 1kW to 2kW would be useful for lighting and some low power appliances (radio, TV etc), 3kW to 4kW would supply medium power appliances (fridge, freezer etc) and over 4kW would supply all the electrical requirements of a house including some water and room heating. Also a shearing shed could be run with about 4kW. Even a small amount of power (1kW to 2kW) would reduce diesel usage and increase convenience, but may not reduce overall costs.

There is therefore a range of powers that would be useful. The aim is to produce as much as possible, up to about 5kW, or, allowing for the inefficiencies of the generator and transmission, 7kW from the turbine.

2.1.2 Speed

The turbine is to drive the generator at 3000 RPM, to produce 50Hz AC power. There are 4 pole generators available to run at 1500 RPM, but they are more expensive and the system would require 4 times the flywheel inertia to give the same stability. It is preferable then to aim for a generator speed of 3000 RPM.

A speed increase through a single stage gearbox or belt drive of 4:1 is straight forward, and up to 6:1 may be possible. In general the turbine speed must be as high as possible.

2.1.3 Flow Rate

A water right was obtained to divert up to $1m^3/s$ of water from the river, this being a quarter of the estimated minimum flow. It is hoped to use an existing culvert which would restrict the flow to about $0.5m^3/s$.

2.1.4 Head

By diverting the river flow where it enters the farmer's property onto a river terrace and dropping it to a lower terrace level near the house, a drop of 2.7m can be obtained (see map, Figure 5.4). To increase this head would mean a large increase in the costs of channels etc, and so would not be viable.

2.1.5 Efficiency

The gross power available with a head of 2.7m and flow rate of $0.5m^3/s$ is 13.5kW. Therefore an overall efficiency of about 40% or turbine efficiency of about 50% would be adequate. It is likely that the speed will be a more important factor than efficiency.

2.2 GENERAL CONFIGURATIONS

2.2.1 **Turbine Axis and Bends**

There are several possible configurations for a propeller turbine, as shown in Figure 2.1. The propeller is shrouded by a straight tube for ease of construction. After the propeller an expanding section (draft tube) is needed to gradually slow the water and recover some of the velocity head (Section 4.2.3).
A,C,D and E could be made free-standing, B and F would suit being buried or formed from concrete.

Configuration F was studied with particular interest in improving the flow around the bend by introducing swirl into the flow. Some tests were done, but the results were not conclusive. One major advantage of configuration F is that the turbine is operating in a high pressure region, which reduces the chance of cavitation problems. However cavitation was not expected to be a problem for a head of 2.7m (see Appendix I.1). As there was sufficient height available the simplest configuration, A, was chosen. For heads above about 5m cavitation would be a problem, and another configuration may be necessary. For a lower head in relation to the turbine diameter, there would be less room for the draft tube, and again another configuration would become necessary.

Bends can be expensive to manufacture. A small diameter turbine may be able to utilise readily available pipe fittings.

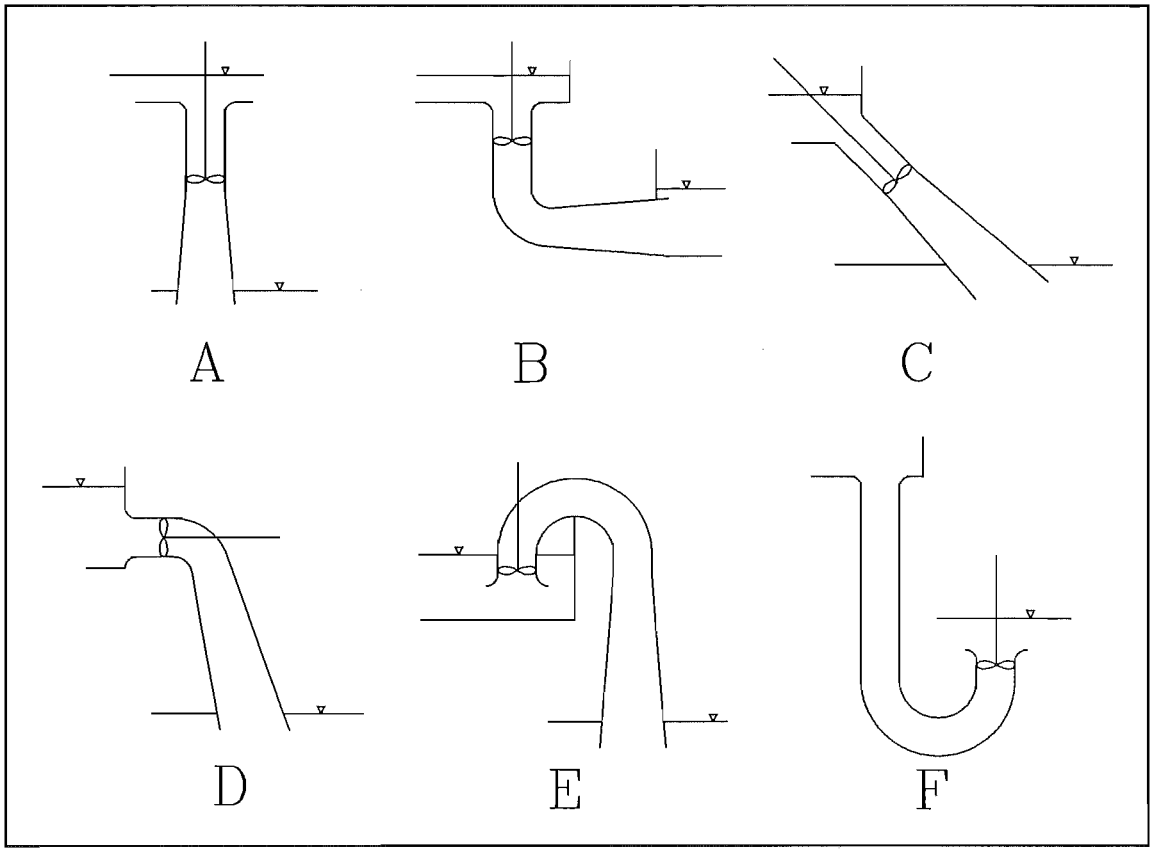

Figure 2.1 Turbine Configurations

A Vertical Axis: simple, compact, a limit to the room for a draft tube, cavitation possible.

B Vertical Axis with Bend: more room for draft tube, careful design required to avoid separation in bend/draft tube.

C Inclined Axis: more room for draft tube.

D Horizontal Axis: easier connection to generator, shaft seal required.

E Syphon: more room for draft tube, installation may be easier, requires priming, shaft seal.

F Inverted syphon: convenient shaft location, very little room for draft tube, bend may disturb flow through propeller.

2.2.2 Guide Vanes

Guide vanes are used to give the flow approaching the turbine blades an initial swirl or tangential velocity component. The turbine blades change the tangential velocity component of the flow, and it is this change in tangential momentum that produces the torque that drives the generator. There is also an axial component of force on the blades, produced by the pressure differential across the blades.

If the swirl or tangential velocity component given to the flow by the guide vanes balances the change in tangential velocity through the blades, the flow will leave the blades with zero tangential velocity, ie, the flow will be purely axial. This is theoretically the most efficient operating point since the tangential velocity can not be recovered as pressure in the draft tube. However some exit swirl may cause improved performance, for example the flow may follow the diverging draft tube walls better.

If the change in tangential velocity through the blades is not large the increase in efficiency with guide vanes fitted may not justify the extra complications in manufacture, ie the turbine could be made with a simpler inlet structure.

There are two basic configurations for the guide vanes, radial and axial, as shown in Figure 2.2. The radial configuration is slightly more compact in the axial direction, making the shaft shorter. Some form of curved surface is required to turn the flow without causing separation, particularly on the "inside" of the bend. The top plate would reduce the tendency for air entrainment and uncontrolled swirl associated with vortices, and so may be necessary for the axial configuration as well. It also provides a mount for a water lubricated bearing to steady the runner. The radial configuration makes the guide vanes easy to adjust.

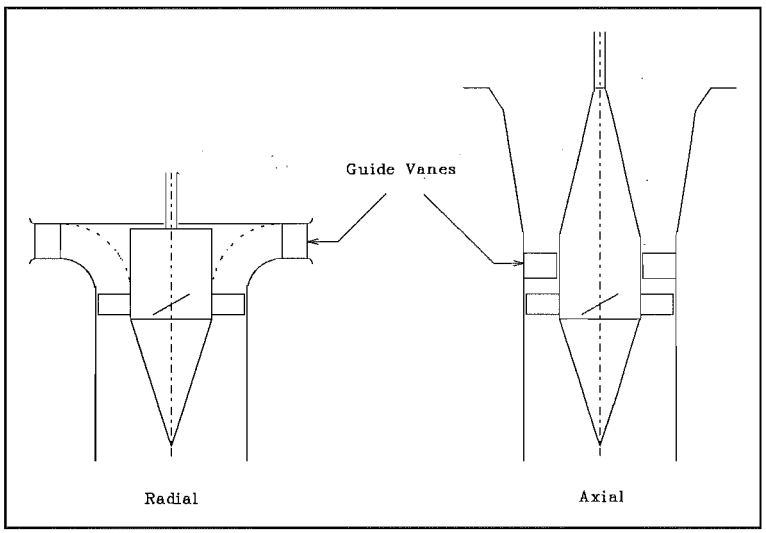

Figure 2.2 Guide Vane Configurations

2.2.3 Turbine Runner

The runner is the rotating part of the turbine, ie, the hub, blades and shaft. It could be fabricated or made from a modified boat propeller. Casting from metal is probably too expensive except for mass production. Fibreglass moulding has been experimented with (Section 1.4) and may be suitable, especially for higher head turbines. A propeller turbine with uniform thickness helical metal blades was tested by Rao (1988).

The purpose of this thesis was to try further simplifications, particularly the use of flat blades. This would give the turbine a greater range of applications, since the manufacture would be less complicated. The runner could then be made with hand tools, a lathe, and welding. Also there would not be any complexly shaped surfaces (possibly critical to the turbine performance) to reproduce from drawings, reducing the amount of skill required to build the turbine and so making it easier for manufacture in developing countries or for users to build themselves.

Blade Angles Ideally the blade angles at their leading and trailing edges should match the relative flow direction at all radii. This would require complicated curvature of the blades or a non-free vortex approach flow. The blade angle should change from leading to trailing edge and with varying radius.

The ideal change in angle from leading edge to trailing edge is determined by the change in tangential velocity component that is required. For a flow having axial and tangential velocity components V_{axial} and V_{tan}, the angle of the flow (β) observed relative to a blade moving with tangential velocity $r\omega$, is given by

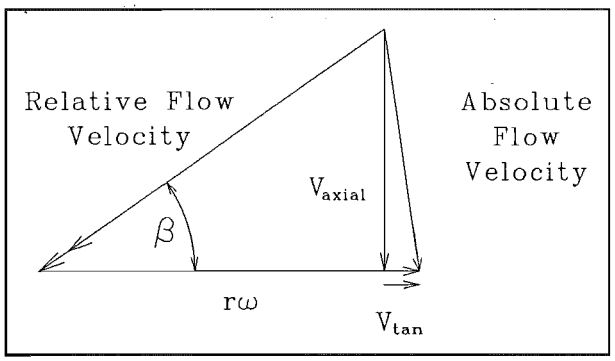

Figure 2.3 Flow Direction Relative to Blade

$$\tan(\beta) = \frac{V_{axial}}{r\omega - V_{tan}} \qquad (2.1)$$

where $V_{axial} \approx Q/A$ (Figure 2.3).

V_{tan} is calculated from the change in tangential momentum that gives the required power. Equating the power produced by the turbine (in terms of head and flow rate) to the rate of change of momentum gives:

$$\eta \rho g H Q = \rho Q \Delta V_{tan} \quad (2.2)$$

Assuming that $\mathbf{V_{tan}=0}$ at the trailing edge, ie, zero outlet swirl, then at the leading edge $\mathbf{V_{tan}=\Delta V_{tan}}$, so from Equation 2.2

$$V_{tan} = \frac{g\eta H}{r\omega} \quad (2.3)$$

(this swirl is provided by the guide vanes)

Taking typical values, for the blade tip: $\eta H = 1.5m$, $Q = 0.5m^3/s$, $A = \frac{1}{4}\pi(0.4m)^2(1-0.66^2)$, $r = 0.15m$, $\omega = 700$ RPM $= 73rad/s$; then Equation 2.1 gives:

β = **36.4°** at leading edge

β = **32.8°** at trailing edge

The change in flow angle from the leading edge to the trailing edge is small (≈3.6°), and so a flat blade could be used with a small angle of attack ($\alpha \approx 3.6°$) at the leading edge. The difference in the angles is small because $\mathbf{r\omega \gg \Delta V_{tan}}$.

Flat blades do not give a match with the flow angle for all radii. The flow direction relative to the blades (β) is a function of the tangential velocity of the blade, which is proportional to radius. Ignoring any swirl in the water flow and any angle of attack, then helical blades will give a match between the flow angle and the blade angle for all radii. If flat blades are used then the hub must be large to limit the variation in tangential velocity. A hub diameter to blade tip diameter ratio of $F = 0.66$ was used. This gave a predicted variation in the angle of attack (α) at the leading edge from 0° at the tip to about 10° at the hub, which is the angle at which stall could be expected to start occurring. (It also corresponded to an available size of material). The model hub was made from PVC water pipe, for ease of manufacture and alterations.

The large hub reduces the flow area so a greater turbine diameter is required to give the same flow, and this reduces the rotational speed. Although this goes against the requirement of high specific speed, it was considered likely to be a

worthwhile trade-off. A modified boat propeller may have been a better solution but it would not have the same universal application, since it may not be available in developing countries.

The initial blade configuration (4 blades, blade angle 22.5°) was designed using recommendations from Stepanoff (1957). These recommendations are for axial flow pumps, but it was thought that since an axial pump can be run in reverse as a turbine the design would provide a useful starting point.

The process of testing and designing better blade configurations is described in Section 3.4.

2.3 MODEL DESIGN

2.3.1 **Model Dimensions**

The model was designed with a blade tip diameter of 172mm and a head of about 1.8m. These dimensions were not critical and so were mainly determined by availability of materials and equipment. The model and prototype can not conveniently operate with the same Reynolds number (Re) but when the flow is well into the turbulent range this does not usually affect the modelling. Re_{model} for flow rates from 30 l/s to 60 l/s is about $0.3x10^6$ to $0.6x10^6$.

The main limitations on the model were a maximum available flow rate of 100 l/s and a maximum dynamometer speed of 2500 RPM.

2.3.2 **Draft Tube**

A draft tube is required to increase the suction on the downstream side of the turbine, ie, to make use of the part of the head after the turbine blades. It is designed to slow the flow down gradually to recover the kinetic energy of the high velocity flow. This energy is recovered in the form of pressure if the flow slows without turbulence being created, ie, if the flow follows the passages without separation. Because a high specific speed is required, the fluid velocity is high, and so recovery of the velocity head is important.

The required length was 0.9m. Doubling of the diameter from the inlet to the outlet of the draft tube gives four times the flow area and a sixteenth of the

velocity head ($V^2/2g$), assuming that the flow is axial and uniform. For an inlet diameter of 172mm and a length of 0.9m, the draft tube cone angle is $2\theta = 10.9°$ (Figure 2.5). Gubin (1973) suggests that angles from 8° to 18° are typically used, so this is a relatively gradual enlargement.

2.3.3 Cone

If the hub is large there is a significant decrease in the flow area at the blades compared to the full turbine tube area. For a hub diameter to blade tip ratio $F = 0.66$ the annulus area is $1-F^2 = 0.56$ of the full area and so the velocity head is 0.56^2 or 3.2 times that in the full area (again assuming uniform axial flow). The velocity head after the hub is 0.56^2, or 31%, of the annulus area velocity head, ie, there is a potential for ⅔ of the velocity head recovery to occur in the straight section of turbine tube, ie, before the draft tube. A cone giving a gradual increase in the flow area, ie, gradual decrease in the hub area, is required to recover this energy.

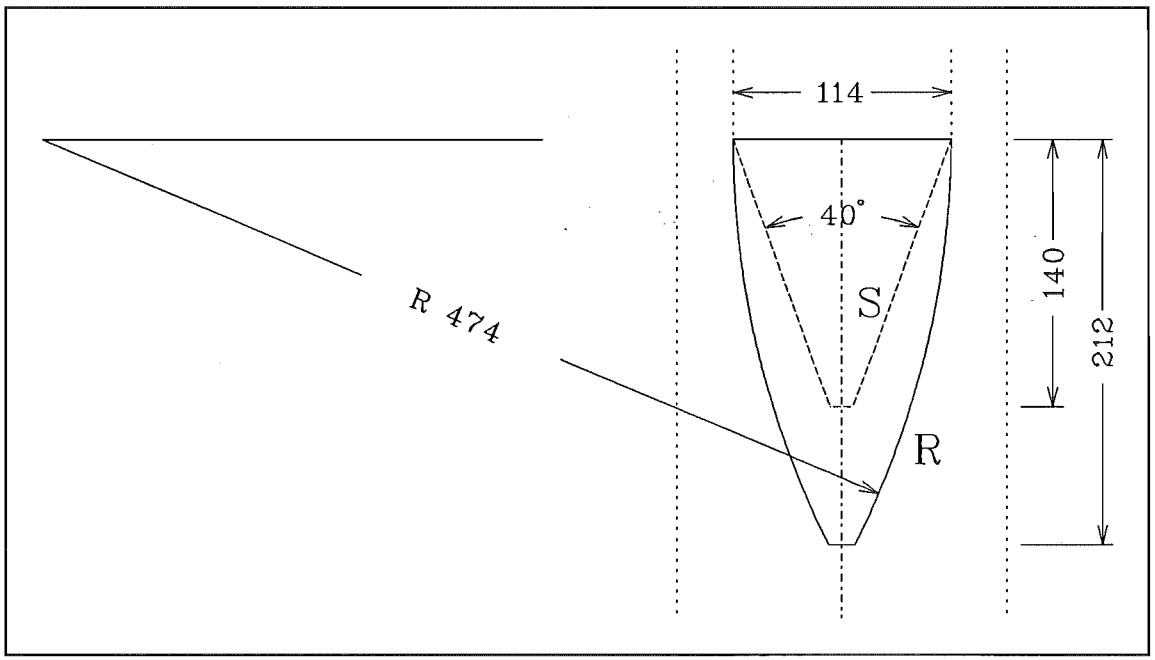

Figure 2.4 Straight and Radius Cones

Firstly a conical or "straight" cone was made with an apex angle of 40°. This was a simple shape to manufacture. Later a "radius" cone was made with a more gradual decrease in area (Figure 2.4).

Gubin (1973) uses an "effective cone angle", which is the "cone angle" (2θ) of a draft tube that would give the same increase in area in the same axial distance,

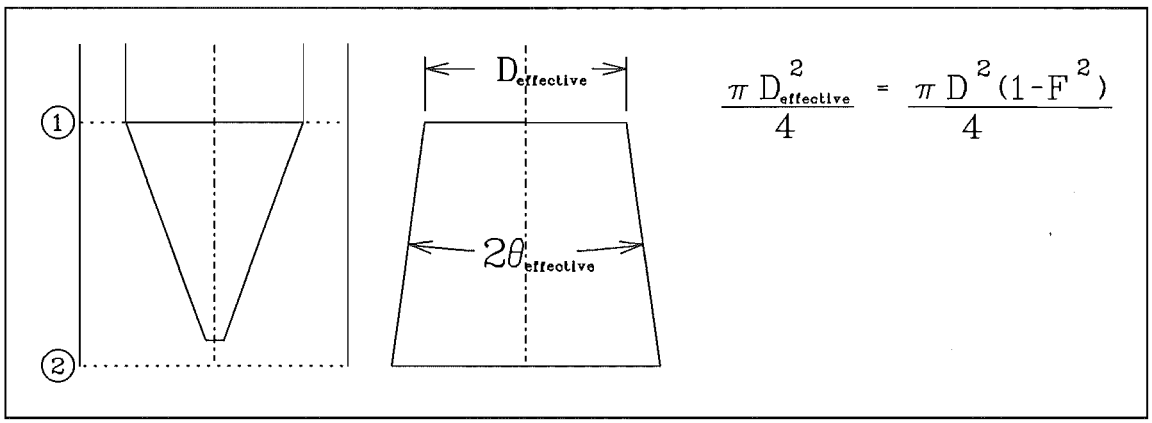

Figure 2.5 Effective Angle of a Cone

for any two cross-sections (Figure 2.5). For the straight cone the effective cone angle ($2\theta_{effective}$) is large at the beginning of the cone. Over the whole cone $2\theta_{effective} = 16°$ but for close sections at the beginning and end of the cone $2\theta_{effective}$ ranges from about 35° to 6° respectively. (The values depend on the distance between the sections.) Since the surface of the radius cone is initially tangential, $2\theta_{effective}$ increases from an initial value of zero. It becomes large near the tip. It was thought that the initially small $2\theta_{effective}$ would reduce flow separation and give better recovery of the velocity head.

2.3.4 Other Design Requirements

Inlet The turbine inlet must be submerged with sufficient space around it to allow the flow to enter uniformly after coming from the approach channel, where it may have a significant velocity. The turbine was mounted in the bottom of an open steel tank (see Figure 3.1). This tank was connected to another similar one containing the supply pipeline.

Turbine Construction To enable observation of the flow through the runner and guide vanes and past the cone, the main turbine tube and top plate were made from clear acrylic. A flat window was provided to observe the blade area without distortion. Flow visualisation was done using cotton tell-tales and streams of air bubbles. Pressure tapping points were provided in the turbine tube, just above the blades and at the bottom of the straight turbine tube. The pressures were measured relative to the outlet water level (Figure 2.6).

The turbine tube was extended beyond the end of the cone so that longer cones could be put in and so that the flow beyond the cone could be observed.

An acetal water lubricated rubbing bearing was used to steady the shaft.

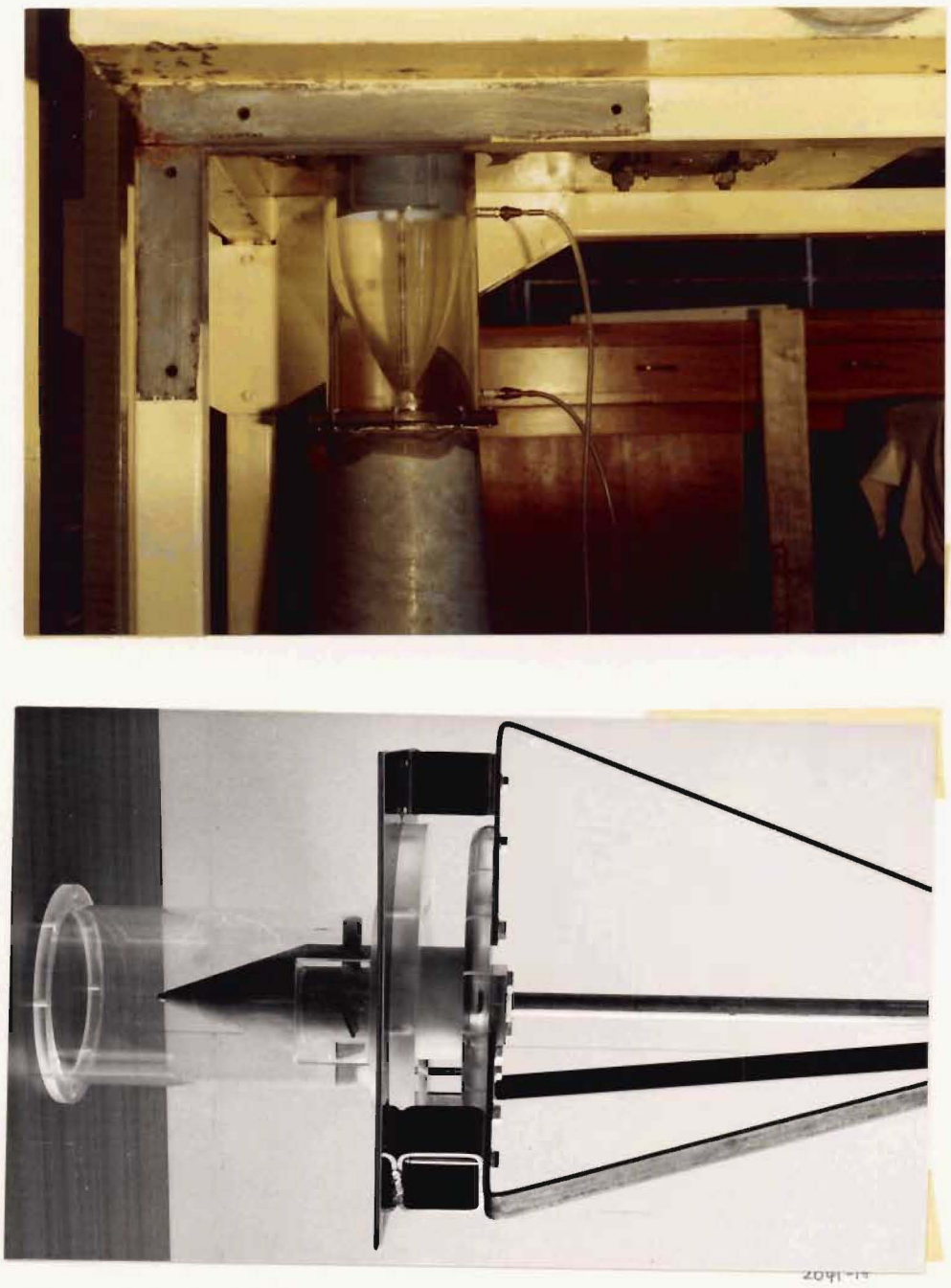

Figure 2.6 Model Turbine

CHAPTER 3

MODEL TESTING

The model turbine was tested in the Fluid Mechanics Laboratory of the Civil Engineering Department, University of Canterbury. The general layout of the test facility is shown in Figure 3.1.

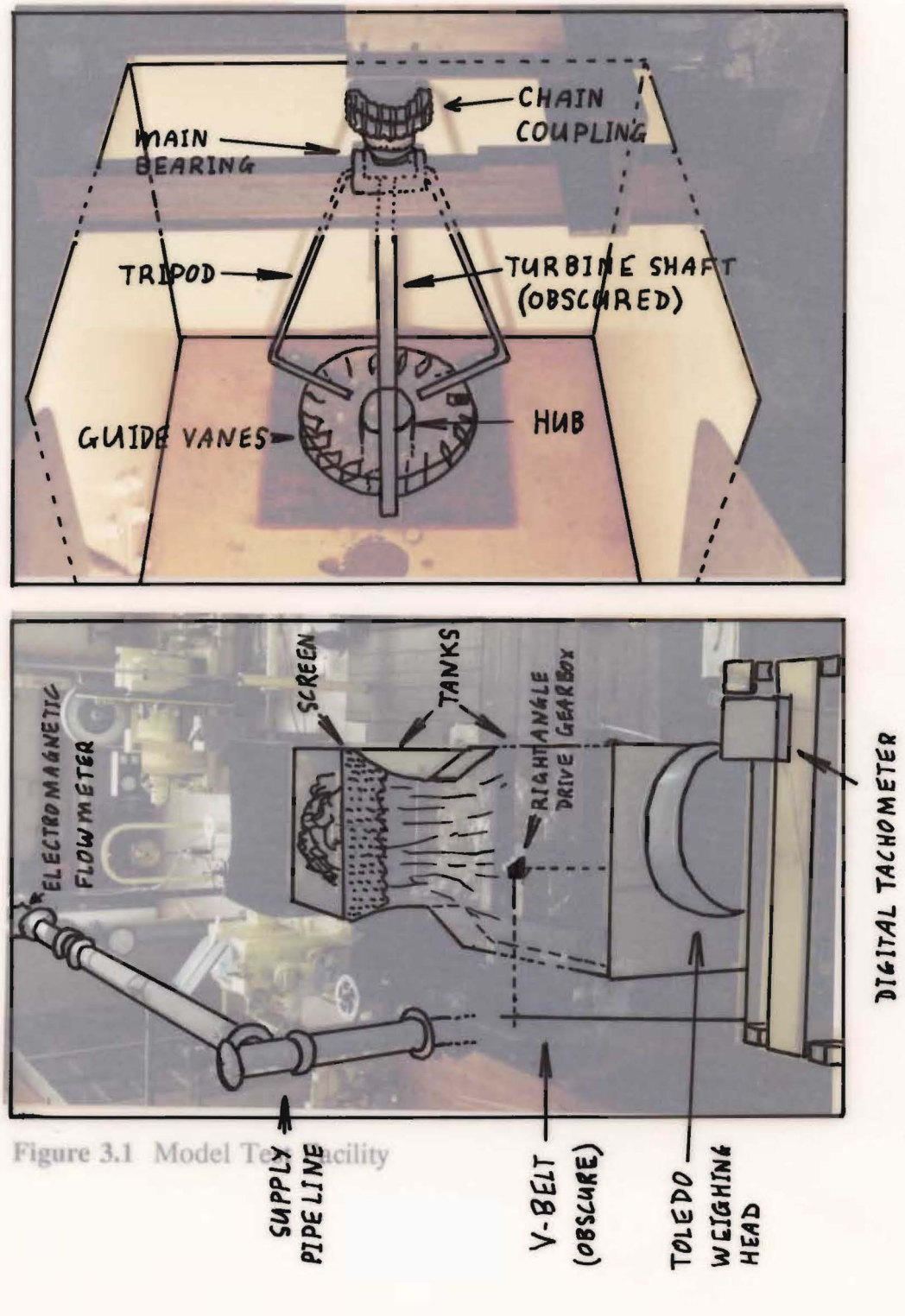

Figure 3.1 Model Test Facility

3.1 MEASUREMENTS

The turbine was connected to a variable speed dynamometer via a flexible chain coupling, right angle drive gearbox, and V-belt drive. The dynamometer used a Schrage motor and could be set to run at any speed from 250 to 2500 RPM. The torque on the dynamometer was measured with a Toledo weighing head on a lever arm (this reading is called S). Digital tachometers gave accurate dynamometer and turbine speeds. (see Section 3.5.2, page 26).

The inlet water level was measured with a piezometer tube on the inlet tank, and the outlet water level with a float gauge. The outlet water flowed over a weir and so the outlet water level varied slightly with flow rate. In the supply pipe line there was a control valve which was used, once the speed had been set, to match the flow rate exactly to keep the inlet water level constant, at a height to give approximately 1.8m head above the outlet water level. The flow rate was measured with an electromagnetic flow meter in the supply pipeline.

The static pressures at the two pressure tapping points (Figure 2.6) were measured using water manometers, giving differentials in head of water. The differentials were measured relative to the outlet water level. Throttling of the upper pressure tapping tube was necessary to stop a slight oscillation in the reading.

3.2 FLOW VISUALISATION

Without complex calculations, the flow through the turbine can only be approximately predicted. Flow visualisation was important to determine the actual flow patterns. The flow directions at various locations were determined with cotton threads and air bubbles.

Cotton Threads These were attached to the blades at various locations from the hub to the tip, on the leading and trailing edges. Observation of the threads with a stroboscope showed the flow direction relative to the blades.

Air bubbles These were introduced through probes just above and below the blades, at varying positions from the hub to the tip, and showed the absolute flow directions. There were also small air bubbles throughout the flow introduced by

turbulence at the supply pipe entry to the inlet tank. These bubbles enabled visualisation of the flow in the area of flow expansion after the hub. By lighting the turbine tube from the side with a narrow beam of light, perpendicular to the direction of observation, a cross section of the flow pattern could be observed. The pattern of moving bubbles was improved by lowering the inlet water level, which, through increased turbulence, increased the number of air bubbles.

3.3 TESTING PROCEDURE

For each turbine configuration (blades, cone, guide vane angle) the performance was measured for a range of speeds. The data for each speed was entered immediately into a spreadsheet program and the calculated performance parameters of power, flow rate, and efficiency were plotted on a graph, so that any readings that did not fit a smooth curve could be retested with another reading at the same speed.

All the recorded performance data is shown in Appendix II. The data is scaled to a consistent head of H = 1.800m, to remove the effect of the slight variation in actual head (the scaling laws are explained in Appendix I.2).

Initially the tests were done over a wide range of speeds, but for later tests only the range from best efficiency point to best power point was covered to save time.

3.4 DRIVE LOSSES

There were significant friction losses in the gearbox and V-belt drive. This meant that the measured torque (S) at the dynamometer was less than the torque produced by the turbine. The amount of friction was estimated by running the dynamometer with the turbine disconnected at the chain coupling.

The gearbox contained gears running in oil. The torque due to friction loss was almost entirely a function of speed, varying with the amount of churning of the oil and also with the temperature of the oil, as this changed the viscosity. The amount of torque transmitted through the gearbox should not affect the friction loss for spur gears.

The friction loss in the V-belt drive was dependent on the transmitted torque since the belt tension increased and the belt was pulled tighter into the pulley grooves at higher torques. It would also have depended on the speed.

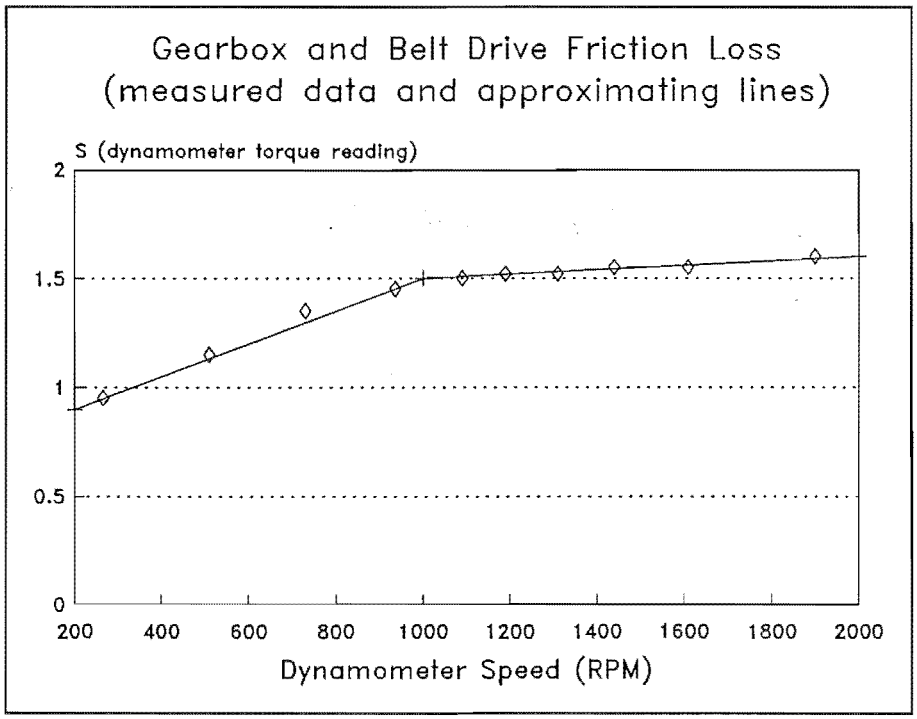

Figure 3.2 Friction Loss Against Speed, No Load

The total friction torque was measured with the dynamometer driving the V-belt and gearbox. The variation in the dynamometer torque reading S is shown in Figure 3.2. In comparison with this friction reading of about 1.5 units, readings with

the turbine running ranged from about 3 to 7 units. The variation in the friction loss with speed was approximated with two straight lines as shown, and the approximate value was added to the S readings made with the turbine running to give the true output of the turbine. The error at the worst point of the curve-fitting (730 RPM) was 1%.

The friction loss when under load was expected to be greater than with no load, since the V-belt tension increases with load. This would mean that the friction correction underestimated the true power produced by the turbine. However an approximate check using a rope brake driven by the dynamometer did not show any measurable rise in the loss with increased load. Therefore it was assumed that using the friction correction value as given in Figure 3.2 would give a good estimate of the true power produced by the turbine.

3.5 ACCURACY

3.5.1 **Temperature Stabilisation**

Because the loss in the gearbox was related to the temperature of the oil, and the temperature increased with increasing speed, the turbine had to run for sufficient time at a constant speed for steady state conditions to be reached. This could take half an hour or more from cold or around 10 minutes for small changes in speed. If readings were taken with insufficient time for equilibrium to be reached, with increasing speed, the gearbox oil would be cooler than when the friction measurements were taken, and so the torque loss would be greater than expected. This would cause an underestimate of the true torque produced by the turbine. Conversely with decreasing speeds the friction loss would be less and the turbine torque would therefore be overestimated.

The effect on the readings when insufficient time was allowed for stabilisation can be seen in Graphs G and H, Appendix II, where two separate lines connect data for increasing or decreasing speeds. Readings were generally taken with increasing speeds, to be conservative, and when a reading was taken out of sequence extra time was allowed for equilibrium to be reached.

3.5.2 Accuracy of Readings

The dynamometer torque reading S was the least accurate measurement taken. The inaccuracy was due to vibrations of the indicating needle. There was a rapid vibration (due to vibration of the internal mechanism of the scale), and a slow oscillation with a period of a few seconds. The average or central position was clear for the rapid vibration but not for the slow oscillation. The error in reading the S value was ± 0.025 units, or under 1% for most readings.

The slow oscillation was due to either a variation in flow through the turbine or some variation in the dynamometer. The oscillation was similar for all turbine configurations. There was an oscillation in the pressure at the top pressure tapping, just after the blades, and in the flow angle just before the blades (Section 4.3.3). While these were not carefully studied, they may have had the same cause, ie, some regular variation in the inlet flow in the inlet tank, guide vanes, or toroid section. The oscillation was about 2% of the measured S values, for the heavily damped dynamometer.

The flow rate and speed measurements were accurate to within 1% of their true values.

CHAPTER 4

RESULTS OF MODEL TESTS

4.1 TYPICAL PERFORMANCE (AND PROTOTYPE DESIGN IMPLICATIONS)

The performance curves for the various turbine configurations tested had the same basic form. A typical set of curves is shown in Figure 4.1 (the data is taken from Graph C, Appendix II). The values have been non-dimensionalised by dividing by the value at the best efficiency point.

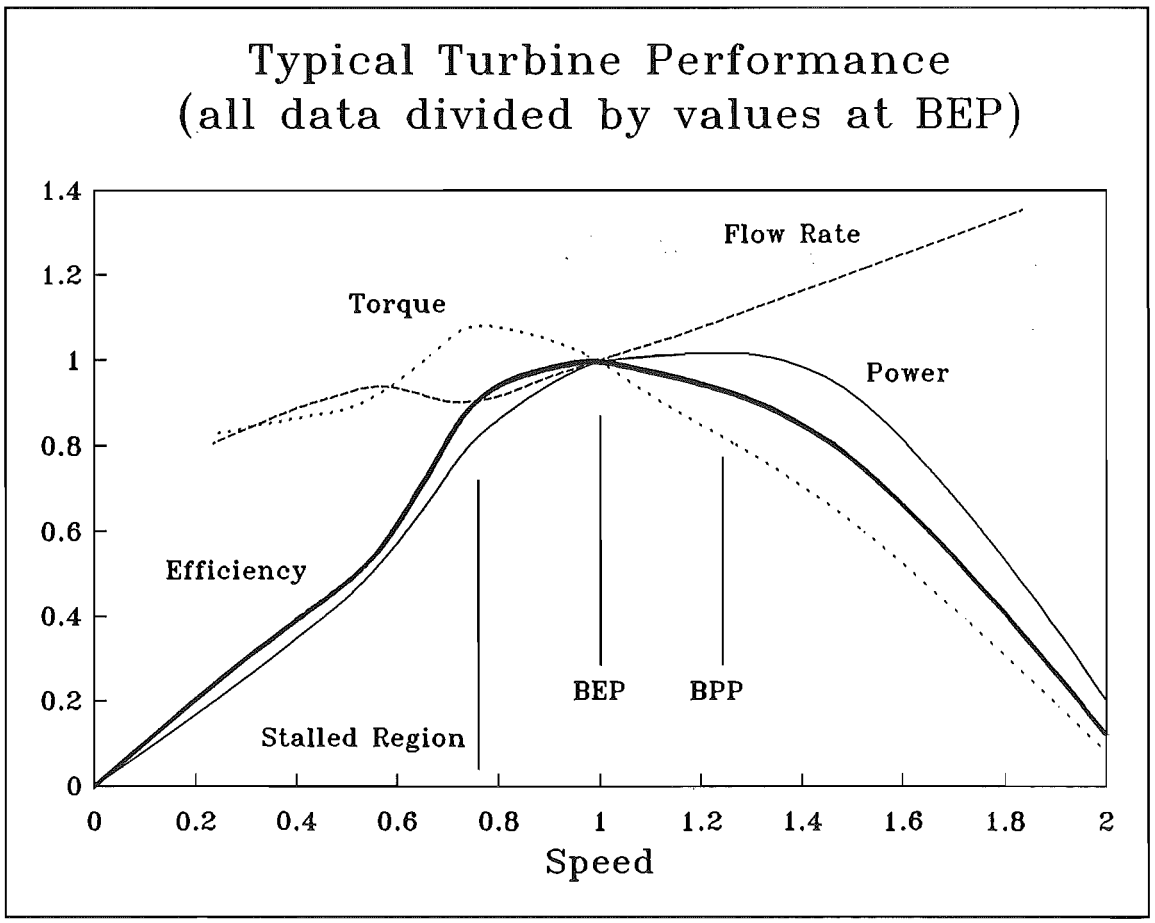

Figure 4.1 Typical Performance Curves at Constant Head

4.1.1 Best Efficiency Point

This is usually the operating point of most interest, as it is usually used as the point at which comparisons between different turbines are made. It is the point at which the flow angles and blade angles are best matched to give minimum losses. It is the performance point used for design of a turbine to produce the maximum amount of power for a given head and flow rate. The turbine configurations tested had a best efficiency ranging from 48% to 64%.

4.1.2 Best Power Point

As the speed is increased above the best efficiency point, the efficiency initially decreases only slightly and the flow rate increases to give a best power point at a higher speed than the best efficiency point. For a given power requirement the required diameter of the turbine is less, giving a further increase in speed. The turbine should therefore be designed to run at this point if high speed is more important than the efficiency.

The speed at the best power point was 15% to 40% higher than the speed at the best efficiency point, for different turbine configurations. The power was about 2% to 11% greater. The efficiency was 92% to 98% of that at the best efficiency point, and the flow rate 10% to 20% greater.

The power curve was flat around the best power point so there was a range of speeds (about 15%) over which the power did not vary significantly. This makes the design point less critical. The speed at which the best power point occurred could only be approximately estimated, and because of this the efficiency and flow rate at the best power point are also approximate.

4.1.3 Runaway Speed

The runaway speed is the speed the turbine would reach with no load. This could happen to the prototype if the drive fails or the electrical load is lost. Since the runaway speed was large (about 2.1 times that at the best efficiency point or 1.7 times that at the best power point) damage could occur, particularly to the generator windings, and so a fail safe brake is required on the prototype turbine. The flow rate was about 1.4 times that at the best power point so if this flow rate is not available the

inlet water level will reduce until air entrainment and other problems occur. There would normally be sufficient volume of water in the supply channel for the turbine to reach its full runaway speed before the water level had dropped significantly.

4.1.4 Zero Speed

When the turbine was stopped there was still a significant torque and flow rate. Their values were about 75% and 65% respectively of their values at the best efficiency point.

4.1.5 Stall Point

When the turbine is running at a low speed the angle of attack on the blades is large and they become stalled. As the speed is reduced from the best efficiency point the angle of attack increases, giving greater torque, until stall starts to occur. The torque then decreases giving a rapid drop in efficiency and an increase in flow rate, since the friction losses ($\propto V^2$) must increase to balance the decrease in power absorbed by the blades.

The maximum torque was about 10% and 35% greater than at the best efficiency point and best power point respectively. The turbine brake must overcome this maximum torque. The speed was about 60% of the speed at the best power point.

4.1.6 Flow Rate

Above the stall point the flow rate against speed was almost exactly a straight line, particularly from the best efficiency point to the best power point.

4.2 CONE AND DRAFT TUBE

4.2.1 **Results of Tests**

The effect of different cones is shown in Table 4.1. The data given is at the best efficiency points and best power points of the configurations as indicated (Graphs D,G,H,X,Z, Appendix II). The Table shows the change in the performance parameters from their value for no cone, as a percentage of the no cone value. The values in brackets are for the performance at the same speed as that of the best power with no cone.

Configuration		Best Efficiency Point				Best Power Point			
	CN	N	Q	P	η	N	Q	P	η
BA35 8MB GVA35	1	0	2	3.6	2	8.4 (**0**)	7.5 (3.3)	6 (5.2)	-2 (2)
BA22.5 4PB GVA32	1	0	0	6	6	0	0	5	5
	2	0	0	0	0	0	0	-2	-2
Percent Increase in value from No Cone value									

BAn : Blade Angle of n degrees GVAn : Guide Vane Angle of n degrees

8MB : 8 Metal Blades 4PB : 4 Plastic Blades

CN=1 : Straight Cone CN=2 : Radius Cone

Table 4.1 Effect of Cone Type on Turbine Performance

No Cone The performance with no cone was better than expected. The overall efficiency was 53% to 58% for the configurations used in Table 4.1, and the maximum efficiency measured with no cone was 64% (Graph O, Appendix II). An increase in efficiency of about 15% (to say 75%) could be expected with a perfect cone and draft tube (Section 4.2.3).

Straight Cone This gave a small but definite improvement in the performance of the turbine, compared with the performance with no cone. In general there was an increase in power and efficiency for the same speed and flow rate, which implies that the effective head was greater, ie, the losses were reduced. This was confirmed by the pressure recovery measurements (Section 4.2.4), which show an increase in the velocity head recovery for the straight cone. For the 8 metal blades at 35°, at the best power point, there was still an increase in power but also an increase in speed and flow rate, and a slight decrease in efficiency. The data for this configuration (Graph Z) was not very good, and so the speed at the best power point is not certain; if a lower speed was chosen the corresponding efficiency would be slightly higher, as indicated by the numbers in brackets in Table 4.1. The data still showed an improvement in the performance.

The small improvement in performance may not warrant the extra manufacturing complexities, so making the turbine with no cone may be preferable in some situations.

Radius Cone This gave no improvement in performance compared with no cone. At the best power point there was a slight decrease in power and efficiency.

4.2.2 Flow Patterns and Explanations of Results

The flow patterns in the turbine tube between the blade outlet and the draft tube inlet, were made visible with small air bubbles, as described in Section 3.2. After the hub there was a wake of stationary or recirculating flow (Figure 4.2). This wake extended well beyond the hub and into the inlet of the draft tube (from there it was not visible). The existence of the wake means that the assumption of uniform flow was not valid at the entry to the draft tube. The area of the wake at this point was difficult to measure because of the distorted view, but was in the order of a quarter of the area of the hub.

The existence of the wake meant that the velocity at the inlet to the draft tube was greater than expected. Hence there was more velocity head to be recovered in the draft tube, but this recovery would not be good because of the non-uniform velocity distribution.

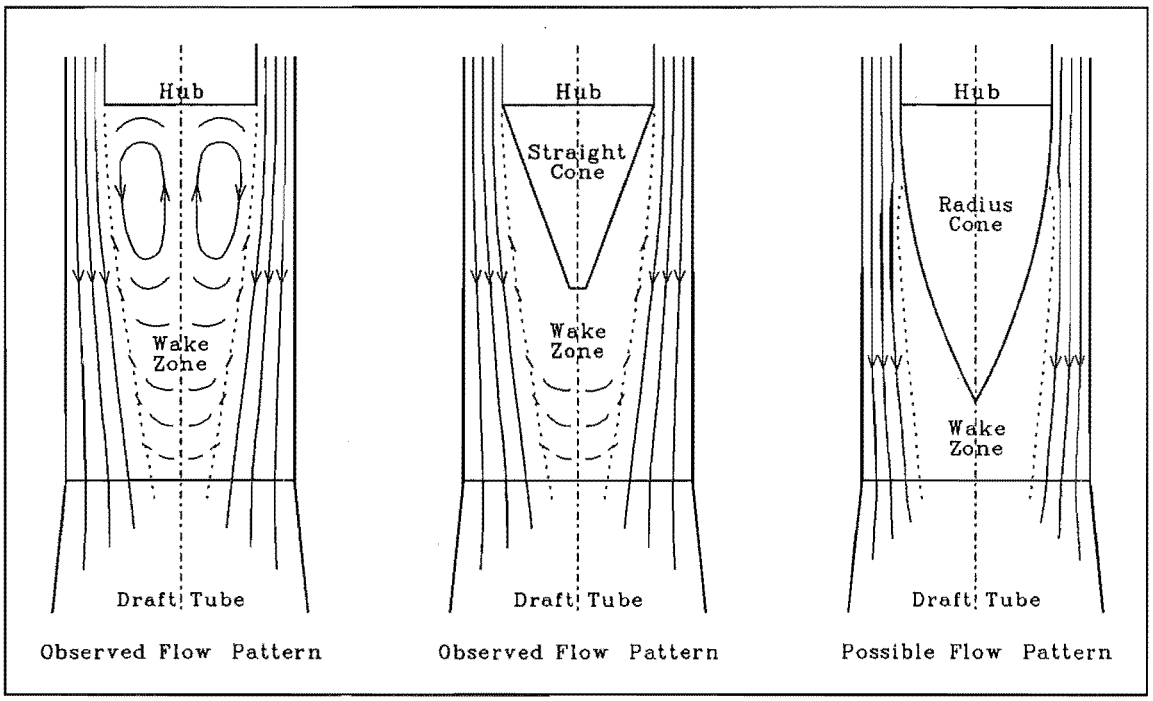

Figure 4.2 Flow Patterns for Different Cones

No Cone The sharp edge of the hub seemed to produce a flow pattern that gave reasonable recovery (Figure 4.2). The zone of fast moving flow appeared to stay separate from the wake zone. It is the interaction and mixing of the fast moving flow with the "stationary" or recirculating wake flow that causes turbulence and losses, and over the observable area (ie, before the draft tube) the wake boundary was fixed and definite. The velocities in the wake appeared to be large, but the flow pattern was steady and smooth, ie, there did not appear to be large amounts of turbulence to cause losses.

It is likely that in the draft tube with the extra expansion and with a small remaining wake area, the boundary between the fast flow and the wake would become less stable and turbulent mixing would occur. A longer straight section before the draft tube could possibly give better pressure recovery, but this could also cause an increase in other losses such as skin friction drag.

Straight Cone There was some improvement in the performance with the straight cone, although the cone was located entirely within the wake (Figure 4.2). The flow did not follow the cone surface, which was not surprising considering the large rate of expansion in flow area and the sudden change in flow direction required.

It is possible that reducing the free area for the recirculating flow to develop in had reduced the losses. If the cone caused a reduction in the size of the wake at the entry to the draft tube then the overall recovery should be better.

Radius Cone This was expected to improve the turbine performance significantly by controlling the flow better at the beginning of the expansion. It was expected to slow the flow more quickly and with less turbulence, by keeping the flow attached to its surface. The reason for the radius cone not giving improved performance was not discovered, although some possible reasons were identified:

i. The extra friction drag due to the increased surface area rotating at a high speed could have counteracted any improvement in velocity head recovery. The torque on the hub, and hence the power lost, was estimated with an approximate analysis of the drag force on the hub, treating the hub surface as a flat plate moving through stationary water, with a velocity equal to the tangential velocity of the surface of the hub ($r\omega$). This approximate estimate (using a drag coefficient of $0.003 \pm .001$) gives a power loss of approximately 5% of the power produced by the turbine (calculated at typical conditions: BPP, Graph V). Therefore the increase in area over which drag was acting with the radius cone attached could have counteracted an increase in performance of a few percent.

ii. If separation was still occurring part way along the cone, then the initially improved recovery may be counteracted by a worse flow pattern after separation. Also because the separation would have occurred closer to the draft tube the wake would not have so far in which to reduce in size before entering the draft tube. Figure 4.2 shows an extreme example of what could have been occurring.

4.2.3 Pressure Recovery Measurements

Velocity Head Using the average axial velocity (Q/A), for typical conditions (BPP, Graph V; Q=57.5l/s), the velocity head $Hv=V^2/2g$ in the annulus area was 0.97m or about 54% of the total head, H. This velocity head ratio Hv/H was 17% at the inlet to the draft tube and 2% at the exit of the draft tube. The swirl velocity (tangential velocity component) was ignored because it would be hard to recover

without straightening vanes, and because the swirl was not large around the best operating points. The point of minimum outlet swirl occurred near the best power point for the metal blades set at angles of 20°-35°.

If none of the velocity head is recovered as pressure then 54% of the available head would be lost. Still using the assumption of uniform flow distribution, ⅔ of the potential velocity head recovery would occur past the cone as the flow slows from its annulus area velocity to the velocity in the full turbine tube area, and ⅓ would occur in the draft tube. The velocity head is only fully recovered as pressure if the flow slows without turbulence occurring, otherwise energy is lost as heat.

Measured Recovery Differential manometers were connected to the pressure tappings in the wall of the turbine tube, just after the blades and just before the draft tube inlet, and between the latter tapping and the outlet free surface water level (Figure 2.6). The manometer differential readings gave the velocity head recovery, ie, the decrease in velocity head minus the head lost through turbulence.

The total recovery of velocity head, for the straight section of turbine tube and the draft tube, was typically about 70% of the velocity head in the annulus area, calculated using the average axial velocity. This figure was generally constant over the range from best efficiency point to best power point.

Therefore at least 30% of the total velocity head was lost, representing about 15% of the total head, so there is potential for a good cone/draft tube design to increase the overall efficiency by around 10%. The remaining losses of approximately 25% were assum ed to occur mainly in the blades.

The measurements showed that approximately equal proportions of the pressure recovery occurred in the cone area and in the draft tube. There was a decrease in the proportion of recovery occurring before the draft tube as the speed was increased from the best efficiency point to the best power point.

The pressure recovery for 8 metal blades at 35° (Graphs X and Z, Appendix II) showed an increase with the straight cone fitted compared with no cone. The pressure recovery for no cone was 62% of the annulus area velocity head, compared with 72% for the straight cone. For no cone this ratio was constant from the best

efficiency point to the best power point but at the best efficiency point for the straight cone it rose to 77%.

Cylindrical Draft Tube If the draft tube did not increase in area, ie, the final outlet diameter was the same as the turbine tube diameter (D), then 17% of the total head would be lost as velocity head at the outlet. This would reduce the overall turbine efficiency by 17% to about 40%, but avoiding the extra expense of the conical draft tube may be more important in some situations. (A straight section after the hub is still required to allow recovery of the initial ⅔ of the velocity head). There would be other effects of having a straight draft tube, eg, increased skin friction loss and possible improvement of the velocity head recovery from the annulus area.

4.3 GUIDE VANES

4.3.1 **Results of Tests**

The guide vanes were set at an angle, GVA, to the radial direction (Figure 4.3) to give the flow swirl in the same direction as the rotation of the blades.

The effect that varying the guide vane angle had on the performance is shown in Figure 4.4. The data shown is for the turbine configuration of 4 plastic blades at 22.5°, straight cone (Graphs A-E, Appendix II). The effect on other configurations was similar.

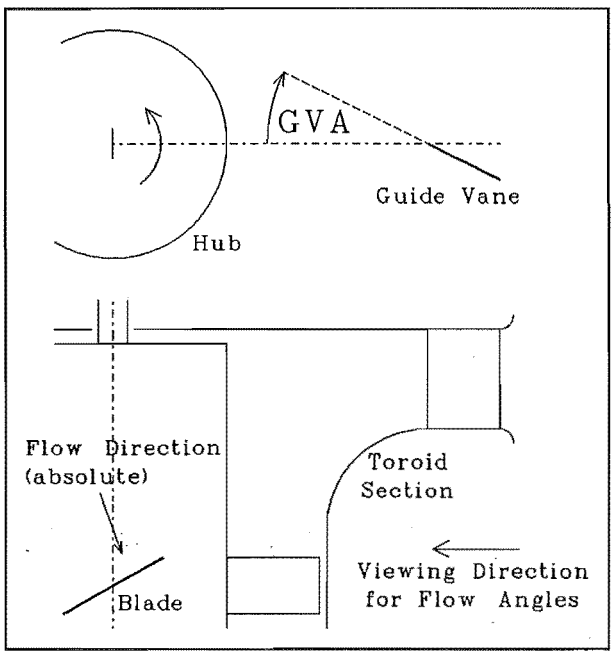

Figure 4.3 Guide Vane Angle

Small changes in the guide vane angle did not make a large difference to the performance, though there was a definite improvement with the guide vanes fitted (at say 30°) compared with no guide vanes (GVA=0). As GVA was increased there was an increase in the efficiency and power, to a maximum at about 45° for the efficiency and 30° for the power. There was no significant change in the speed of the best operating points. The flow rate dropped as GVA increased, ie, the increase in efficiency was greater than the increase in power.

If the power is the most important parameter then GVA≈30° would be best. To maximise the efficiency a larger GVA could be used; the efficiency was possibly still increasing at 45°.

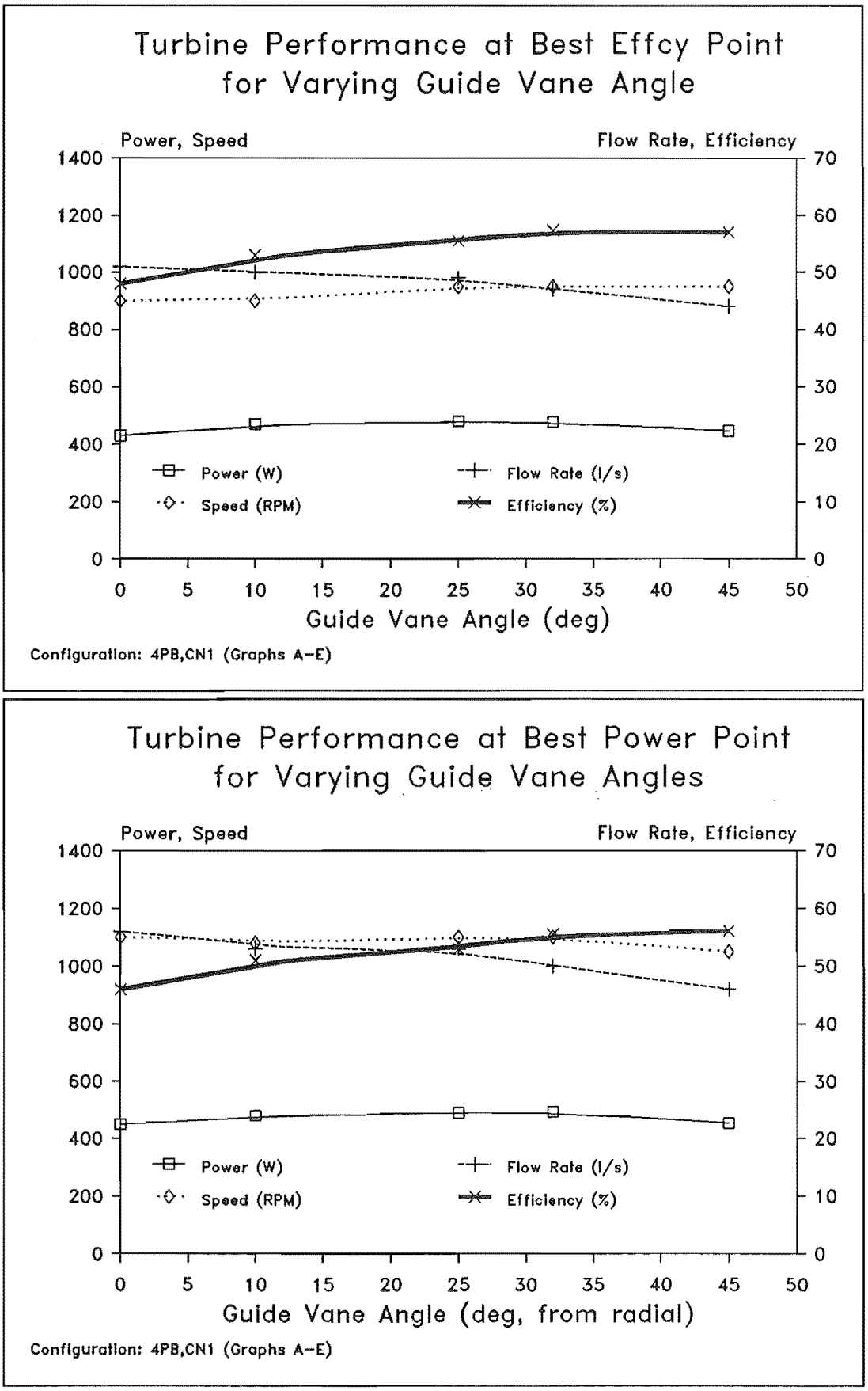

Figure 4.4 Effect of GVA on Turbine Performance at Constant Head

4.3.2 Losses

The losses through the guide vanes and inlet passages through to the turbine tube just above the blades were measured with GVA=25°. For a flow rate of 40.3l/s the pressure at the outside wall of the turbine tube was zero (ie, atmospheric pressure). This was determined from a probe hole in the tube wall, just above the blades, which had no flow of water or air through it when open (at other flow rates air was sucked in or water forced out of the probe hole). The annulus area was $0.01303m^2$ giving an average axial velocity $V_{axial}=3.09m/s$. The observed flow angle was approximately 20° from axial giving the average resultant velocity $V=3.09/\cos 20°=3.29m/s$. The velocity head is therefore $V^2/2g=0.55m$. The pressure tapping point was 0.58m below the inlet water free surface. Using Bernoulli's equation for energy changes from the inlet free surface (1) to the probe hole (2), including the loss H_{loss}, gives

$$\frac{p_1}{\rho g}+z_1+\frac{V_1^2}{2g} = \frac{p_2}{\rho g}+z_2+\frac{V_2^2}{2g}+H_{loss}$$

where $p_2=p_1=p_{atm}$, $V_1=0$, $z_1-z_2=0.58m$, so:

$$H_{loss} = (z_1-z_2)-\frac{V_2^2}{2g}$$

$$= 0.58m-0.55m \approx 0.03m$$

This was about 1.7% of the total head. The swirl would have caused a radial pressure distribution with a higher pressure at the outer wall than the average pressure, so p_2 would be less than the measured value and hence H_{loss} becomes greater. The increase in the pressure head ($p/\rho g$) at the outer wall due to the centrifugal force of the rotating flow was calculated, assuming a free vortex swirl distribution, as 0.026m, giving $H_{loss}\approx 0.06m$ or about 3% of the total head.

The total inlet loss was not large. At large guide vane angles the guide vanes could stall giving increased losses and reduced swirl but this was not observed at the maximum GVA tested of 45°.

4.3.3 Flow Angles

The absolute flow angle just before the turbine blades was measured by observing a stream of bubbles released from a probe. The angle was measured from the axial direction (Figure 4.3). The angle was difficult to measure exactly because it varied slowly by 5° to 10°. The fluctuation had a variation of a few seconds; it was similar to the fluctuation in the dynamometer torque, and hence may have been related. No regular variation at the inlet free surface was noticed.

The average flow angles for GVA=25° were measured at varying radii as about 15° at the tip position (outer radius of annulus area), 20° midway, and about 30° at the hub (inner radius of annulus area). For GVA=32° the average tip angle was 22°, varying from 15° to 25°, and the hub angle about 30°. As expected, the flow angles did not appear to vary with flow rate, for a fixed geometry.

There were three possible reasons for the variation in the flow angles with radius. Firstly the tangential swirl velocity varied with radius, due to conservation of angular momentum, ie, assuming a free vortex swirl distribution. The theoretical tangential velocity is therefore inversely related to radius and V_{tan} at the hub is greater than V_{tan} at the tip by a factor $F^{-1}=1.51$, where F is the hub diameter to blade tip diameter ratio. Secondly the axial velocity was probably not uniform from hub to tip. As the flow was turned from the radial direction through the guide vanes to the axial direction in the turbine tube, there may have been an increase in the velocity on the "inside" of the bend, ie, the outside of the turbine tube. There would have been a matching decrease in the velocity at the "outside" of the bend, ie, at the hub (Ward-Smith, 1980). Thirdly the area of stationary or recirculating flow around the top of the hub (ie, the "outside" of the bend) may have influenced the flow, particularly near the hub.

Assuming uniform axial velocity (Q/A) and conservation of momentum, the calculated flow angles for GVA=25° are 15.7°, 18.7°, and 23.0° for the tip, middle, and hub positions respectively. For GVA=32° the angles are 21.4°, 25.2°, and 30.6°, which is very close to the measured values above. This is partly chance since the flow angles could not be measured accurately (the error was about ±2°). There is a difference between the measured and calculated value for GVA=25°. If the angular momentum is not conserved then it is more likely that the tangential velocity at the

hub will be less than predicted, which gives a smaller calculated flow angle at the hub rather than the larger angle measured. Therefore to match the measured values the axial velocity must have varied. The ratios of the actual axial velocities to the average value (Q/A), that matches the calculated flow angles with those measured are 1.05, 0.93, and 0.74 at the tip, middle, and hub respectively (still using the assumption of conservation of angular momentum). These do not give the correct average of 1, indicating that the actual GVA was slightly greater than measured. Using GVA=27° in the calculations gives a match with an axial velocity distribution of 1.15, 1.0, and 0.8. The guide vanes were accurately set at the same angle using a template, but the actual angle could not be accurately measured. The increase in the axial velocity at the tip position was expected, if the flow around the toroid section was similar to flow in a bend.

4.3.4 Guide Vanes made with a Varying Angle

The flow angles do not match the turbine blade angle for all radii, because the tangential velocity of the turbine blades is large in comparison to the flow velocity and it varies in proportion to the radius. Normally the blades are curved to give a perfect match. An attempt was made to match the flow angles to the straight blades by giving the inlet flow more swirl at the tip position. This was done with flat guide vanes, angled at 45° from vertical, to give GVA=20° at the top (hub position) and GVA=45° at the bottom (tip position). The guide vane arrangement is shown in Figure 4.5.

However the results showed no improvement in performance (Graphs J,K, Appendix II). This was probably because the flow did not follow the guide vanes properly and so the full variation in swirl did not occur.

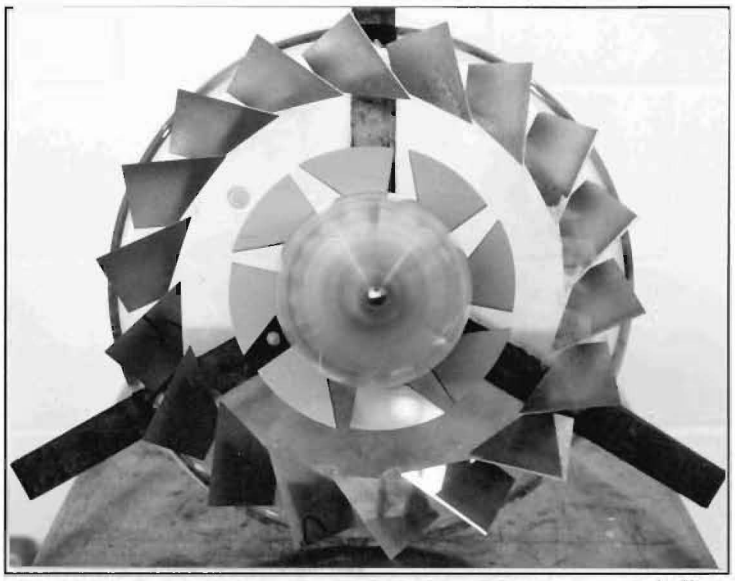

Figure 4.5 Varying Angle Guide Vanes

Also the areas of varying swirl may have mixed, giving an averaging effect. It was also found that the increased angle of attack towards the hub gave a more consistent outlet swirl distribution, since the flow nearer the hub did not follow the blade angle exactly (Section 4.4.2).

4.4 TURBINE BLADE CONFIGURATION

Various types of flat blade were tested. The blade angle, β (or BA), is measured from the tangential direction as shown in Figure 4.6, ie, $\beta = 0^\circ$ means the blade is perpendicular to the axial flow direction.

4.4.1 First Configuration

Design The initial blade configuration was determined using axial flow pump design guidelines. Axial flow pumps can be run in reverse as turbines so it was thought that the guidelines would have some relevance, even if only as a starting point. The required specific speed of the prototype was estimated and this value used in guidelines presented by Stepanoff (1957). However the hub diameter was made larger than that indicated by the guidelines, since a large hub was required to reduce the effect of the flat blades (Section 2.2.3). The guidelines recommended 3 or 4 blades and suggested a blade angle of 22.5° as a typical angle used for axial flow pumps.

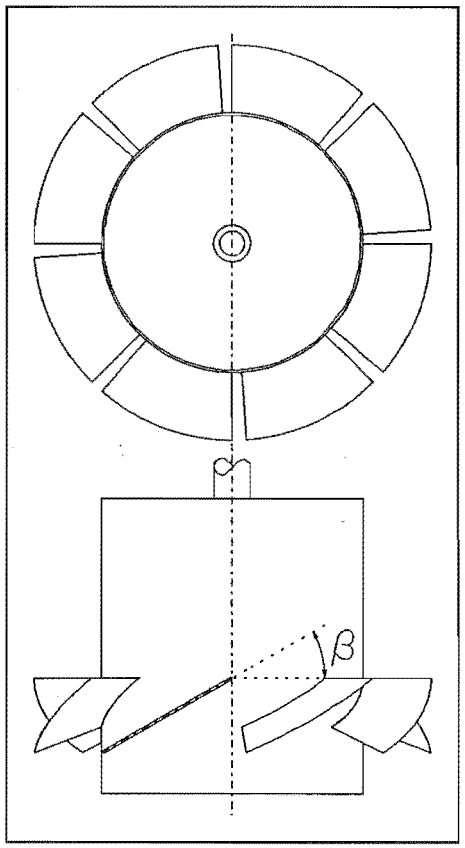

Figure 4.6 Blade Angle

The blades were made from 3mm sheet PVC plastic glued into slots milled in the hub, which enabled easy and accurate assembly. The first blade design is shown in Figure 2.6.

Results The performance data is given in Graphs A-I, Appendix II.

Flow visualisation showed that most of the flow through the blades was at a steeper angle than the blade angle. Only close to the blades did the flow follow the blade angle, and then only while passing the blades. As soon as the blades were passed the flows of differing directions combined.

The effective blade angle, ie, the typical flow angle relative to the moving blades or hub, was about 30°, compared with the actual blade angle of 22.5°. It was thought that more blades would control the flow better so that it followed the blade angle more closely. This would reduce the losses caused by the mixing of the different flows after the blades.

4.4.2 Second Configuration

The number of blades was increased to 8, still using PVC plastic. At the same time an attempt was made to get a varying trailing edge blade angle, so that the outlet swirl would be the same at all radii. Fig 4.7 shows β_L and β_T, the blade angles at the leading and trailing edges respectively, of a blade set square to the hub at the leading edge.

$$\tan\beta_T = x/y$$

$$x = z\tan\beta_L$$

$$z = r\sin\phi$$

$$y = r\tan\phi$$

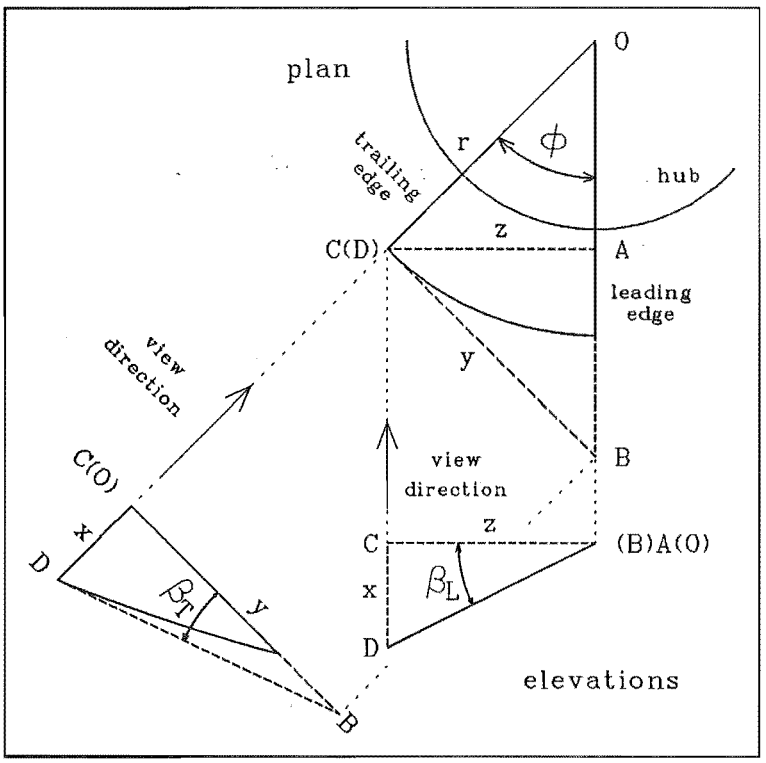

Figure 4.7 Blade Angles at Leading and Trailing Edges

so $$\tan\beta_T = \frac{r\sin\phi\tan\beta_L}{r\tan\phi}$$

or $$\beta_T = \tan^{-1}(\cos\phi\tan\beta_L) \qquad (4.1)$$

The blade angle, β_T, becomes smaller as ϕ gets larger, until at $\phi=90°$ the blade angle is zero.

The blades were made with a cut-away trailing edge (Figure 4.5), so that ϕ ranged from 25° at the hub to 40° at the tip. This gave a varying β_T from 18.3° at the hub to 15.6° at the tip ($\beta_L=20°$).

Results The performance for this blade configuration is given in Graphs J-N, Appendix II. In general there was an increase in the efficiency but a decrease in the flow rate and power, with the speed remaining constant.

Flow visualisation showed that the flow angle through the blades followed the blade angle at the tip, but differed significantly towards the hub. This was mainly due to the increasing angle of attack at the leading edge. Because the flow was not following the blade angle closely, the blade angle at the trailing edge did not determine the outlet swirl, except at the tip of the blade. The flow left the blades with less variation in swirl with radius than was expected assuming conformity of the flow to the blade angle.

The fact that the flow rate decreased for the same running speed indicates that the effective blade angle had reduced, ie, the general flow was following the blade angle more closely.

4.4.3 Blade Thickness

Calculations and the results for various cone configurations showed that the large velocity head in the hub annulus area was a significant cause of losses (Section 4.2). Therefore the further increase in velocity due to the blockage of the blades could be significant. With 8 blades of thickness 3mm, the decrease in flow area was 15% of the annulus area, which would increase the velocity head by a factor of 1.37. This

represents about 10% of the total head at typical conditions. Since it is likely that the recovery of this extra velocity head would be poor, there is potential for improved efficiency with thinner blades.

4.4.4 Third Configuration

The blades for this configuration were made from 0.5mm sheet steel, attached with two bent tabs screwed to the hub. They were cut from a single sheet as shown in the drawings for the prototype turbine, Appendix III. The blade angle was 20° as for the second configuration. The performance data is given in Graphs O and P, Appendix II, and summarised in Table 4.2.

There was a small increase in efficiency, but a drop in the power at the best operating points, because these occurred at lower speeds and correspondingly lower flow rates. There was a slightly greater drop in the flow rate than there was in the speed indicating that the flow was following the blade angle more closely.

Config.	Best Efficiency Point				Best Power Point			
(GVA= 33°)	N (RPM)	Q (l/s)	P (kW)	η (%)	N (RPM)	Q (l/s)	P (kW)	η (%)
8PB (thick)	880	35	.37	60.5	1000	37	.38	59
8MB (thin)	800	30	.33	62	950	32	.345	61

Table 4.2 Effect of Thin Blades on Turbine Performance

Flow visualisation confirmed that the flow was following the blade angle more closely. There was still a tendency for the flow nearer the hub to have a steeper angle than that of the blades, due to the increasing angle of attack. This reduced the variation in outlet swirl at different radii.

4.4.5 Blade Angle

Progressively through the previous configurations the effective blade angle was decreased as the flow followed the blade angle more closely (there was also a slight decrease in the actual blade angle). This resulted in a gradual improvement in efficiency but a decrease in the power and speed at the best operating points. Initially it was thought that a smaller blade angle would give a higher running speed, but, although this does increase the speed for a given flow rate, it was found that the effect of the smaller blade angle was to move the best operating points to lower speeds, with correspondingly lower flow rates and lower power. This is similar to Kaplan turbines in which the blade angle is reduced to maintain a high efficiency at part load, with the speed remaining constant. It became apparent that larger blade angles should give improved performance.

Results The effect of varying the blade angle is shown in Figure 4.8. The guide vane angle was kept at 25°, except for the run with a blade angle of 20°, where the guide vane angle was 33°. This should not make a significant difference to the results. The full data for the four different blade angles tested is given in Graphs O-X, Appendix II. There was some uncertainty in the data, particularly the speed at the best operating points, since estimating the maximum points was difficult. It is possible that inaccuracies in the manufacture of the blades may have caused some of the variation in the results. The blades were made by hand to give a tip clearance of up to 1mm (it was particularly large for the 35° blades), compared with the blade width of 29mm. The blade angle was accurate to within 1° of the nominal value. The blades were all of the same length so that as blade angle increased the effective length decreased slightly. The spacing of the blades also increased.

The graphs in Figure 4.8 show an initially large increase in the power, levelling out at a blade angle of about 30°. The speed was highest at 30°. Therefore 30° was the optimum blade angle, since maximising power and speed was more important than maximising the efficiency. The efficiency dropped slightly as the blade angle increased.

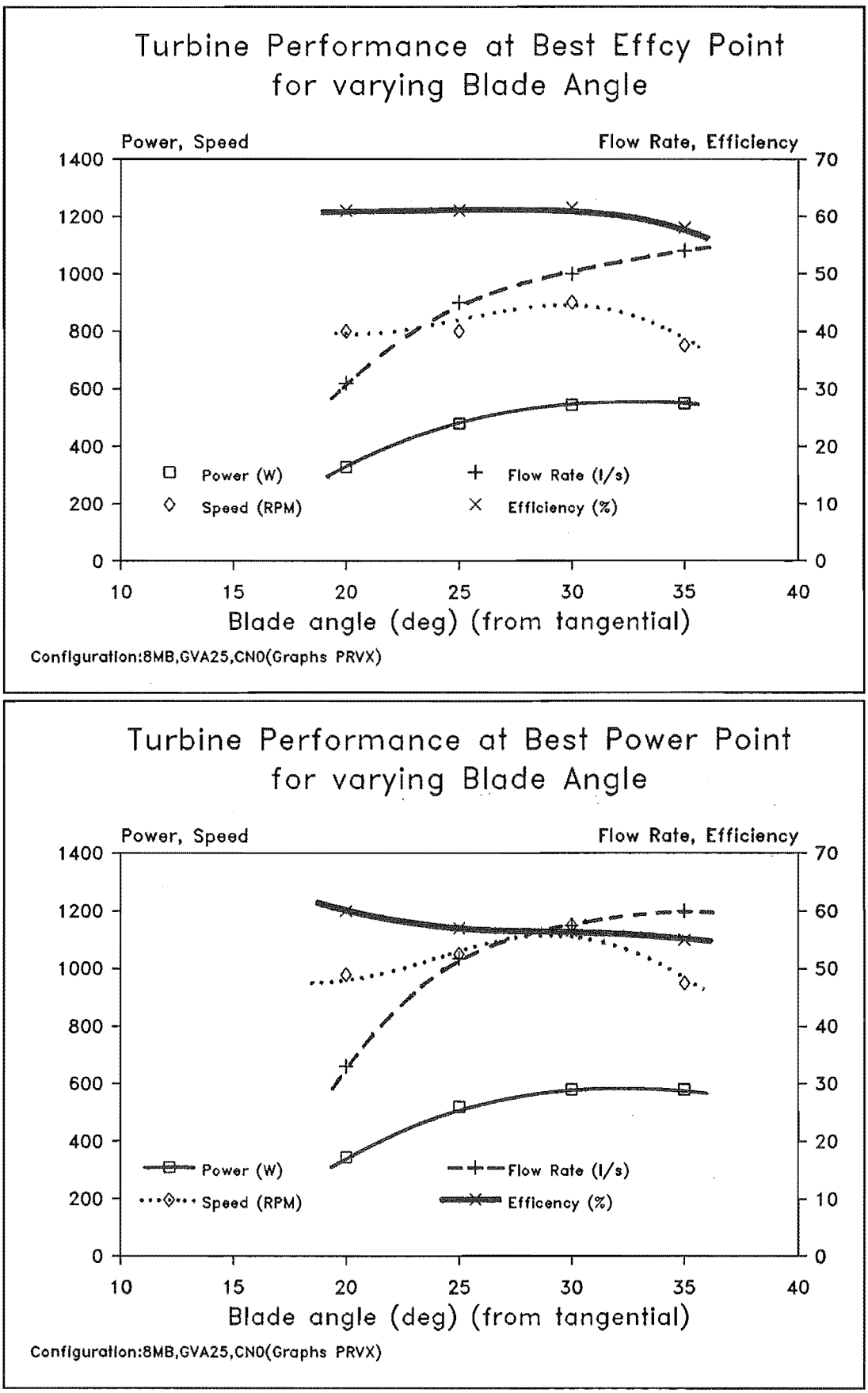

Figure 4.8 Effect of Blade Angle on Turbine Performance at Constant Head

Explanation of Results When the turbine was operating at its best power point, which was the case for the results shown in Figure 4.8, the fluid velocity at the blade exit was close to the axial direction. Assuming it to be exactly axial, the velocity triangles would be as shown in Figure 4.9. The flow rate through the turbine is given by

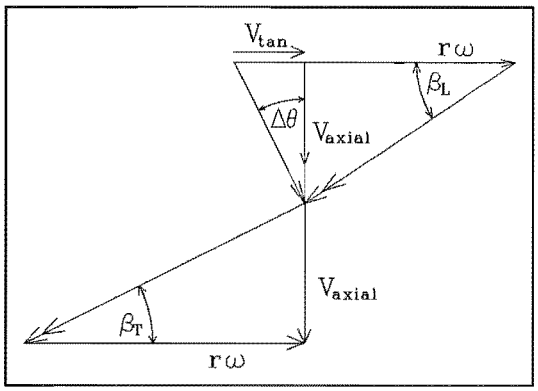

Figure 4.9 Flow Angles

$$Q = V_{axial}A_{annulus} = r\omega\tan\beta_T A_{annulus}$$

(at some typical radius)

The angles are related by

$$\tan\Delta\theta = \frac{1}{\tan\beta_T} - \frac{1}{\tan\beta_L}$$

($\Delta\theta$ is the typical change in the absolute fluid flow angle through the blades.)
The power produced by the turbine is given by

$$P = \rho Q \Delta V_{tan} r\omega = \rho Q^2 / A_{annulus} \tan(\Delta\theta) r\omega$$

$$= \rho(\tan\beta_T)^2\left(\frac{1}{\tan\beta_T} - \frac{1}{\tan\beta_L}\right)(r\omega)^3 A_{annulus}$$

$$\propto \tan\beta_T \left(1 - \frac{\tan\beta_T}{\tan\beta_L}\right)N^3$$

This shows the effect the blade angle has on the power. As β_L and β_T are increased, more water goes through the turbine, and so more power is produced. There is however a limit to the increase in power as the increasing friction and turbulence losses ($\propto Q^2$) mean that the efficiency decreases. This moves the best power point to a lower speed and lower flow rate, giving less power.

4.4.6 Conformity of Flow to Blade Angle

From flow visualisation it was found that the flow followed the blades more closely as the number of blades was increased. With the final blade configuration of 8 thin metal blades, at various angles, the flow was observed to follow the blade angle closely at the tip (measurement of the flow angle had an uncertainty of a few degrees). The calculated flow angles also indicated that the flow was following the blades reasonably closely at the tip. Table 4.3 shows the calculated flow angles at the best power point, for the various blade angles tested. BA is the nominal blade angle, also equal to the actual blade angle at the leading edge, ie, $\mathbf{BA}=\beta_L$. The actual blade angle at the trailing edge is β_T, given by Equation 4.1. The calculated flow angles under the heading "Average" was calculated using the tangential blade velocity at the tip ($r\omega$) and the average axial flow velocity, **Q/A**. Under the heading "Estimate" the true axial flow velocity was estimated using the approximate distribution found in Section 4.3.3, ie, **1.15Q/A**. It was assumed that the flow leaving the trailing edge had no tangential component, ie, zero swirl, which was approximately true near the best power point. The difference between the flow angle "Estimate" and β_T is the equivalent for the trailing edge of α (angle of attack at the leading edge). It is small indicating that the flow followed closely to the blade at the tip. Towards the hub the flow did not follow the blade angle at the trailing edge, because of the increasing angle of attack. The reason for the larger difference for BA=25° (and for the same calculated flow angles for BA=25° and BA=30°) is not known.

Blade Angles		Calculated Flow Angles		
BA (β_L)	β_T	"Average"	"Estimate"	difference (approximate)
20°	16°	16°	18°	3°
25°	20°	23°	26°	6°
30°	24°	23°	26°	2°
35°	28°	28°	32°	4°

Table 4.3 Flow Angles

CHAPTER 5

PROTOTYPE DESIGN

5.1 SELECTION OF TURBINE CONFIGURATION AND OPERATING POINT

In Chapter 4 the effect of various changes in configuration was discussed, and the optimum of each variable was individually found. This process is confirmed by the more general approach described below.

The optimum turbine configuration and operating point depends on which performance parameters are to be maximised. The requirements vary for different applications, with the overall objective being to minimise the cost.

There are three common parameters that can be used to compare different turbine configurations and operating points: η, N_S, and k_S.

The efficiency, $$\eta = P/(\rho g H Q) = (P/\rho)Q^{-1}(gH)^{-1}$$

is maximised to get the maximum Power for a given Flow Rate and Head (or minimum Flow Rate for a given Power and Head).

The Specific Speed, $$N_S = NP^{1/2}H^{-5/4}$$

is maximised to get the maximum Speed for a given Power and Head (or maximum Power for a given Speed and Head).

The Characteristic Number, $$k_S = \omega Q^{1/2}(gH)^{-3/4}$$

is maximised to get the maximum Speed for a given Flow Rate and Head (or minimum Flow Rate for a given Speed and Head).

The Specific Speed (N_S) can be written in a fully non-dimensional form as

$$n_S = \omega(P/\rho)^{1/2}(gH)^{-5/4}$$

Note the similarity in form of the equations for η, n_S, and k_S, and that

$$n_S = k_S\eta^{1/2}.$$

In k_S, Q is raised to a positive power (compared to the negative power in η), since as the turbine is scaled up to take a greater flow rate, the speed decreases. n_S (and N_S) indicates how well a turbine performs, in terms of both speed and power, for a given head (the effect of the flow rate cancels out since it has an opposite effect on the power and speed).

In general the limiting factor with low head turbines is their low running speed, and so the speed is usually of most importance. Therefore N_S or k_S should be maximised. However since k_S does not include the power or efficiency, it is high for high speed, inefficient turbines (for instance the shortened blade configurations,

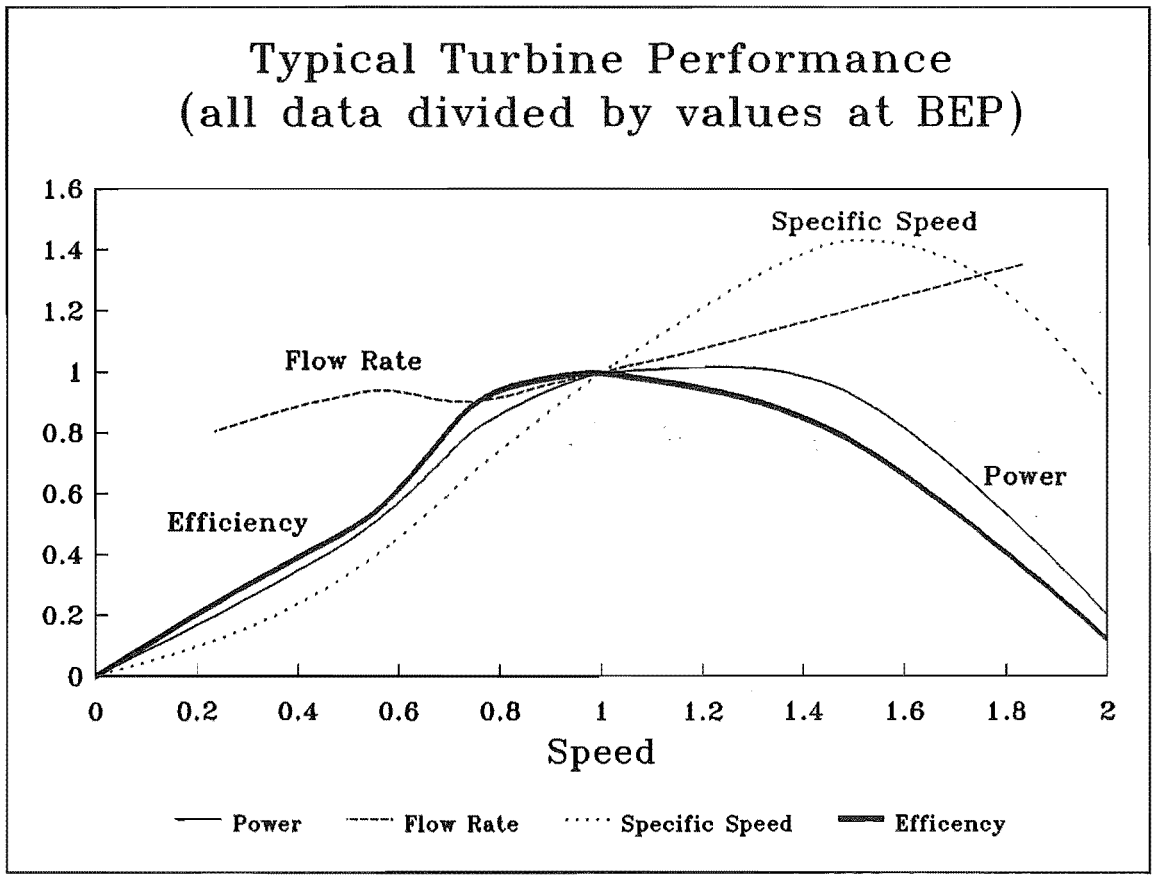

Figure 5.1 Typical Performance Curves including Specific Speed, at Constant Head

(Graphs T,W), Table II.2, Appendix II). Also it continues to rise past the best power point and is still rising at the runaway speed (where no power is produced), so it is not in fact a useful parameter. N_S reaches its maximum value at a higher speed than that

of the best power point, as shown in Figure 5.1 (typical performance, from Graph C, Appendix II). The reason for this is that above the best power point the power does not initially decrease enough to overcome the effect of the increasing speed. N_S reaches a maximum at a speed of about 1.2 times the speed at the best power point, but the drop in efficiency at this point is significant. The larger flow rate and size of the turbine would increase the overall cost, so it would normally be better to use an operating point nearer the best power point.

For the prototype designed in this project the performance goals were:

Speed: as high as possible, to reduce the cost of the speed increasing transmission. The speed should be high enough to be able to get to 3000 RPM with a single stage speed increase (4:1 to 5:1).

Power: as high as possible, up to the limits of the generator to be used, which can produce a maximum of about 4.8kW.

Flow Rate: effectively no limit on availability, but the cost of the channels, concreting, and turbine increase as the volume of water being carried increases. In this case there is an existing culvert that can carry up to about $0.5m^3/s$, which would be expensive to replace.

Head: an increase would give an improvement regardless of what performance is the most important. To get a higher head would require more extensive channels etc, and would not be cost effective.

The parameter of most interest was N_S. This was maximised with the configuration of Graph V (BA=30°, GVA=25°, CN=0). The full data for η, k_S, and N_S at the best operating points is given in Table II.2, Appendix II. There would be a further improvement in N_S with GVA=30° (Section 4.3) and with a straight cone fitted (Section 4.2).

The configuration chosen for the prototype turbine was 8 blades, with a leading edge blade angle of 30° (Figure 4.6), and a guide vane angle of 30°. The operating point that was finally chosen was at a slightly higher speed than that of the best power point.

5.2 PERFORMANCE PREDICTION AND SELECTION OF SIZE AND OPERATING POINT

5.2.1 Scaling Laws

If a prototype is to be built of a different size to that of the model, and operating under a different head, then its performance can be predicted using the scaling laws derived in Appendix I.2. The laws apply if the model and prototype are "similar". This requires that the flow patterns in each must be the same and that they are the same shape, ie, have a consistent scale ratio throughout. The size of the turbine is given by a characteristic dimension, which in this case is D, the blade tip diameter. The scaling laws can be arranged into various forms and three useful sets of equations are:

$$\frac{P_{proto}}{P_{model}} = \left(\frac{H_{proto}}{H_{model}}\right)^{5/2} \left(\frac{N_{proto}}{N_{model}}\right)^{-2} \qquad (5.1a)$$

$$\frac{Q_{proto}}{Q_{model}} = \left(\frac{H_{proto}}{H_{model}}\right)^{3/2} \left(\frac{N_{proto}}{N_{model}}\right)^{-2} \qquad (5.1b)$$

$$\frac{D_{proto}}{D_{model}} = \left(\frac{H_{proto}}{H_{model}}\right)^{1/2} \left(\frac{N_{proto}}{N_{model}}\right)^{-1} \qquad (5.1c)$$

$$\frac{P_{proto}}{P_{model}} = \left(\frac{H_{proto}}{H_{model}}\right)^{3/2} \left(\frac{D_{proto}}{D_{model}}\right)^{2} \qquad (5.2a)$$

$$\frac{N_{proto}}{N_{model}} = \left(\frac{H_{proto}}{H_{model}}\right)^{1/2} \left(\frac{D_{proto}}{D_{model}}\right)^{-1} \qquad (5.2b)$$

$$\frac{Q_{proto}}{Q_{model}} = \left(\frac{H_{proto}}{H_{model}}\right)^{1/2} \left(\frac{D_{proto}}{D_{model}}\right)^{2} \qquad (5.2c)$$

$$\frac{Q_{proto}}{Q_{model}} = \left(\frac{H_{proto}}{H_{model}}\right)^{-1} \left(\frac{P_{proto}}{P_{model}}\right) \quad (5.3a)$$

$$\frac{N_{proto}}{N_{model}} = \left(\frac{H_{proto}}{H_{model}}\right)^{5/4} \left(\frac{P_{proto}}{P_{model}}\right)^{-1/2} \quad (5.3b)$$

$$\frac{D_{proto}}{D_{model}} = \left(\frac{H_{proto}}{H_{model}}\right)^{-3/4} \left(\frac{P_{proto}}{P_{model}}\right)^{1/2} \quad (5.3c)$$

(η is theoretically constant.)

The values for the model performance are obtained from testing. Two variables can be set independently for the prototype; the other performance variables are then determined by the scaling laws. Since the flow must remain "similar" there are limits to the range over which the scaling laws apply. For instance, if the head is increased above about 5m (or 10m if the turbine hub is located low down near the outlet water level), cavitation will occur and there will be a drop in performance.

Figure 5.2 shows the turbine performance as the head and size of the turbine is changed. The performance is scaled from the model turbine performance, for the best configuration (BA=30°, GVA=30°) at its best power point, using Equations 5.2. The efficiency at this operating point was 57%. An increase in power of about 5% is expected with a straight cone fitted (Section 4.2.1). Generally as the size and head of the turbine increases there will be a small increase in efficiency, due to the increase in Reynolds number and a decrease in the relative size of manufacturing inaccuracies, clearances, and roughness.

5.2.2 **Required Power**

The maximum power that can be produced by the system was determined by the thermal limit of the generator. The generator chosen was a Markon 2 Pole Single Phase Brushless Synchronous generator, with a maximum capacity of 6kVA. A larger generator would not be cost effective because the extra power would not often be utilised. The limit is on the current, which increases when the power factor of the

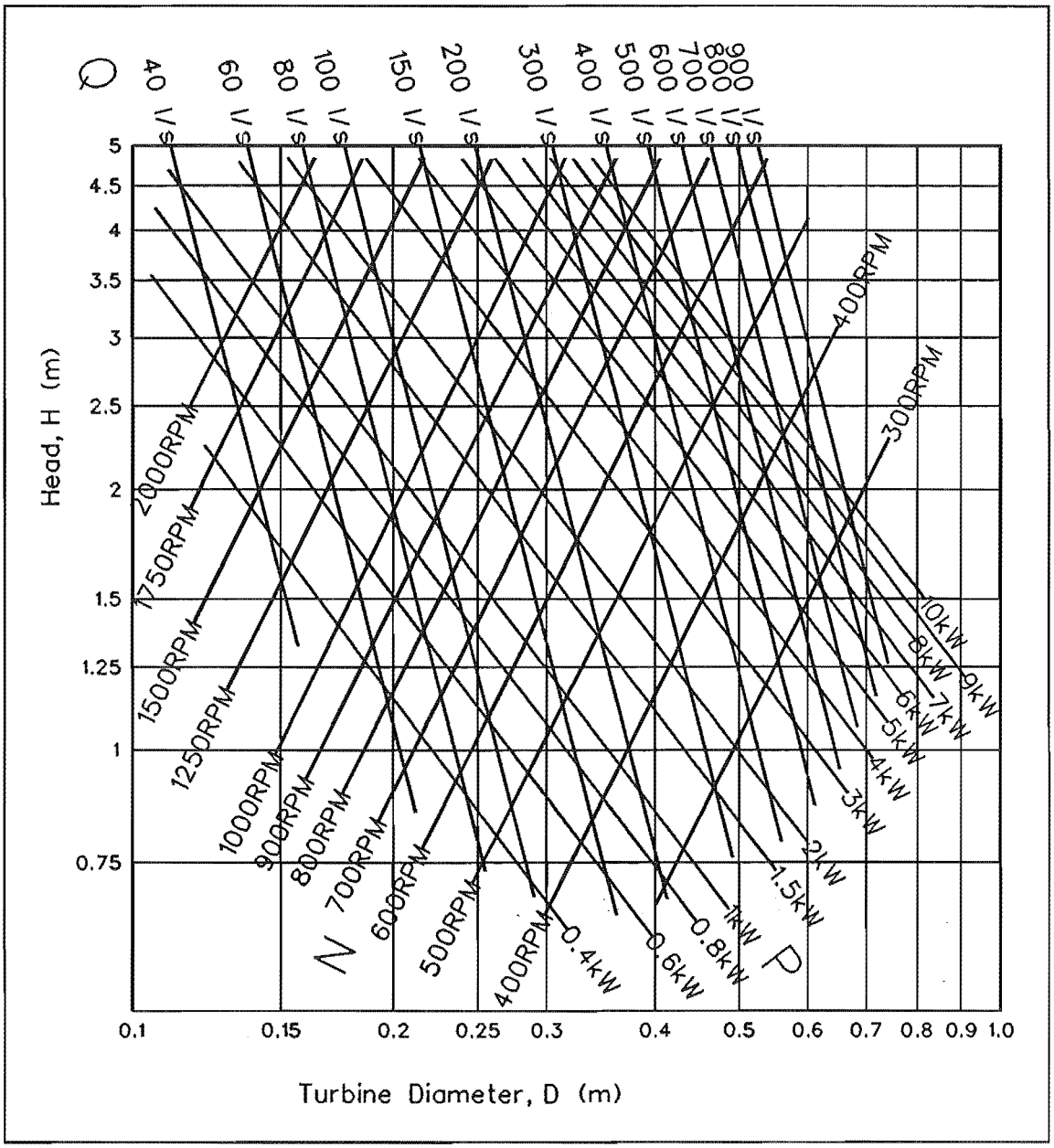

Figure 5.2 Scaled Turbine Performance at Best Power Point

system is less than unity. With a load consisting of electromagnetic motors and resistance loads, the power factor can typically drop to around 0.8. This limits the maximum power output from the generator to about 4.8kW. The generator can take larger currents for short periods of time, which could occur when large motors are started.

The manufacturer gave the efficiency of the generator as 75%, and the gearbox was expected to have an efficiency of 95%, so the maximum power that can be produced by the turbine is **4.8kW/(75%*95%) = 6.7kW.**

The model performance at best power point of P=0.58kW, N=1150 RPM, Q=57.5l/s, with H=1.8m, and D=0.172m, can be scaled to find the parameters of a turbine that will produce 6.7kW from a head of 2.7m. Using Equations 5.3a,b,c gives: **N=562 RPM, Q=0.44m^3/s,** and **D=0.43m.** Operating above the best power point will give an increase in speed and flow rate.

5.2.3 Required Speed (Final Selection)

If the speed step-up ratio is chosen, then the prototype speed is set, and if the head is known then the other parameters of the prototype can be determined. The gearbox that was finally chosen (Section 5.3.4) had a speed ratio of 4.9:1, giving a

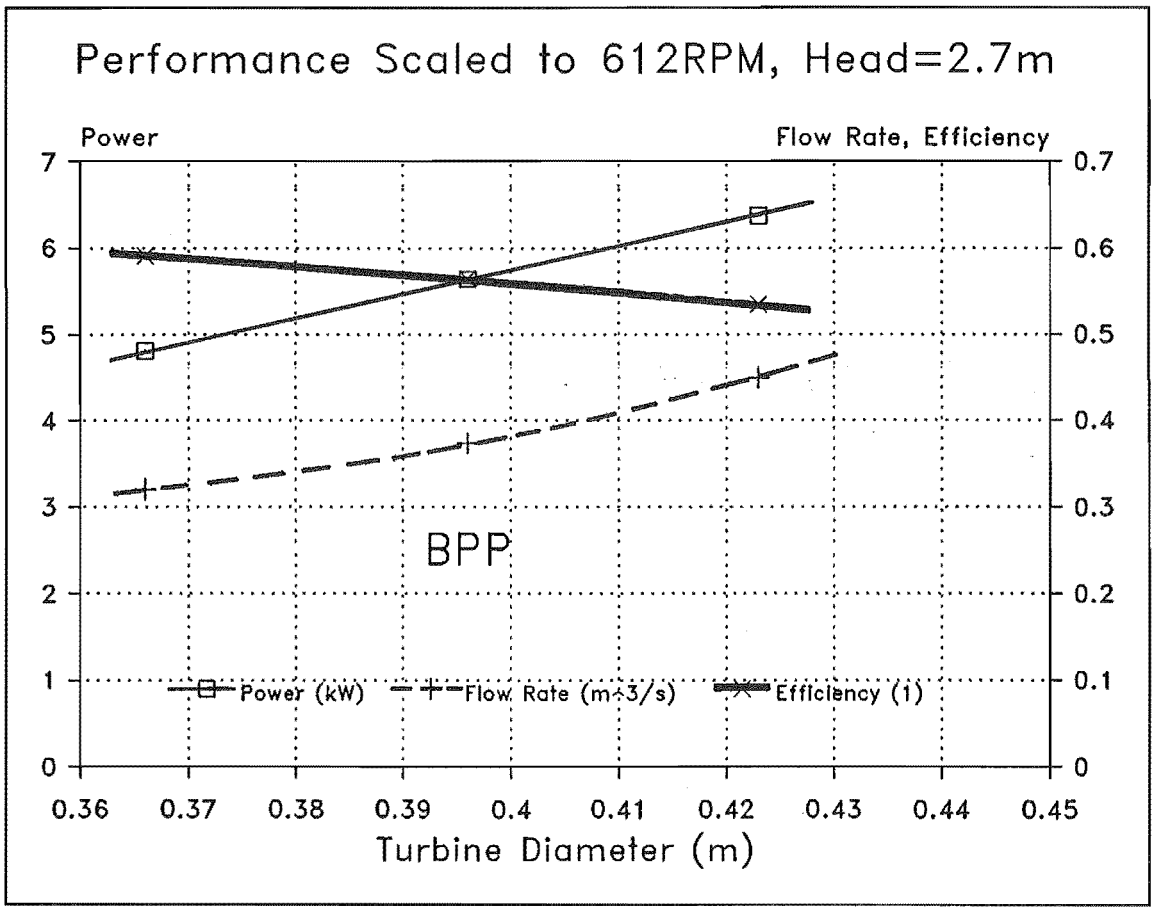

Figure 5.3 Turbine Performance at Different Operating Points, Constant Head

turbine speed of 612 RPM. Figure 5.3 shows the predicted performance at different operating points around the best power point, when scaled using Equations 5.1a,b,c to give a speed of 612 RPM and a head of 2.7m.

The turbine size chosen was D=0.410m, which gives a predicted power of 6.0kW with a flow rate of 0.41m^3/s and an efficiency of 55%. With a straight cone fitted the power would be expected to increase by 5%, giving a power of 6.4kW, and the predicted electrical power produced by the generator would then be **6.4kW*95%*75%=4.5kW.** There is some uncertainty in the model power and hence the predicted prototype power, and there may be an increase in the efficiency of the prototype, due to scale effects. Therefore the prototype power could be greater than 6kW, but if it produces slightly too much power the head could easily be reduced to give a power that would not overload the generator.

5.3 DESIGN

5.3.1 General

The scope of this Thesis includes the design of the prototype turbine, draft tube, transmission, flywheel, and brake. It does not include design of electrical controls, concrete structures, channels or other civil works, though these are briefly described for completeness.

The turbine dimensions were primarily determined by scaling from the model, having decided on a turbine dimension of D=0.410m. The scale ratio is **0.410m/0.172m = 2.38.** However in some cases the dimensions had to be changed to suit strength or manufacturing requirements. There were some other small changes made to the design, which should not affect the performance significantly.

The turbine and transmission were designed with an emphasis on avoiding complicated or critical machining. There are many parts which can not be made accurately, so provision was made for adjustment so that the correct alignment could be achieved on assembly. The prototype turbine was manufactured in a well equipped workshop, but the limitations of a less well equipped workshop (for example in a developing country) was kept in mind. Design for one-off manufacture and ease of assembly and maintenance on site were also important factors.

The turbine was made predominantly from steel. Parts exposed to the air were painted for protection after assembly. Corrosion should not be a problem for parts that stay submerged.

5.3.2 Design Calculations

Some typical calculations are described below. Calculations of bearing life, stresses, etc, are not described. Sizing of the flywheel and brake is described in Section 5.3.5.

Axial load The blades experience a force which has two components, tangential, which causes a torque on the turbine shaft, and axial, which causes an axial load on the turbine shaft. An approximate estimate of the axial force on the hub and blades is obtained by calculating the pressure difference corresponding to the total head acting on the turbine, and assuming it acts over the entire hub and blade area.

$$F_{axial} = pA = \rho gH.\pi D^2/4 = 3.6kN$$

This is an over-estimate since some of the total head is lost, and so the effective head across the turbine blades is less the total head. Taking the effective head as ηH (and assuming it also acts across the hub) gives

$$F_{axial} = pA = \eta\rho gH.\pi D^2/4 = 2.0kN$$

This is an under-estimate because some of the losses causing a drop in the power output do not reduce the effective head across the blades or the hub. The axial load on the blades can also be calculated using the torque, which gives the other component of the total force perpendicular to the blade surface. This gives a similar result to that obtained using ηH as the effective head. For the design of components, bearing life etc, an axial load of 2.7kN was used.

Blade thickness This is not determined simply by scaling the thickness of the model blades, since the bending moment at the blade root is not just a function of the size of the turbine. The force on each blade is proportional to the total head, H, and the area of the blade, which is proportional to D^2. The distance of the force from the root of the blade is proportional to the size of the turbine, D. Therefore the bending moment is proportional to HD^3. The strength of the blade in bending is proportional to the allowable stress in the blade root, the length of the blade, and the thickness squared. From these relationships the thickness of blades (t) can be scaled by the relationship $t \propto DH^{½}$, to give the same stress level in the blade root as in the model blades, which showed no signs of bending. An extra allowance for safety was made, giving a blade thickness of 3mm.

5.3.3 Steadying Bearing, Cone, and Draft Tube

The axial load on the turbine blades is supported by the main bearing at the top of the turbine shaft, which is above water. A steadying bearing is required to position the hub accurately in the turbine tube. This bearing must be submerged unless a cantilever arrangement is used with the steadying bearing located just above the water level. On the model the steadying bearing was located above the hub on the top plate to which the guide vanes are attached (Figure 2.6). When designing the prototype it was decided to mount the steadying bearing below the hub, supported by four fins in the turbine tube (Appendix III). The bearing used was a "Thordon" water lubricated plain bearing, mounted in the bottom of the turbine shaft. It runs on a stainless steel shaft attached to the four fins.

The fins may improve the efficiency slightly by straightening the flow as it leaves the hub. They also allow a cone to be mounted in the turbine tube, which would be stationary, compared with the cones on the model which rotated with the hub. This should reduce the small loss due to skin friction on the hub (Section 4.2.2).

The draft tube was made from available cones, to reduce the cost. The outlet diameter was less than it should be if scaled from the model dimension (0.620m instead of 0.834m). This would cause a drop in efficiency of 2% because of the increased velocity head at the outlet, though the more gradual expansion may partly offset this loss.

5.3.4 Speed Increase

A speed increase of about 4:1 to 5:1 was required to drive the generator at 3000 RPM. If a 4-pole generator running at 1500 RPM was used then half the speed increase would be required. However four times the flywheel inertia would be required and the generator would be more expensive. Either V-belts or a gearbox could be used for the speed increase. A right angle change in direction is required, since the turbine shaft is vertical and the flywheel shaft should preferably be horizontal for ease of assembly and for a better load direction on the flywheel bearings.

A V-belt transmission was sized, to show its feasibility. It requires two stages, since the quarter turn drive can not incorporate a large enough speed ratio. The minimum centre distance for the quarter turn drive is given by $C=5.5(D+W)$ where

D is the pitch diameter of the larger pulley and W is the total width of the belt or belts (DAYCO, 1981). To minimise the centre distance the quarter turn drive is put after the speed increase, so that the torque transmitted is less and hence smaller pulleys can be used. To transmit the power at 3000 RPM two V-belts with pulleys with a pitch diameter of 117mm are required. This gives a minimum centre distance of about 820mm. The speed increase requires two V-belts on pulleys with pitch diameters of 483mm and 93mm. The minimum centre distance is about 400mm.

The main advantage of a V-belt drive is that it is cheap. However it would take up extra room, and would require adjustment and periodic replacement of the belts.

A suitable gearbox was found with a speed ratio of 4.9:1. It is usually used for speed reduction, but can be used in reverse. A gearbox with a worm gear would not be able to be reversed. The advantages of a gearbox are its compactness and the simplicity of the overall design. It is however more expensive and may require periodic replacement of bearings.

5.3.5 Flywheel and Brake

Two requirements of the design are that the system have sufficient inertia to prevent any instability of the electronic speed governor, and that there be a brake to ensure the turbine and generator can not over-speed if the load is lost. These requirements can be simply achieved with a combined flywheel and disk brake.

The frequency sensing electronic governor controls the generator speed by changing the dump load in steps of $^1/_{15}$ of the total power produced. The step-wise control is smoothed by mechanical inertia in the system. A large inertia also increases the stability of the system when large loads are switched on or off by the user. When electric motors are started there can be a temporary load in excess of the rated capacity of the generator, which the generator can tolerate, provided that there is sufficient inertia to ensure that it does not slow down significantly. The manufacturer of the electronic governor that was used, Delphi Industries, recommends a flywheel inertia given by

$$J = 0.02\ P\ (3000/N)^2$$

where J is the polar moment of inertia in kgm^2, P is the generator rating in kW or kVA, and N is the flywheel speed in RPM. For P=6kW and N=3000 RPM, $J=0.12kgm^2$. However from experience it has been found that a larger inertia is beneficial for better stability when switching large loads (Giddens, 1991). The size chosen for the flywheel was a diameter of 470mm and a thickness of 12mm. This gave $J=0.46kgm^2$. During manufacture it was found that the disk had been distorted enough during cutting to cause noticeable dynamic imbalance. It was machined down to a thickness of 10.9mm, giving $J=0.42kgm^2$, which is 3.5 times the recommended inertia.

A calliper brake operates on the flywheel disk and is held open in normal operation by a solenoid. The brake is operated by a spring. If the electronic governor senses that the speed is outside set limits it will deactivate the solenoid allowing the brake to operate. The system is fail safe since if power is lost to the governor the solenoid also loses its power and the brake operates.

The brake must overcome the maximum torque produced by the turbine and provide sufficient torque to decelerate the flywheel. The total inertia of the high speed shafts was approximately $0.5kgm^2$. For a stopping time of 3 seconds the rate of deceleration is 100 rad/s^2, which requires a torque of 50Nm. The torque produced by the turbine at its normal operating speed is 100Nm. It increases at lower speeds to a maximum of about 140Nm (Section 4.1.5). This torque is reduced by the gearbox speed ratio to 30Nm, giving a total torque the brake must provide of 80Nm.

5.3.6 Submergence and Overflow

To minimise the length of the turbine shaft and tripod support structure the hub should be located as high as possible. The limit is the critical submergence of the intake to the turbine, required to avoid vortex generation and air entrainment. The required depth was estimated from the model, with no inlet vortex generation observed with an inlet submergence of 0.2m. The critical submergence is mainly a function of the inlet velocity head (Knauss, 1987), which from the scaling laws (Appendix I.2) is proportional to the total head on the turbine, H. Therefore the required depth of submergence is given by **0.2m(2.7m/1.8m) = 0.3m.**

The generator and flywheel must be located sufficiently high above the normal water level to allow for the rise in water level when the turbine is stopped or if the up stream control gate is accidentally opened too much. At normal operating conditions a small amount of water goes over a spillway, so that the correct inlet water level is maintained. When excess water goes over the spillway the water level will rise.

5.3.7 Debris Protection

The turbine can run with a small amount of sand and silt in the water, since there are no fine running gaps. The water lubricated bearing is tolerant of some abrasive material but should be kept as free of it as possible, to ensure a long life. The water flowing through the bearing is sucked through from a hole in the turbine shaft, above the hub and the top plate of the inlet and guide vane structure. It is covered with a fine mesh screen.

Larger debris such as leaves, grass etc, can catch on the blades and reduce the efficiency; on the model leaves were observed to remain caught on the blades for an indefinite length of time. A mesh screen surrounds the turbine inlet to stop larger debris from entering the turbine. This may need cleaning occasionally. The intake channels incorporate settling ponds so there would be minimal amounts of sand and silt in the flow.

5.3.8 Low Flow

For the site where the prototype is to be installed, insufficient flow rate is not expected to be a problem since only a small part of the river's normal minimum flow is diverted to the turbine. However low flow can often be a problem at sites with less flow available, since there is usually an annual variation. This means that the turbine must either be designed to use only the minimum flow rate, or it may not be able to operate throughout the year.

Often there will only be short periods of insufficient flow, and ideally the turbine should still be able to produce a small amount of power, to supply essentials such as a few lights. Higher head turbines with long supply pipelines and air removing valves can operate under low flow conditions as the pipeline only partially fills with water, giving a reduced head and hence reduced flow rate.

However the propeller turbine is not so well suited as low flow will cause substantial air entrainment with shock loads on the hub and rapidly varying torque. If an easily changeable speed ratio could be incorporated in the drive, for instance with two pulley sizes on a V-belt drive, then the turbine speed could be moved to the best efficiency point instead of the best power point, with a drop in flow of approximately 15% (Section 4.1.2). Another alternative would be to raise the outlet water level with a variable height weir, to give a reduced head and hence reduced flow rate. There is a large decrease in power due to the reduced flow rate and also a decrease in the efficiency, as the operating point moves towards the runaway speed (if the running speed remains the same as the head is reduced).

5.3.9 Civil Works

A map of the installation site is shown in Figure 5.4. It is situated at the top end of a large established shingle fan. The intake from the river leads directly to a settling pond. There is a multiple gate and weir system which ensure that the correct flow reaches the turbine, with little variation as the river level changes. The excess water is diverted back to the river. The water from the turbine is discharged into an old stream bed which leads it back into the main river.

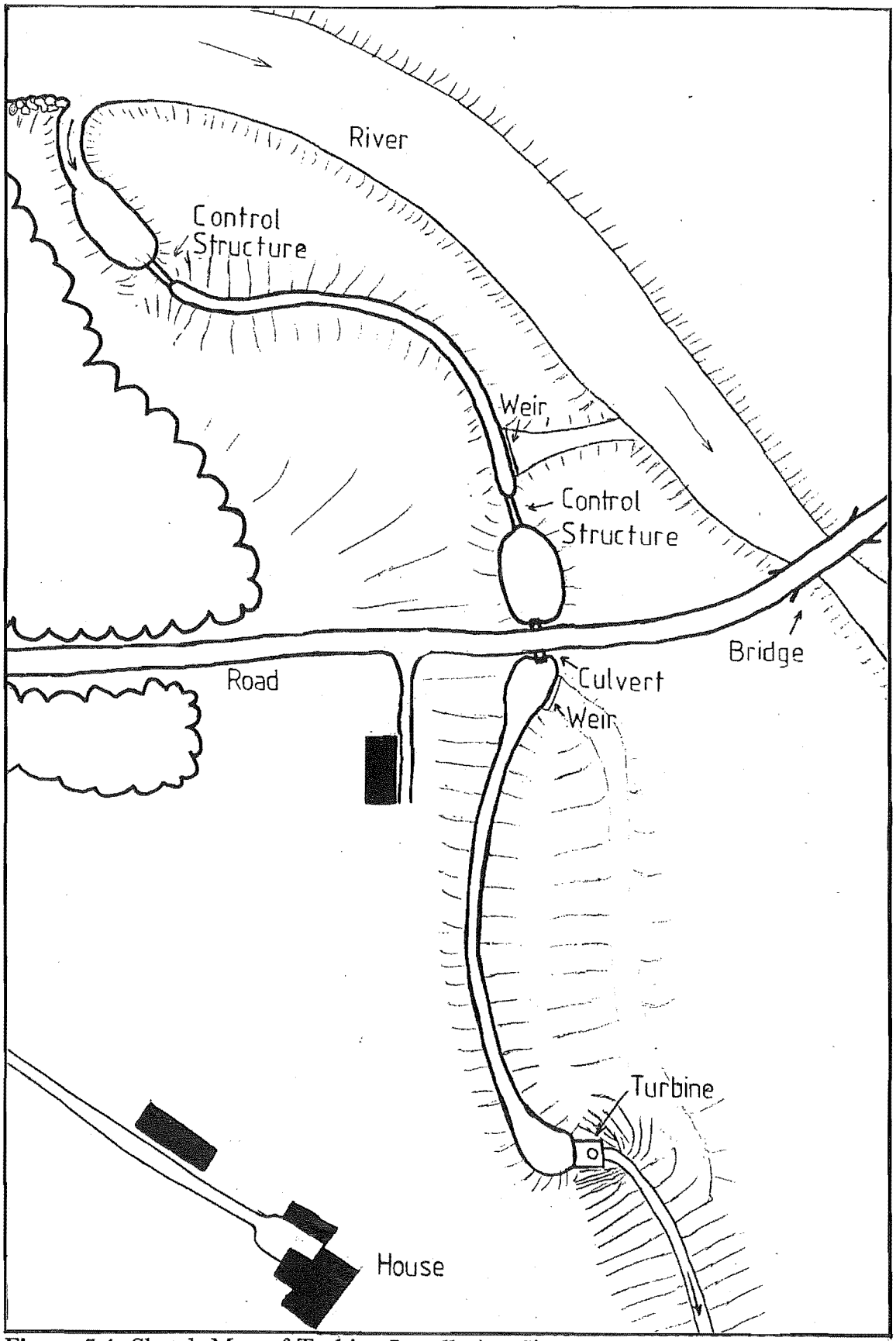

Figure 5.4 Sketch Map of Turbine Installation Site

CHAPTER 6

CONCLUSIONS

A model propeller turbine has been tested to find a design that gave good performance but was not complicated to manufacture. Various configurations of blades, guide vanes, and cones were tested to find the optimum design. Because of the simplified design, particularly the use of flat blades, the flow was complicated, and could not be predicted accurately by theory. Hence flow visualisation was important in determining the reasons for poor performance in the configurations first tested. From the measured performance and flow visualisation, better configurations were designed, until a suitable configuration was found. This configuration was used to design the full size prototype turbine.

6.1 PERFORMANCE

From the model testing the best blade configuration was found to be 8 metal blades, with a blade angle of 30° from tangential (Figure 4.6). The optimum guide vane angle was about 30° from the radial direction (Figure 4.3).

The best efficiency of the model was measured as 62% with no down stream cone on the hub. The efficiency at the best power point was 57%. With a straight sided ("straight") cone the best efficiency would be about 63%. There is some uncertainty in the measured power and hence in the efficiency (Sections 3.4, 3.5), and there may be some increase in the efficiency of the prototype due to scaling effects (Section 5.2.1) and use of a fixed cone rather than one revolving with the hub (Section 5.3.3).

The prototype turbine has been designed to run at 612 RPM, and has a predicted power of 6.0kW (4.3kW produced by the generator) from a flow rate of $0.41 m^3/s$ and a head of 2.7m. This gives a specific speed of N_S=433 RPM (kW,m) or 502 RPM (hp,m). The operating point is at a slightly higher speed than that of the best power point, and hence the efficiency is reduced to 55%. The overall efficiency of the turbine and generator unit is predicted to be 40%. The design would be

suitable for a wide range of heads and flow rates, with predicted performance as given in Figure 5.2. The main constraint is in the head, since cavitation would be expected to occur with heads above 5m to 10m, depending on the height of the blades above the outlet water level (Appendix II.1).

6.2 MAJOR CAUSES OF LOSS

When operating near the best operating points, the major losses occurred at the expansion in flow area at the end of the hub, and at the blades, which because of being flat had a large angle of attack at the hub.

In order to get as high a running speed as possible the fluid velocity past the blades must be large. This is because of the direct effect on the blade velocity, and also because a higher fluid velocity means a smaller turbine diameter for the same flow rate, and hence the same power, which gives a further increase in rotational speed. The high fluid velocity means that the losses due to turbulence, which are proportional to the velocity head, $V^2/2g$, will be large. The velocity head at the outlet from the blades is about 60% of the total head. Hence it is important to recover a large proportion of the velocity head as pressure, by slowing the flow with a minimum of turbulence.

The most significant reduction in velocity head (⅔ of the total reduction, Section 2.3.3) occurs between the hub and the inlet to the draft tube, as the flow area increases from the blade annulus area $\frac{1}{4}\pi D^2(1-F^2)$ to the full turbine tube area $\frac{1}{4}\pi D^2$. A cone on the end of the hub was expected to improve the recovery of velocity head (and hence give a better efficiency), but it was found that while the "straight" cone made a small improvement the carefully shaped "radius" cone made no improvement. However the performance with no cone was still good, since reasonable recovery of the velocity head occurred in the straight section of turbine tube after the end of the hub.

Further recovery of velocity head occurs in the draft tube. It is possible to get good recovery with a gradually enlarging conical draft tube, provided that the flow entering the draft tube is reasonably uniform and non-turbulent (Gubin, 1973). Hence it is important that the straight section of turbine tube after the hub is long enough for

the flow to become reasonably uniform. The length of the straight section from the end of the hub to the beginning of the draft tube was 1.3D on the model (D is the turbine blade tip diameter), which is considered to be a minimum, as it was observed that the full velocity flow had not completely filled the centre of the tube on entry to the draft tube, ie, a small central area of wake still existed (Section 4.2.2). For the prototype the length of the straight section was increased to 1.7D, which may improve the velocity head recovery and hence slightly increase the efficiency.

Recovery of the velocity head is an important factor in the efficiency of the turbine. There is potential for improved efficiency with a better design of cone and draft tube. An alternative arrangement, to avoid the problem of the large expansion in flow area after the hub, would be to have a non-revolving continuation of the hub extending into the draft tube, with the draft tube beginning immediately after the blades.

The diameter of the hub is an important compromise. A large hub reduces the losses due to the miss-match of the blade angle (ie, the large angle of attack - beyond the angle of stall), but increases the losses as the flow slows down to fill the whole turbine tube area after the hub. Hence there will be an optimum hub diameter for best efficiency. The power (or the speed if the turbine is scaled to keep the power the same) is increased with the larger flow rate obtained with a smaller hub. There is expected to be an overall decrease in the efficiency with small hub diameters so there would be an optimum hub diameter to give maximum power, which would be smaller than the optimum for efficiency.

The best compromise for F depends on what parameters (particularly efficiency or running speed) are the most important in a particular situation. The effect of varying the hub diameter ratio was not tested but the value used for the prototype ($F=0.66$) is thought to be a reasonable compromise.

6.3 MANUFACTURE

The purpose of the project was to design a turbine that was appropriate for manufacture in a small workshop on a one-off basis. The prototype turbine (including transmission, flywheel, etc.) was built using a mill, lathe, rolling machine, and welding equipment plus various hand tools. The only difficulty experienced was with distortion of the top plate when welding the guide vanes to it, which could be rectified with different detail design. The blades in particular were easy to cut out, weld, and machine to give an accurate outer diameter. A lathe of sufficient capacity was needed to machine the blades and the flywheel disk, but this could be avoided if the blade tips were finished with a grinder, and the flywheel disk was cut out without it becoming distorted. The other requirement for machinery that may not always be available was in making the turbine tube, which was rolled from 5mm steel plate. The accuracy is important to give a small gap between the blade tips and the turbine tube; the variation of the inside radius of the tube was about 0.5mm, which is more than adequately accurate. Use of available pipe (steel, plastic, or possibly concrete) would make the manufacture simpler.

6.4 COMPARISON WITH OTHER TURBINES

The helical bladed turbine tested by Rao (1988) is similar in design to the flat bladed turbine, apart from the blade shape. The efficiency for the helical bladed turbine is given as 67%. It produces 5kW from a head of 5m, but the running speed is not given. For the flat bladed turbine the best efficiency was 62% without a cone. Apart from this improvement in efficiency, there is a further advantage of helical blades, since they allow a smaller hub to be used. This means for the same size of turbine, the flow rate and hence power increases, or for the same power the required size is less, giving a greater speed. The hub diameter ratio F for the helical bladed turbine was 0.42 compared with 0.66 for the flat bladed turbine.

Even though there is a decrease in efficiency and speed with flat blades, the simplification in manufacture may make them preferable when there is limited money or facilities for manufacture.

The turbine described by Susanto (1983) was expected to produce 2.5kW (using an assumed efficiency of 86%) from a head of 2.0m and a flow rate of $0.15m^3/s$, and run at 1000 RPM. This gives a specific speed of $N_S=665$ RPM (kW,m), compared with 433 RPM (kW,m) for the flat bladed turbine. A "similar" turbine (ie, scaled using the scaling laws in Appendix I.2) to produce 6.0kW from a head of 2.7m would have a size D=247mm, a speed N=940 RPM, and a flow rate $Q=0.27m^3/s$. This is significantly better than the flat bladed turbine, which runs at 612 RPM and has a flow rate of $0.41m^3/s$, for the same power.

There are two reasons for the better performance of Susanto's turbine. Firstly the hub to tip diameter ratio (F) is smaller (0.44 compared with 0.66), so that the speed is greater. Secondly the efficiency is much higher. However this assumed efficiency of 86% is optimistic; the turbine has moulded blades, which would be expected to give a better efficiency than flat ones, but it also has an abruptly ended hub, and immediately after the hub there is a right-angle bend leading into the draft tube. It is likely that turbulence due to the enlargement in area after the hub combined with the right-angle bend, will cause extra losses that do not occur in the flat bladed turbine, and that the non-uniform flow will reduce the performance of the draft tube. Hence an efficiency of say 70% might be more reasonable, which would give a

turbine power of 2.1kW, N_S=603 RPM (kW,m), and a turbine scaled to give 6.0kW from a head of 2.7m would have N=850 RPM, Q=0.32m^3/s, and D=0.27m. Although the performance figures given by Susanto have not been confirmed by testing, they show the potential improvement with specially shaped blades.

6.5 FURTHER WORK

During the project a number of areas were noted where further development would be worthwhile. There is no limit to the number of variations that could be made to try to improve the performance of the turbine, since the design is simplified, but most of these variations would involve greater complexity of manufacture or would not give significant improvement. Some simple modifications that are thought likely to give improved performance are described below.

6.5.1 **Hub Size**

The hub diameter is an important compromise when using flat blades. The power and speed is expected to increase with a smaller hub (relative to the turbine diameter, D), and the efficiency to decrease (Section 6.2). The optimum hub diameter will depend on the specific requirements of each application. The effect of the hub diameter could be determined by further testing.

6.5.2 **Cone and Draft Tube**

Various configurations of cone attached to the revolving hub were tested, including no cone. Another alternative is to have a stationary cone fixed in the turbine tube. The optimum length and shape for this type of cone is not known.

Since the recovery of velocity head as pressure in the straight section of turbine tube after the hub is important to the turbine performance, there would be an optimum length for the straight section. This length must be designed in conjunction with the draft tube, for which the effect of length and divergence angle is better understood (Gubin 1973).

6.5.3 Blades

Further testing could be done to confirm the optimum blade angle. It is possible that more blades would control the flow better, but this would also decrease the flow area. The length could also be optimised. There may be simple ways to bend the blades to get better matching of the flow angle at the hub, however an attempt at this was made which gave no improvement in performance (Graph Y, Appendix II).

6.5.4 Inlet and Guide Vanes

If as a simplification it was decided to not use guide vanes, then the toroid section and inlet used for the model and prototype would not be needed, which would give further simplifications in the design. The effect of using flat guide vanes in an axial configuration (Section 2.2.2) could be studied.

6.5.5 Other Alternatives

Use of standard boat propellers has been mentioned in various literature, but there is little information on performance, etc. This may be a suitable solution, but would depend on what is available in different countries.

The Deriaz (diagonal flow) turbine may be suitable for simplified manufacture as it avoids the problem of the cone, and appears to have nearly flat blades, but it does not have such a high specific speed as the propeller turbine (Davis and Sorensen, 1969).

REFERENCES

Blakely, R.J. (1981) *Present and potential use of micro-hydro-electric schemes in remote locations.* New Zealand Energy Research and Development Committee, Report number 68.

Chapman, G.C. (1986) *Water wheel or turbine?.* Newsletter of the National Association of Water Power Users, Great Britain.

Davis, C.V. and Sorensen, K.E. (1969) *Handbook of applied hydraulics.* McGraw-Hill Book Company, USA. 3rd Ed.

DAYCO (1981) *Dayco engineering guide for V-belt drives.* Dayco Corp., USA.

Giddens, E.P. (1991) Pers. Comm.

Gubin, M.F. (1973) *Draft tubes of hydro-electric stations.* (trans. from Russian). Amerind Publishing Co. Pvt. Ltd., India.

Inversin, A.R. (1987) *Micro-hydropower sourcebook.* NRECA International Foundation, 1800 Massachusetts Avenue, N.W. Washington, DC 20036.

Knauss, J. (1987) *Swirling flow problems at intakes.* Hydraulic structures design manual 1. International Association for Hydraulic Research.

Monition, L. (1984) (and Le Nir, M., Roux, J.) *Micro hydroelectric power stations.* (trans. from French). John Wiley and Sons inc., Great Britain.

Nechleba, M. and Kopecky, V. (1986) *Mini and micro hydro in Czechoslovakia.* International Water Power and Dam Construction, Vol 38 n4.

Rao, G.J. (1988) (and Prasad, R., Kulkani, B.S.) *Simplified turbine runner shows good cavitation resistance.* International Water Power and Dam Construction, Vol 40 n8.

Stepanoff, A.J. (1957) *Centrifugal and axial flow pumps.* John Wiley and Sons inc., USA. 2nd Ed.

Susanto, D. (1983) *Micro-hydro axial flow turbine for a battery charging system in remote areas.* Small hydro power for Asian rural development. (Workshop on small-scale hydro-power technology applications in Asian rural settings, Bangkok, 1981). National Rural Electric Cooperative Association.

VITA (1985) *Small Mitchell (Banki) turbine: a construction manual.* Volunteers In Technical Assistance, 1815 North Lynn Street, Suite 200, Arlington, Virginia 22209, USA. (reprint).

Ward-Smith, A.J. (1980) *Internal fluid flow.* Clarendon Press, Oxford / Oxford University Press, New York.

APPENDIX I

BACKGROUND THEORY

I.1 CAVITATION

The blades in a propeller turbine act as wings; the force on each blade is developed by a pressure differential across the blade. The fluid on the lower side of the blade is at a lower pressure than the surrounding fluid, by an amount proportional to the net pressure change through the blades, ie, the net head. The surrounding fluid, at the downstream side of the blades, is below atmospheric pressure due to the effect of the draft tube. If the local pressure drops below the vapour pressure of the fluid, then bubbles of vapour will form. As soon as the pressure increases the bubbles will collapse causing shock waves, and there will be damage to the turbine and a drop in performance.

The drop in pressure head at the blades is taken as proportional to the net head across the blades, which is proportional to the gross head, H, for any particular turbine, so it equals σH (σ has a different value for different turbines). The local absolute pressure head is given by

$$H_{atm} - H_{suc} - \sigma H$$

where: H_{atm} is the atmospheric pressure head,

H_{suc} is the suction head caused by the draft tube.

Cavitation will start to occur when the local pressure is equal to the vapour pressure head of the fluid, H_{vap}, ie, when

$$H_{atm} - H_{suc} - \sigma H = H_{vap} \qquad (I.1)$$

By rearranging Equation I.1, σ can be calculated for a particular turbine at any operating conditions.

$$\sigma = \frac{H_{atm} - H_{suc} - H_{vap}}{H} \qquad (I.2)$$

The value of σ at the operating conditions at which cavitation just starts to occur is taken as $\sigma_{critical}$; if the σ values at other operating conditions are greater than $\sigma_{critical}$ then cavitation will not occur. σ is usually calculated using a suction head, H_{suc}, equal to the elevation of the turbine blades above the exit water level, ie, not taking into account the drop in pressure due to velocity head recovery in the draft tube. This alters the values of σ but they can still be used for comparison if they are calculated consistently. This form of σ is known as Thoma's cavitation parameter.

The $\sigma_{critical}$ values for various turbines has been measured and tabulated, and has been found to be mainly a function of specific speed (N_S). The values for propeller turbines range from about 0.2 to 3.5, increasing as the specific speed increases. Davis and Sorensen (1969) give a graph of $\sigma_{critical}$ against N_S. The approximate specific speed for the turbine being designed, using initial estimates of P=6kW=8hp, H=2.7m=8.9ft, N=750 RPM, is $\mathbf{N_S = 140\ RPM\ (hp,ft)}$. The $\sigma_{critical}$ value corresponding to this is 1.0.

σ for the turbine was estimated using H=2.7m, H_{atm}=10.0m, H_{vap}=0.1m, and H_{suc}=2.5m, which gives σ=2.7. This is greater than $\sigma_{critical}$ so cavitation should not occur. If the turbine blades are near the inlet water level then H_{suc} approaches H. (For a syphon configuration H_{suc} can be greater than H). Taking $\mathbf{H_{suc} = H}$ and neglecting H_{vap} gives

$$\sigma \approx \frac{H_{baro} - H}{H} \qquad (I.3)$$

For $\mathbf{\sigma_{critical} = 1.0}$ cavitation will become a problem when H is about half of H_{atm}, ie, **H≈5m**. If the turbine blades are located near the bottom of the turbine, ie, at about the exit water level, then H_{suc} approaches zero. Equation I.2 then becomes

$$\sigma \approx \frac{H_{atm}}{H} \qquad (I.4)$$

For $\mathbf{\sigma_{critical} = 1.0}$ cavitation will start to be a problem when H approaches H_{atm}, ie, when **H≈10m**.

From the predicted performance of the prototype turbine, ie, P=6.0kW, H=2.7m, and N=612 RPM, a better estimate of N_S can be obtained. This value is

$N_S = 120$ RPM (hp,ft) for which the $\sigma_{critical}$ value indicated by Davis and Sorensen is 0.75. This means that the limits on the head H given above are conservative. As a comparison the helical bladed turbine tested by Rao (1988) had $\sigma_{critical} \approx 0.8$, however the specific speed is not given.

I.2 MODELLING: SCALING LAWS AND SPECIFIC SPEED

If a model and prototype are "similar", ie, their shape is the same (at a different scale) and the flow patterns (streamlines) are the same throughout, then they will have the same efficiency at any particular operating point. The scale ratio of the size of the turbines is determined using a typical dimension, which for turbines is usually the blade tip diameter (D). To get "similar" flow Reynold's number (Re) should be equal for the model and prototype. However it is generally accepted that for turbulent flow (ie, large Re) the flows will be sufficiently similar even if Re is not equal.

$$Re = \rho VD/\mu \qquad (I.5)$$

As well as changing the size of the prototype, the head can also be changed. For the prototype to be at the same operating point as the model, the axial velocity of the flow must remain in proportion to the tangential velocity of the blades. This gives the same flow angles relative to the blades and hence the same flow patterns, so that similarity is maintained. For the efficiency to be the same, the total losses through the turbine must vary in proportion to the head, H. For turbulent flow the losses are proportional to the velocity head, Hv, for any particular flow situation.

$$Hv = V^2/2g$$

therefore $H_{loss} \propto Hv \propto V^2$

and since we require $H \propto H_{loss}$

then $H \propto V^2$

or $V \propto H^{1/2}$ (I.6)

This must hold when scaling (known) model conditions to prototype (predicted)

conditions. Equation I.6 is equivalent to $$\frac{V_{proto}}{V_{model}} = \left(\frac{H_{proto}}{H_{model}}\right)^{1/2}$$

At any particular cross section through the turbine the flow rate Q is a product of the velocity and the area. Since the area when scaling is proportional to the square of the size of the turbine (as represented by D), then

$$Q \propto VA \propto VD^2$$

substituting for V using Equation I.6 gives $$Q \propto H^{1/2}D^2 \qquad (I.7)$$

The rotational speed of the turbine (N) is proportional to the tangential velocity of the blades (V_{blades}), divided by the radius. The radius is proportional to the diameter D, so $$N \propto V_{blades}D^{-1}$$

V_{blades} is proportional to the axial flow velocity V, since the flow angles must stay the same, so $$N \propto VD^{-1}$$

substituting for V using Equation I.6 gives $$N \propto H^{1/2}D^{-1} \qquad (I.8)$$

The power (P) is proportional to the head (H) and the flow rate (Q), so

$$P \propto HQ$$

substituting for Q using Equation I.7 gives $$P \propto H^{3/2}D^2 \qquad (I.9)$$

The three Equations I.7, I.8, and I.9 can be written in equivalent form as

$$\frac{Q_{proto}}{Q_{model}} = \left(\frac{H_{proto}}{H_{model}}\right)^{1/2} \left(\frac{D_{proto}}{D_{model}}\right)^2 \qquad (I.10a)$$

$$\frac{N_{proto}}{N_{model}} = \left(\frac{H_{proto}}{H_{model}}\right)^{1/2} \left(\frac{D_{proto}}{D_{model}}\right)^{-1} \qquad (I.10b)$$

$$\frac{P_{proto}}{P_{model}} = \left(\frac{H_{proto}}{H_{model}}\right)^{3/2} \left(\frac{D_{proto}}{D_{model}}\right)^2 \qquad (I.10c)$$

They can be used to predict the performance of a prototype from the performance of the model, given the prototype's size, D_{proto}, and head, H_{proto}. The prediction is for performance at the same operating point. The equations are only valid if the model and prototype are "similar", so for example if the prototype head is increased enough for cavitation to occur, the performance will be different from what was predicted. The efficiency theoretically stays constant, but in fact tends to increase slightly as Re increases. Also as the turbine size increases the relative size of manufacturing inaccuracies, roughness, etc, gets smaller, giving a small increase in efficiency.

The three Equations I.10a,b,c can be rearranged to allow prediction of the prototype performance once any two variables are set. The indices of all the combinations of equations are given in Table I.1. The Equations I.10a,b,c are represented in the first column.

	H,D	H,Q	H,N	P,H	P,N	P,D	P,Q	N,D	N,Q	Q,D
D		$-1/2, 1/2$	$1/2, -1$	$1/2, -3/4$	$1/5, -3/5$		$3/2, 2$		$-1/3, 1/3$	
H					$2/5, 4/5$	$-3/2, -3$	1,-1	2,2	$4/3, 2/3$	2,-4
Q	$1/2, 2$		$3/2, -2$	1,-1	$3/5, -4/5$	$-3/4, 1/2$		1,3		
N	$1/2, -1$	$3/4, -1/2$		$-1/2, 5/4$		$1/3, -5/3$	$3/4, -5/4$			1,-3
P	$3/2, 2$	1,1	$5/2, -2$					3,5	$4/3, 5/3$	$-4/3, 2/3$

Table I.1 Indices for Scaling Equations

As an example the equation to predict the ratio of operating speeds between the model and prototype in terms of ratios of the power produced and the head is represented in the fourth column:

$$\frac{N_{proto}}{N_{model}} = \left(\frac{P_{proto}}{P_{model}}\right)^{-1/2}\left(\frac{H_{proto}}{H_{model}}\right)^{5/4}$$

The speed of a "prototype" at standard conditions is known as the specific speed, N_S.

$$\frac{N_S}{N_{model}} = \left(\frac{P_S}{P_{model}}\right)^{-1/2}\left(\frac{H_S}{H_{model}}\right)^{5/4}$$

Common values for the "standard" conditions are P_S = 1hp (metric) and H_S = 1m. If the "model" is any turbine for which the specific speed is required,

then

$$\frac{N_S}{N_{model}} = \left(\frac{P_{model}}{1hp}\right)^{1/2}\left(\frac{H_{model}}{1m}\right)^{-5/4}$$

or

$$N_S = N\, P^{1/2} H^{-5/4} \qquad (I.11)$$

This is the normal equation for the specific speed. The value of N_S depends on what standard conditions are being used, ie, it depends on the units of P and H, and so is not fully non-dimensional. Other commonly used units are imperial (hp,ft), and metric (kW,m). Alternatives to N_S are discussed in Section 5.1.

APPENDIX II

DATA FROM MODEL TESTS

The complete data obtained for each turbine configuration tested is given in Graphs A-Z. The data has been scaled to a constant head of 1.8m, as each individual reading had a slightly varying head, from about 1.7m to 1.9m. The scaling laws are described in Appendix I.

There are occasionally readings that do not fit a smooth curve. When these were noticed during a test a repeat reading was taken. It was assumed that since the graphs usually had smooth curves, any irregular data was due to errors in the measurements, rather than any unusual turbine performance.

The performance of the different configurations is summarised in Table II.1, which gives the performance at the Best Efficiency Point and Best Power Point. Because the power curve is flat at its maximum point, it is not possible to give an accurate value of the speed, and hence efficiency and flow rate, at the best power point.

Table II.3 describes each configuration, giving the blade type and angle, guide vane angle, and type of cone.

Abbreviations

BAn	Blade Angle = n deg. (approximate, from tangential)		
GVAn	Guide Vane Angle = n deg. (approximate, from radial)		
CN0	no cone		
CN1	"straight" cone	**nPB**	n plastic blades
CN2	"radius" cone	**nMB**	n metal blades

Notes: In Graphs A-Z the power is divided by 10, ie, to get the power (in Watts), multiply the number on the graph scale by 10.

The Graphs are for a constant head of 1.8m.

Graph no.	Best Efficiency Point Speed N (RPM)	Flow Q (l/s)	Power P (kW)	Effcy E (%)	Best Power Point Speed N (RPM)	Flow Q (l/s)	Power P (kW)	Effcy E (%)
A	900	51	.43	48	1100	56	.45	46
B	900	50	.47	53	1080	53	.48	51
C	950	49	.48	55.5	1100	53	.49	53
D	950	47	.477	57.3	1100	50	.493	55.5
E	950	44	.445	57	1050	46	.453	56
Q	1150	44.5	.44	56	1250	46	.45	55
F	950	47.4	.45	54	1100	50.5	.47	53
G	950	47	.45	54	1100	51	.46	52
H	950	46.7	.45	54	1100	50	.47	53
I	900	47	.44	53	1050	50	.45	51
J	850	34	.35	58	1050	38	.37	55
K	950	35.5	.37	58	1050	37.5	.38	57
L	900	35.5	.37	58	1000	37.5	.38	57
M	880	35	.37	60.5	1000	37	.383	59
N	850	33	.37	63	1000	35.5	.38	60
O	800	28.5	.32	64	900	30.5	.34	63
P	800	30	.33	62	950	32	.345	61
R	800	45	.48	61	1050	51.8	.52	57
S	800	46	.48	59	1100	55.5	.525	54
U	850	51	.53	59	1100	60	.58	55
V	900	50	.545	61.5	1150	57.5	.58	56.5
X	750	54	.55	58	950	60	.58	55
Z	750	55	.57	59	1030	64.5	.615	54
T	900	58	.54	53.5	1100	65	.58	51
W	800	52.5	.52	56.5	1150	62.5	.565	51
Y	850	51	.53	59.5	1050	56	.565	57

Table II.1 Performance Data at Best Operating Points

Graph no.	Best Efficiency Point k_S (1)	Best Efficiency Point N_S (RPM) (hp,m)	Best Power Point k_S (1)	Best Power Point N_S (RPM) (hp,m)
A	2.48	330	3.18	413
B	2.46	345	3.03	418
C	2.57	368	3.09	431
D	2.51	367	3.00	432
E	2.43	354	2.75	395
Q	2.96	427	3.27	469
F	2.52	356	3.02	422
G	2.51	356	3.03	417
H	2.50	356	3.00	422
I	2.38	334	2.86	394
J	1.91	281	2.50	357
K	2.18	323	2.48	362
L	2.07	306	2.36	345
M	2.01	299	2.35	346
N	1.88	289	2.30	345
O	1.65	253	1.92	293
P	1.69	257	2.07	312
R	2.07	310	2.92	423
S	2.09	310	3.16	446
U	2.34	346	3.29	469
V	2.46	372	3.36	490
X	2.13	311	2.84	405
Z	2.15	317	3.19	452
T	2.64	370	3.42	469
W	2.24	323	3.51	483
Y	2.34	346	3.03	441
max.	2.96	427	3.51	490

Table II.2 Characteristic Number k_S, and Specific Speed N_S, at Best Operating Points

Graph no.	Description			
	BA	GVA	CN	
A	22.5	0	1	4PB
B	22.5	10	1	4PB
C	22.5	25	1	4PB
D	22.5	32	1	4PB
E	22.5	45	1	4PB
Q	20	33	0	4MB
F	22.5	32	2	4PB
G	22.5	32	2	4PB
H	22.5	32	0	4PB
I	22.5	25	0	4PB
J	20	45-20	2	8PB(CUTAWAY)
K	20	45-20	0	8PB(CUTAWAY)
L	20	25	0	8PB(CUTAWAY)
M	20	33	0	8PB(CUTAWAY)
N	20	40	0	8PB(CUTAWAY)
O	20	40	0	8MB
P	20	33	0	8MB
R	25	25	0	8MB
S	25	15	0	8MB
U	30	15	0	8MB
V	30	25	0	8MB
X	35	25	0	8MB
Z	35	25	1	8MB
T	25	15	0	8MB(SHORTENED)
W	30	25	0	8MB(SHORTENED)
Y	35-30	25	0	8MB(TWISTED)

Table II.3 Description of Turbine Configurations

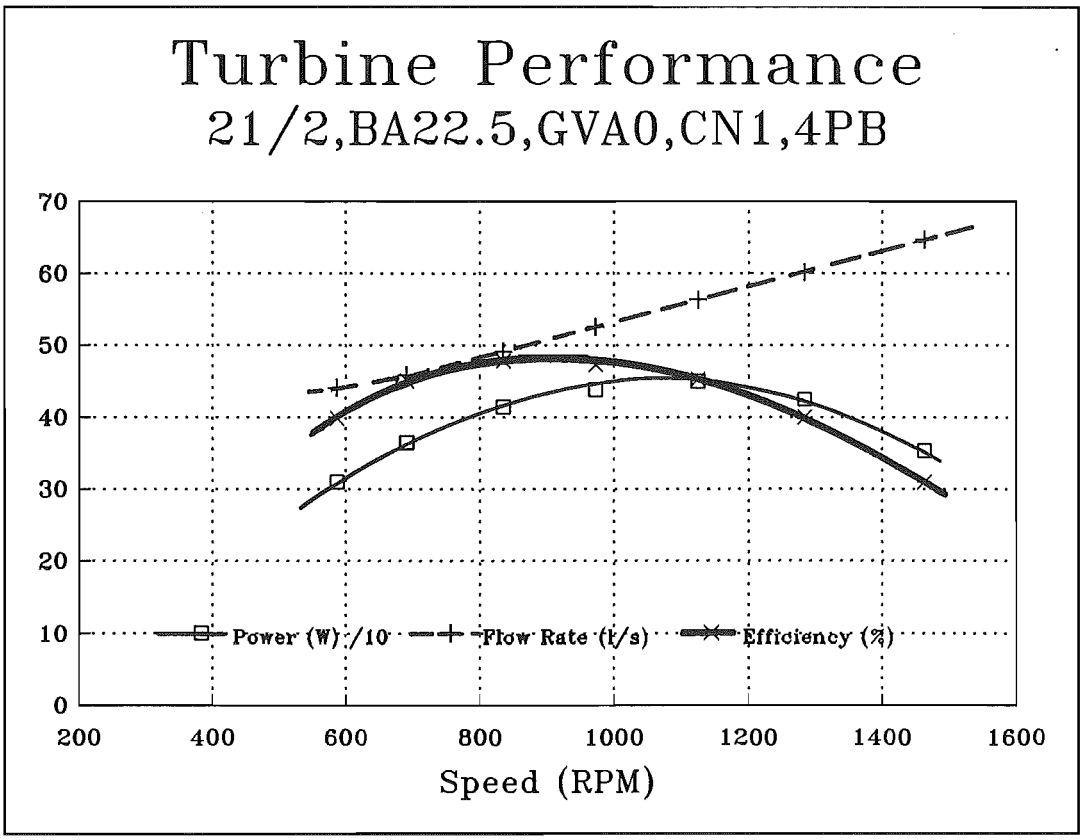

Graph A

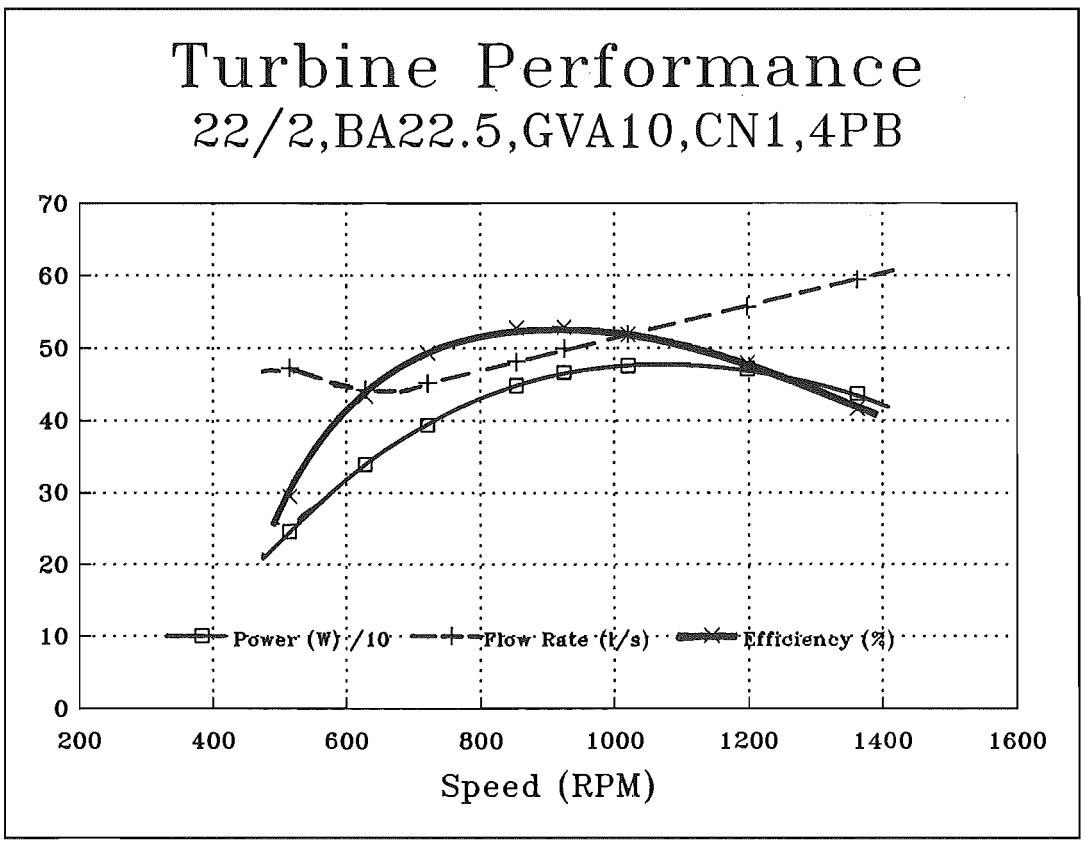

Graph B

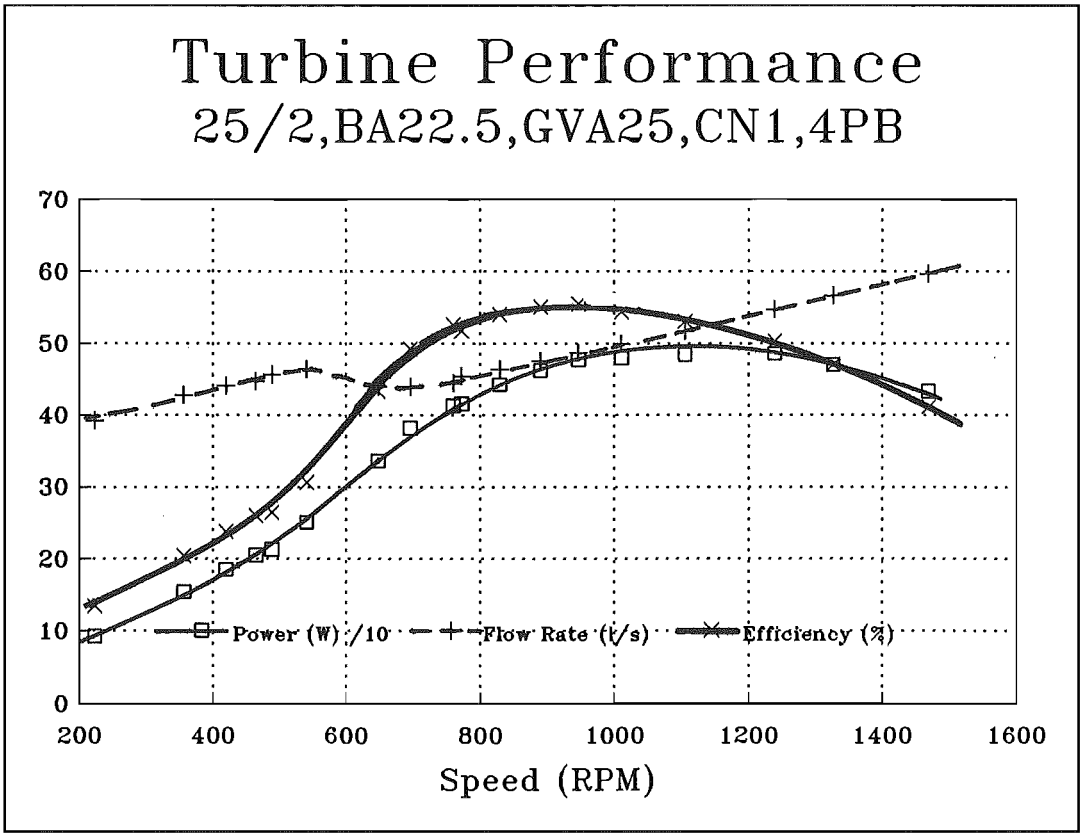

Graph C

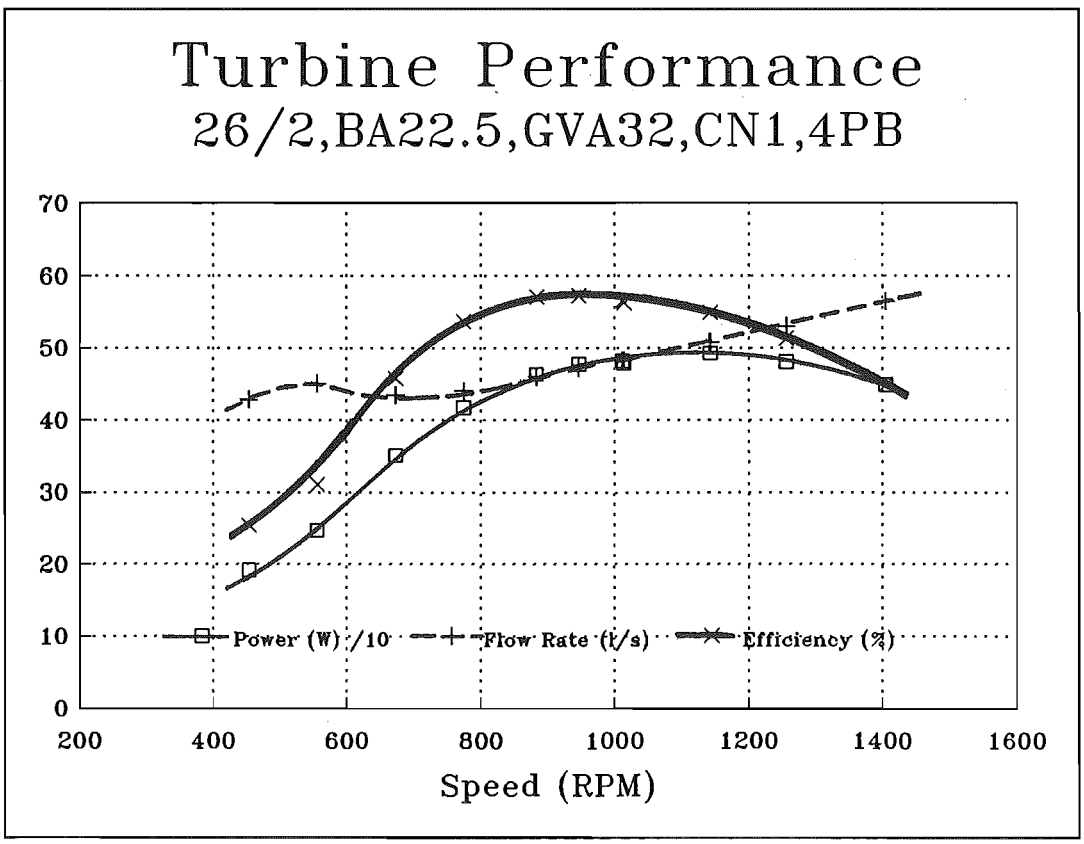

Graph D

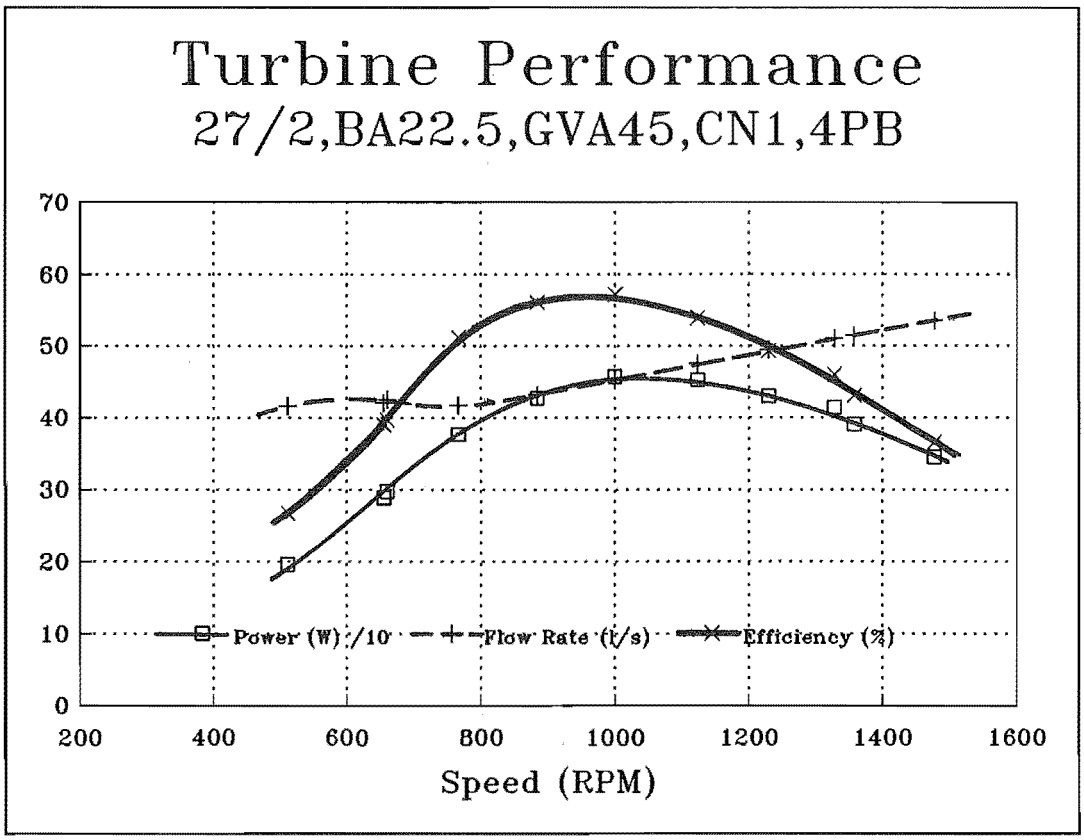

Graph E

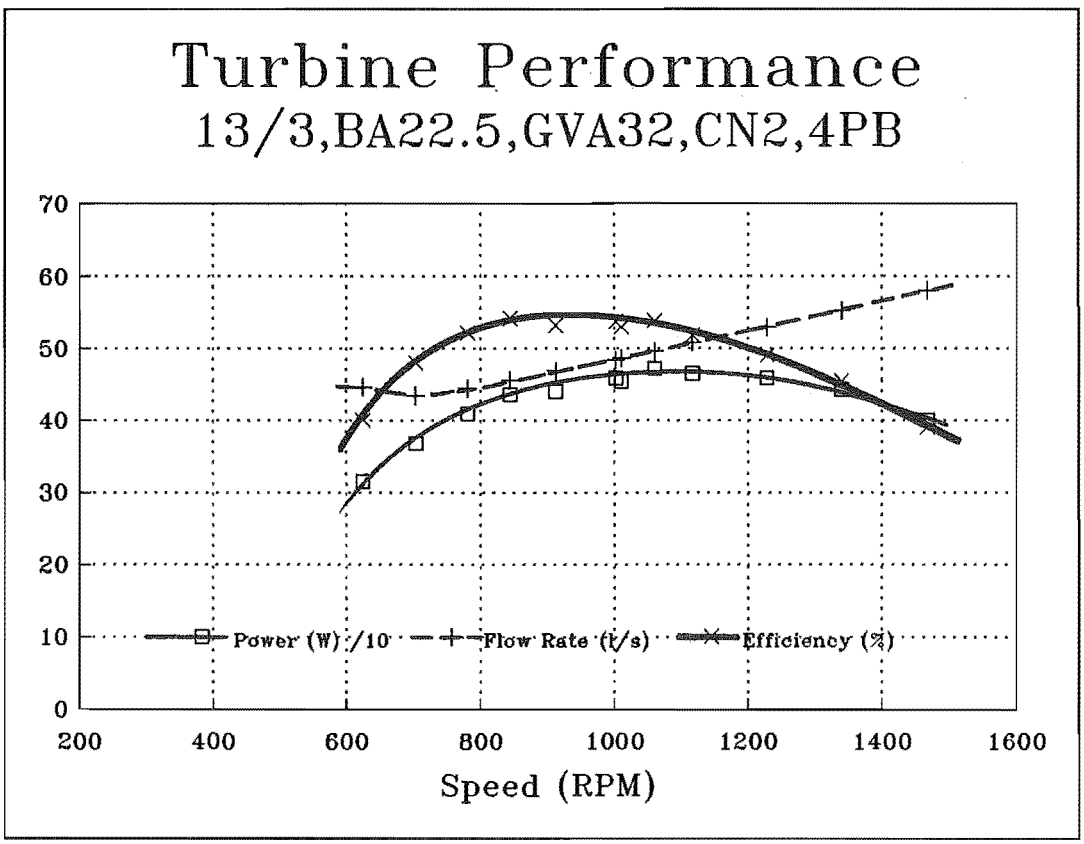

Graph F

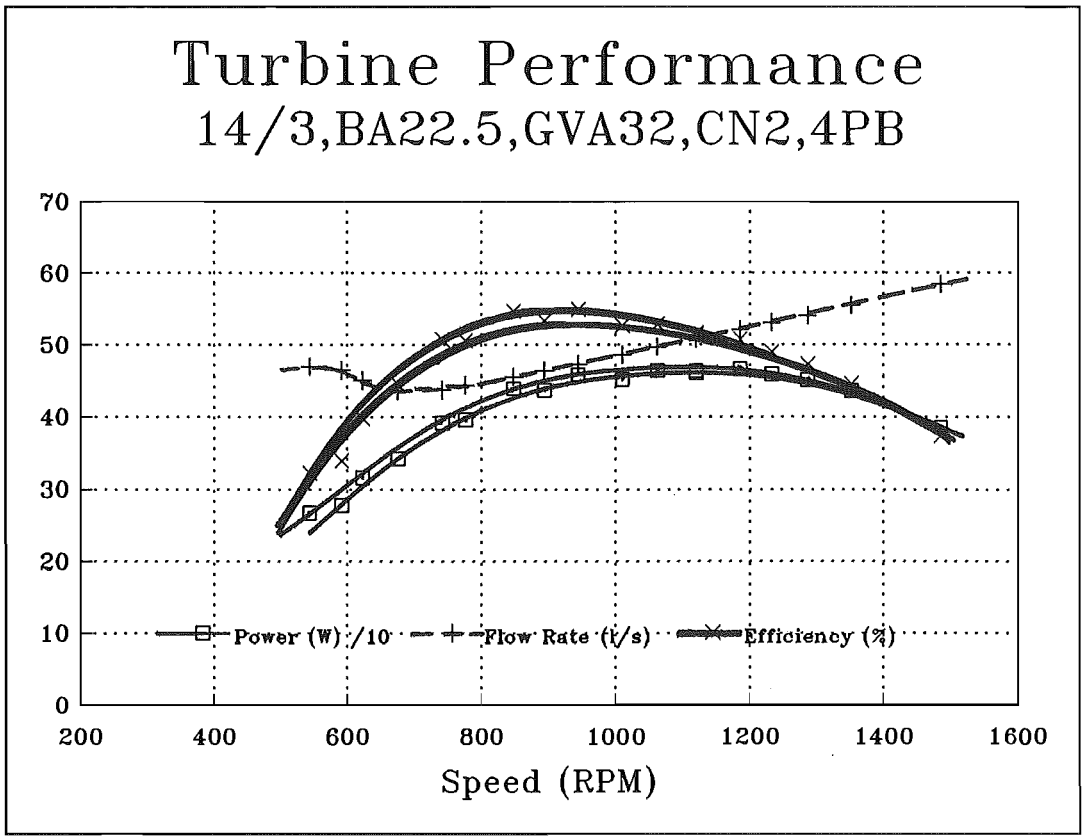

Graph G

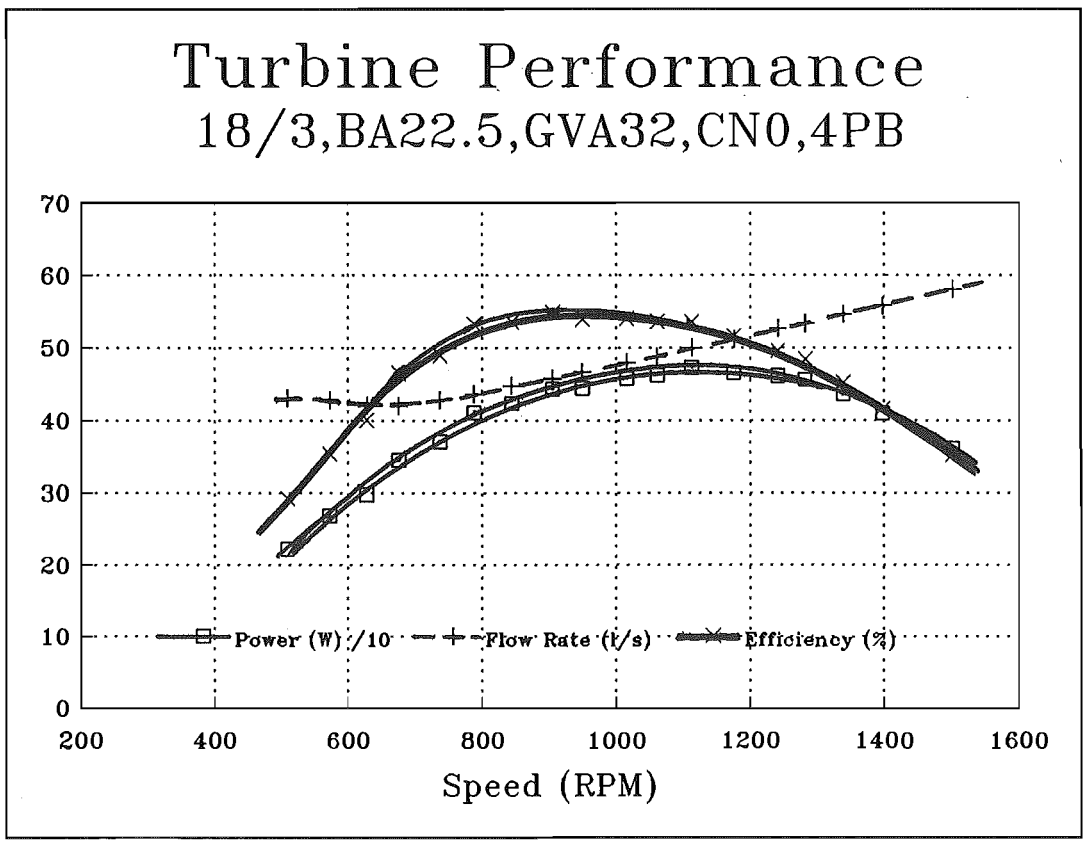

Graph H

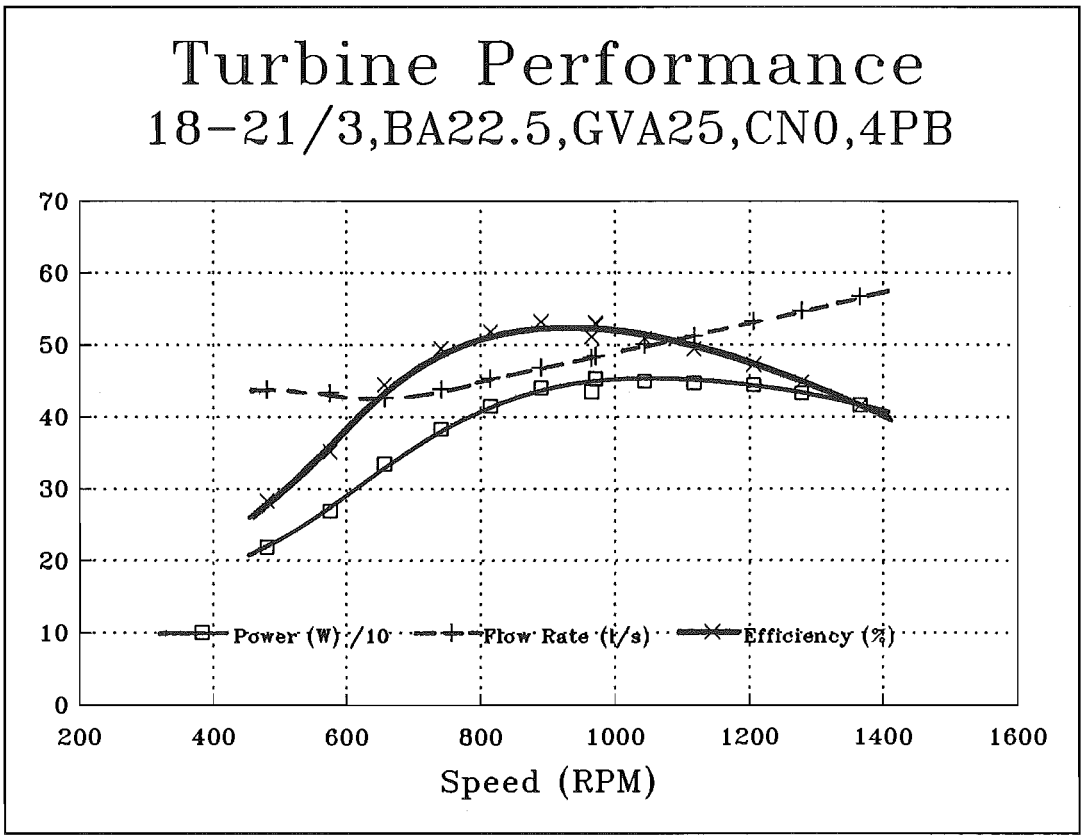

Graph I

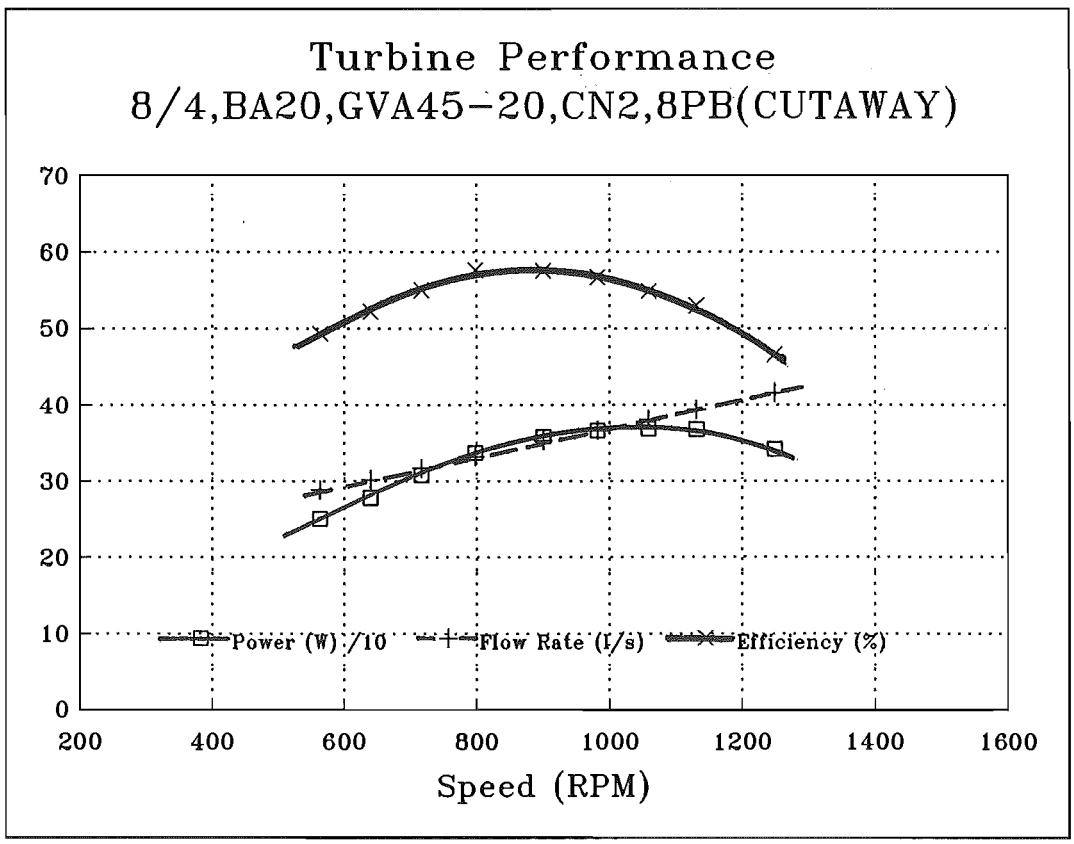

Graph J

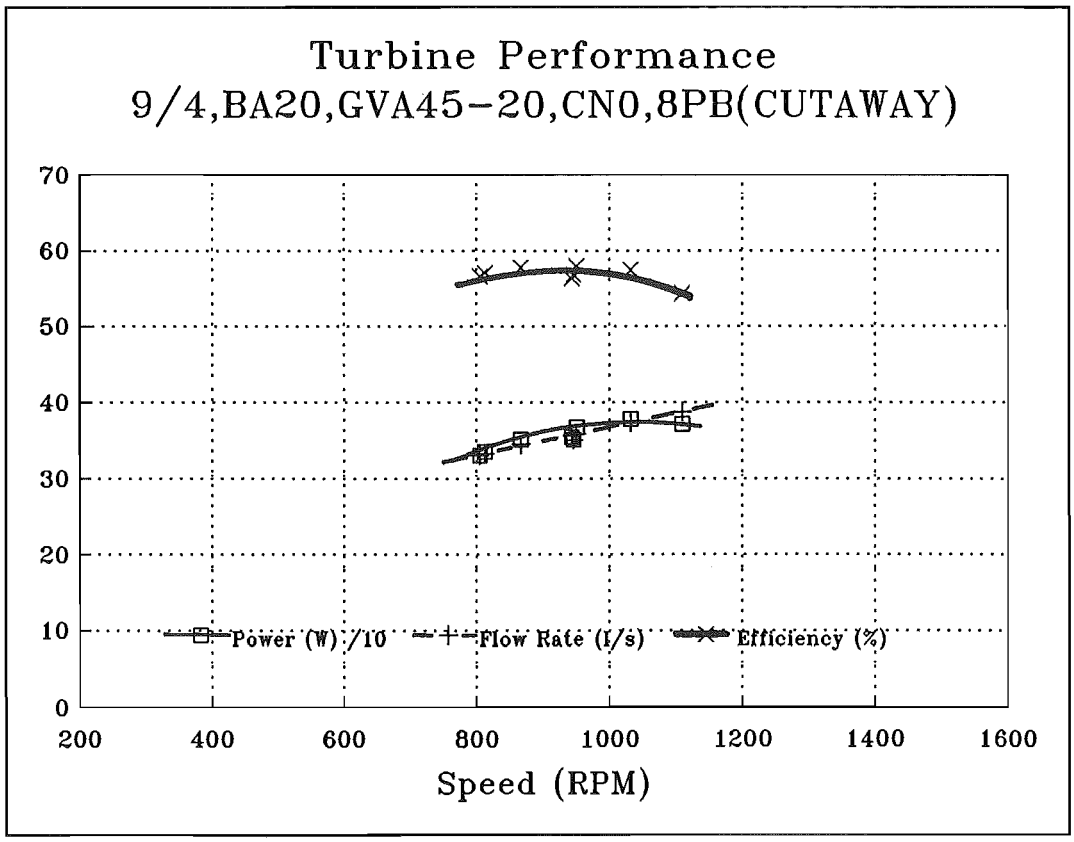

Graph K

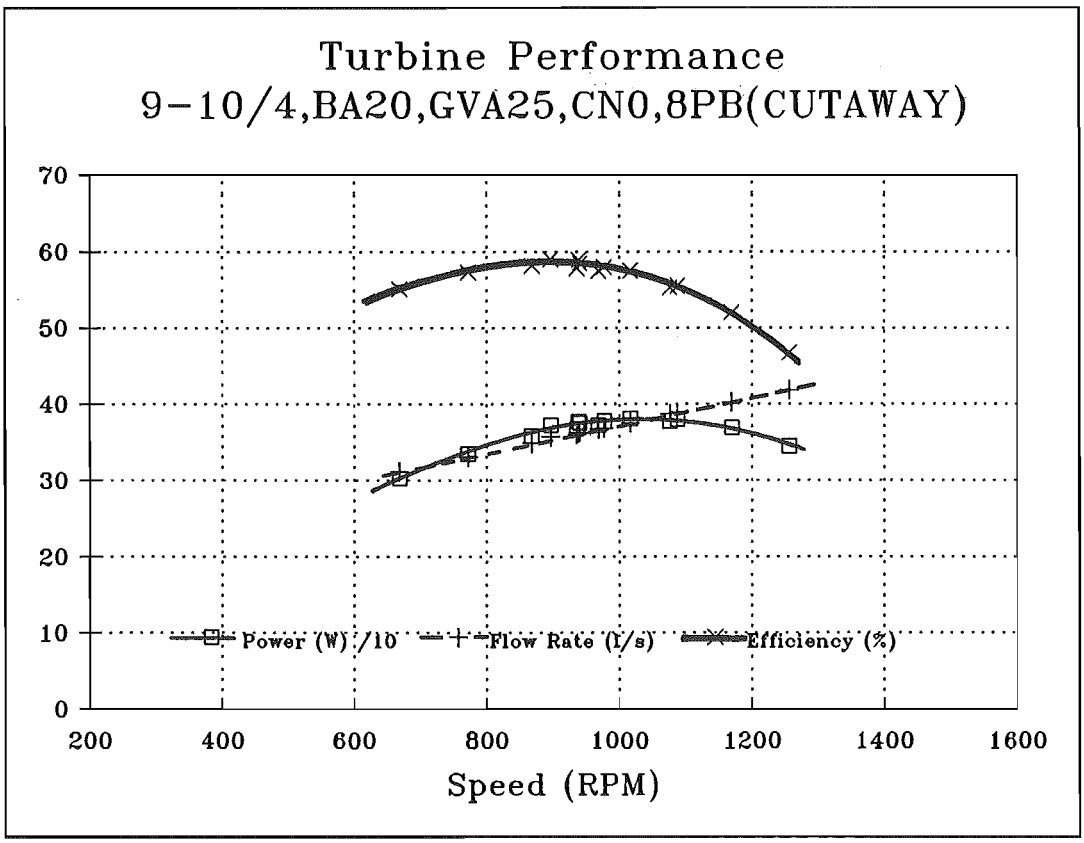

Graph L

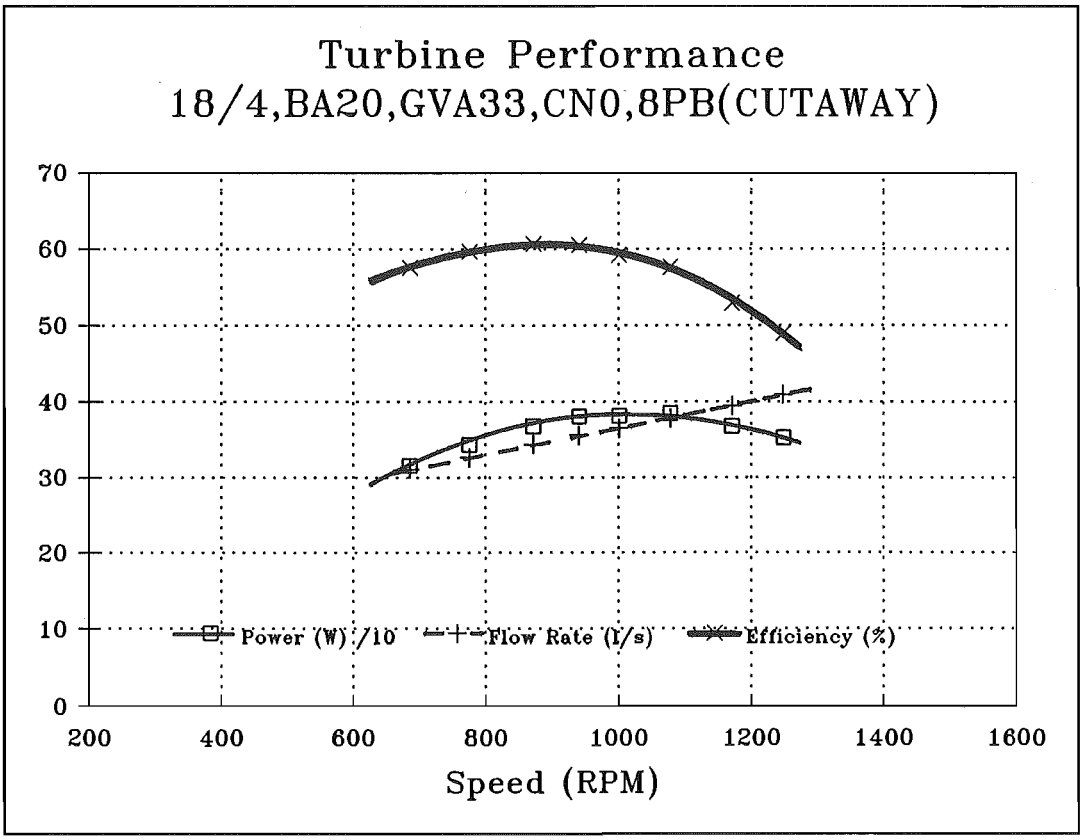

Graph M

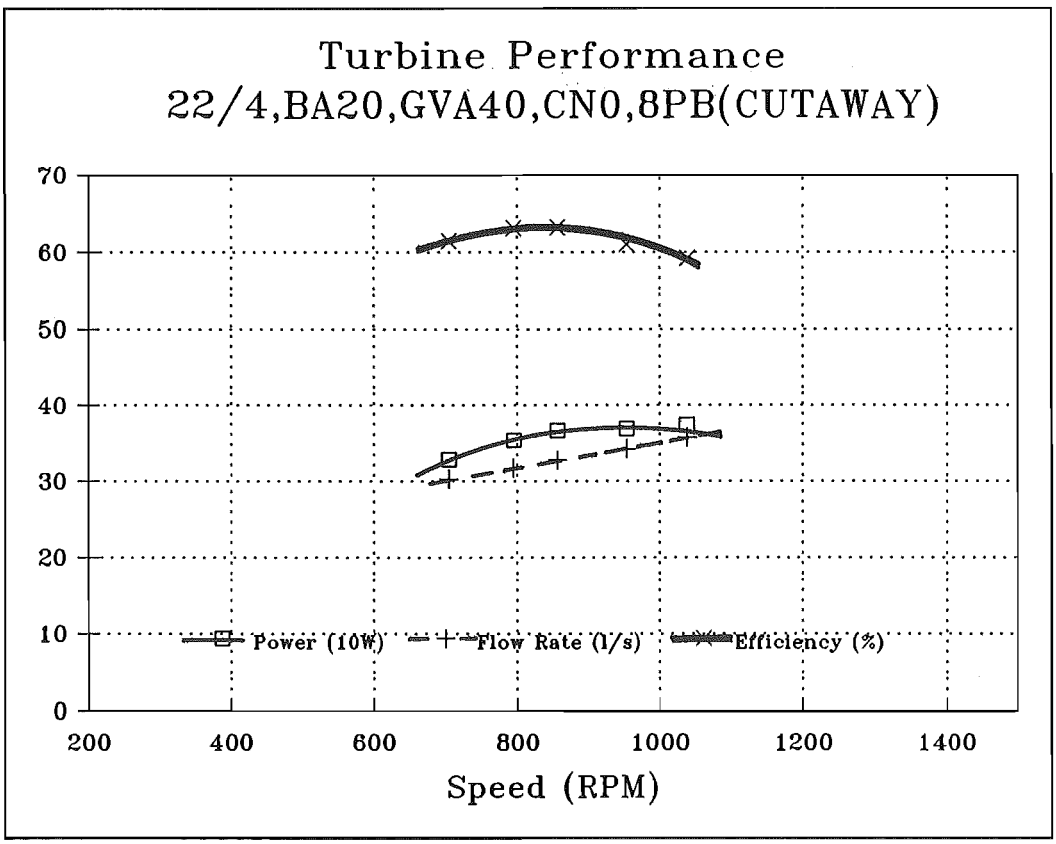

Graph N

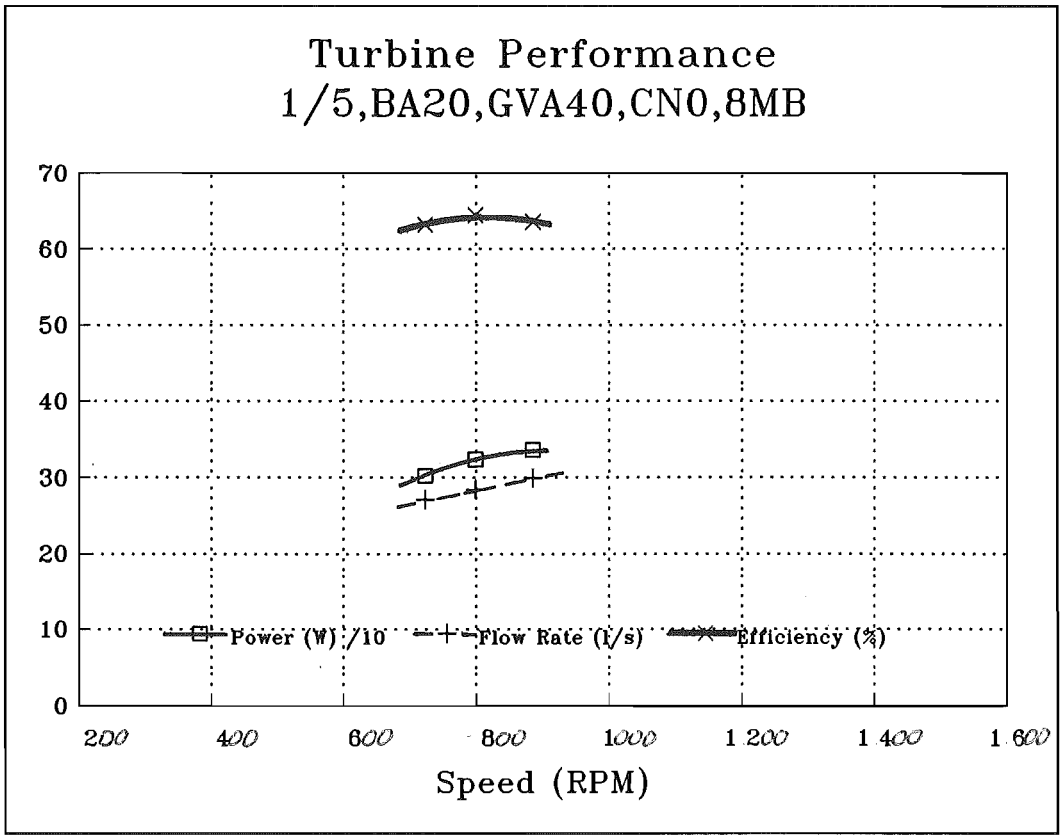

Graph O

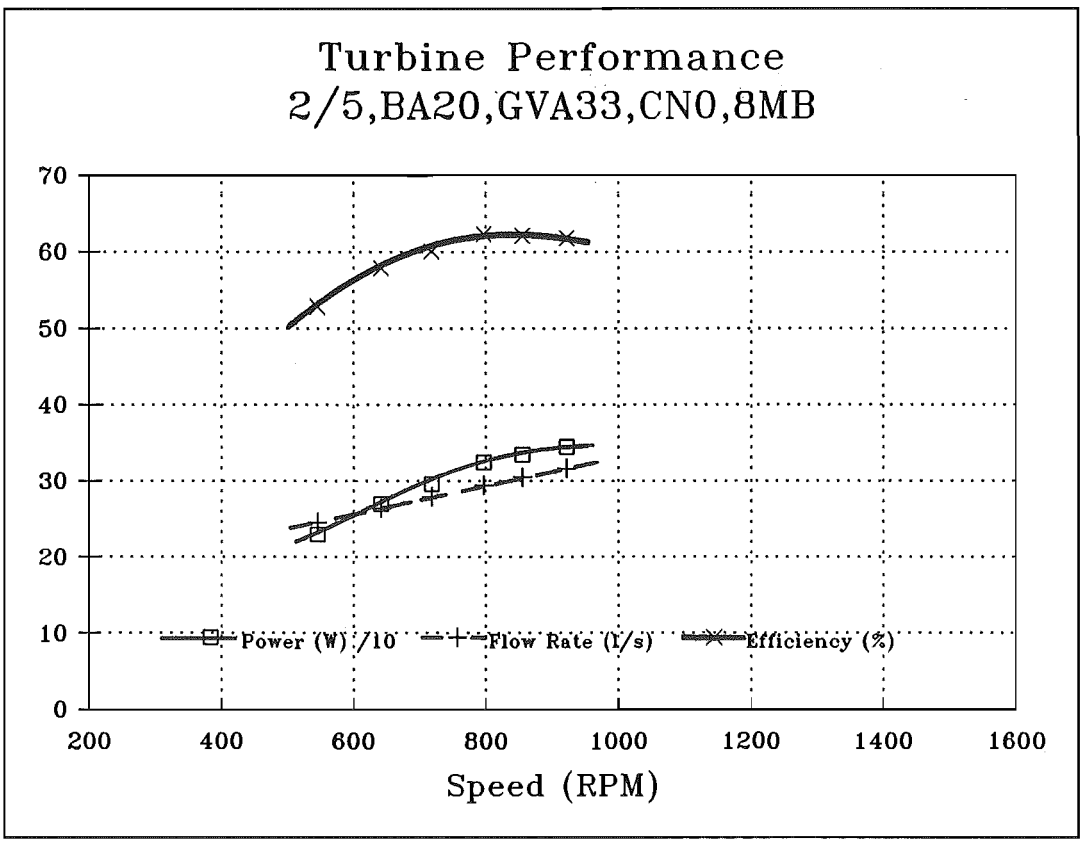

Graph P

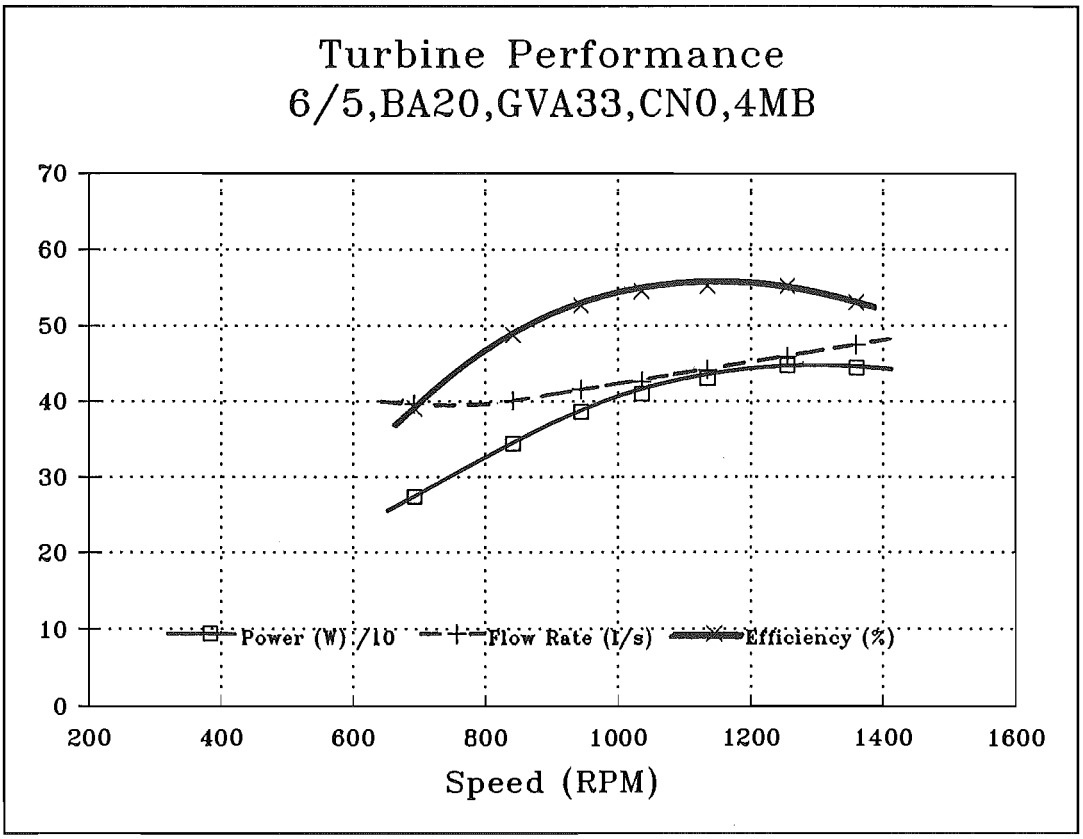

Graph Q

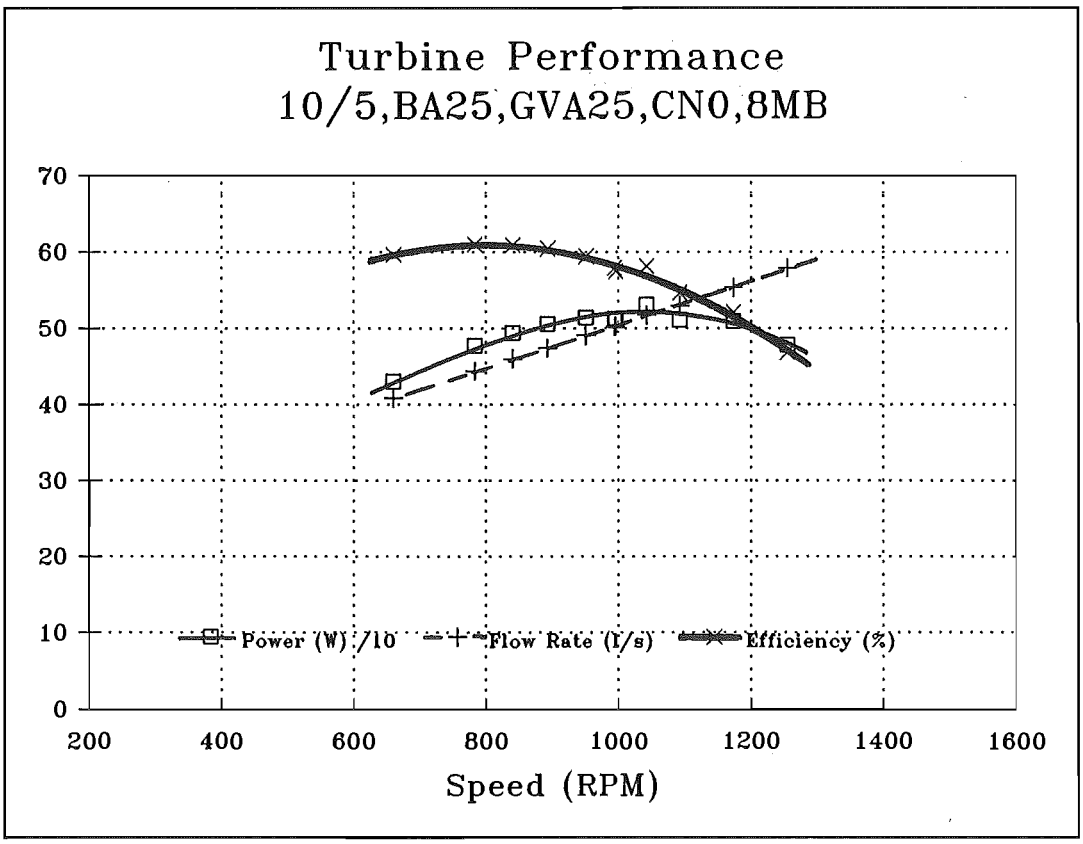

Graph R

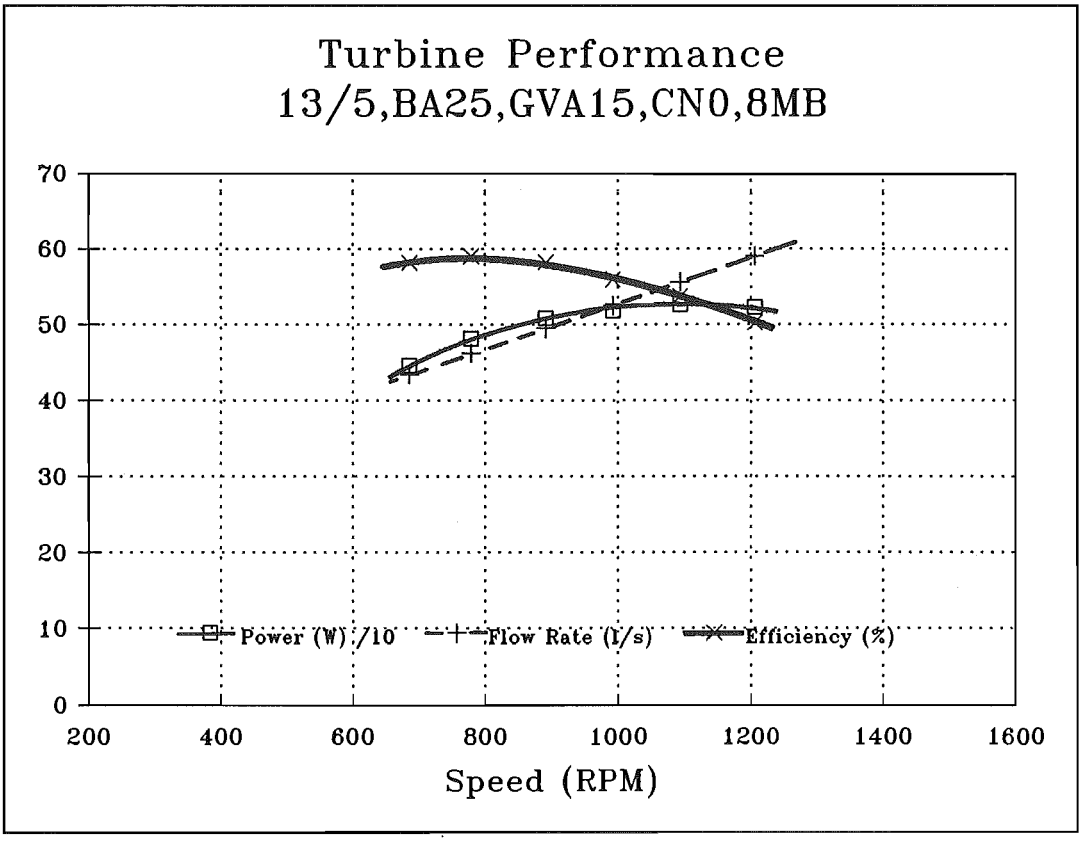

Graph S

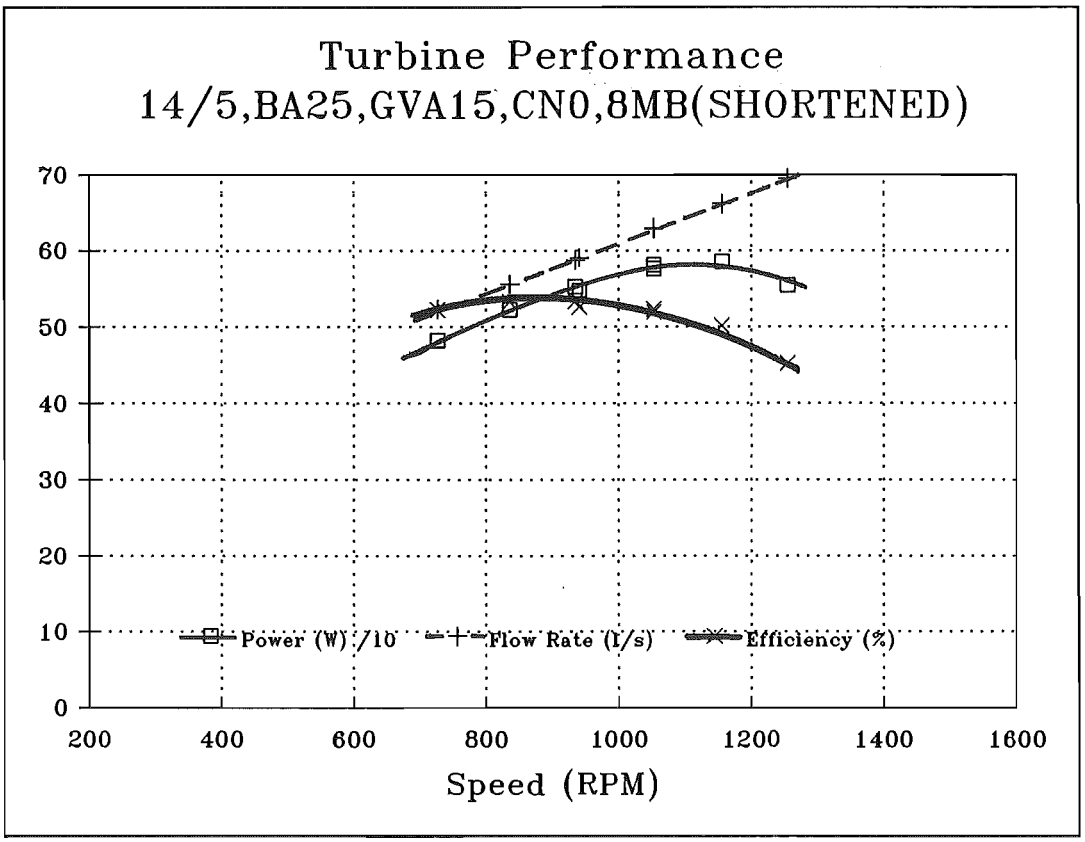

Graph T

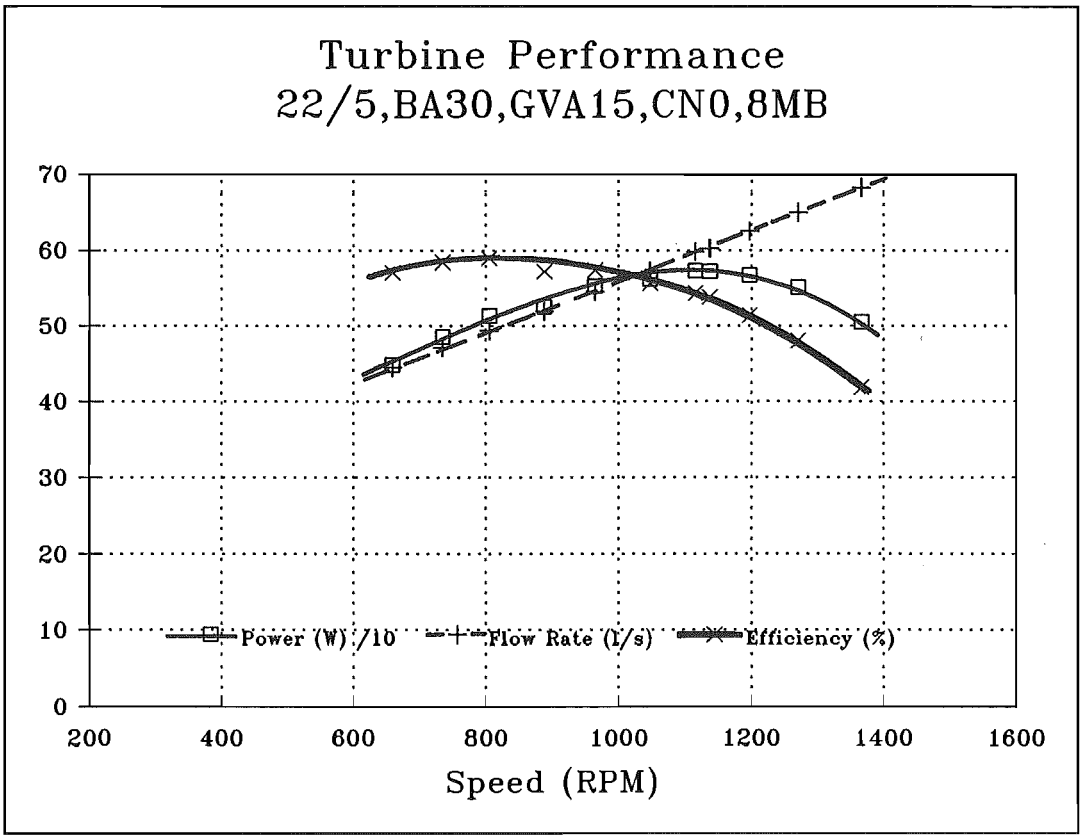

Graph U

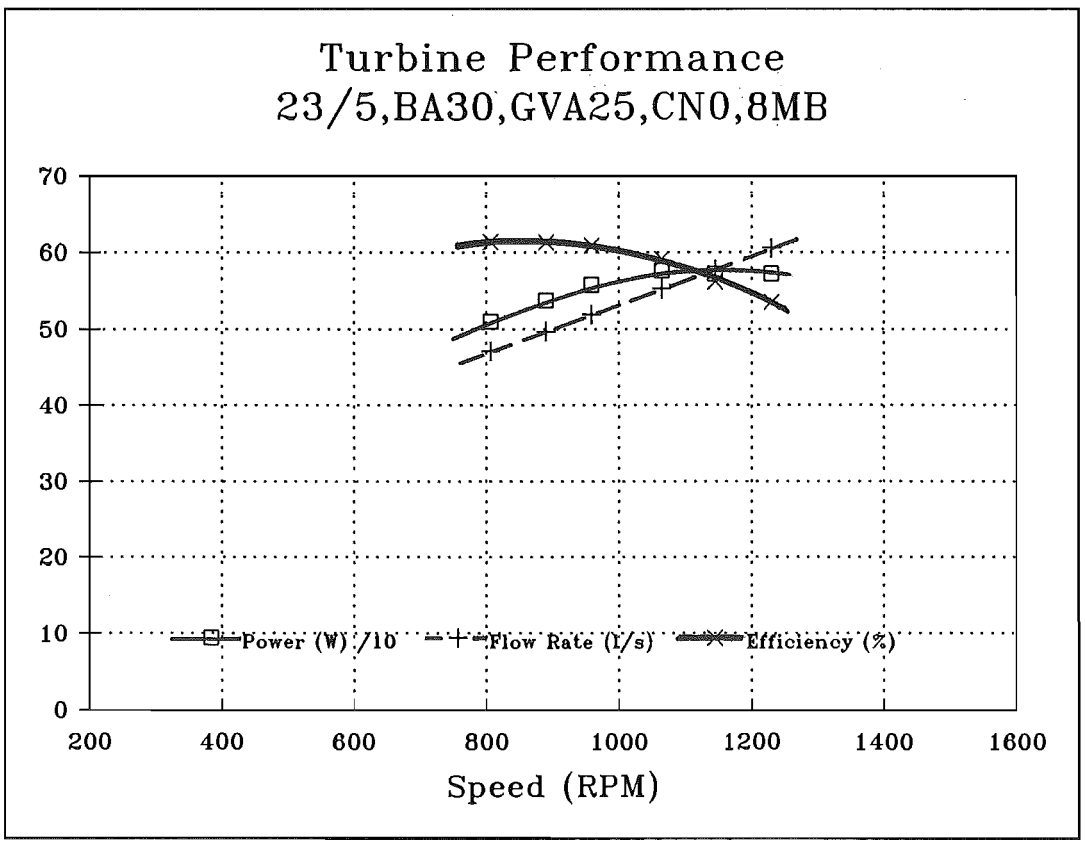

Graph V

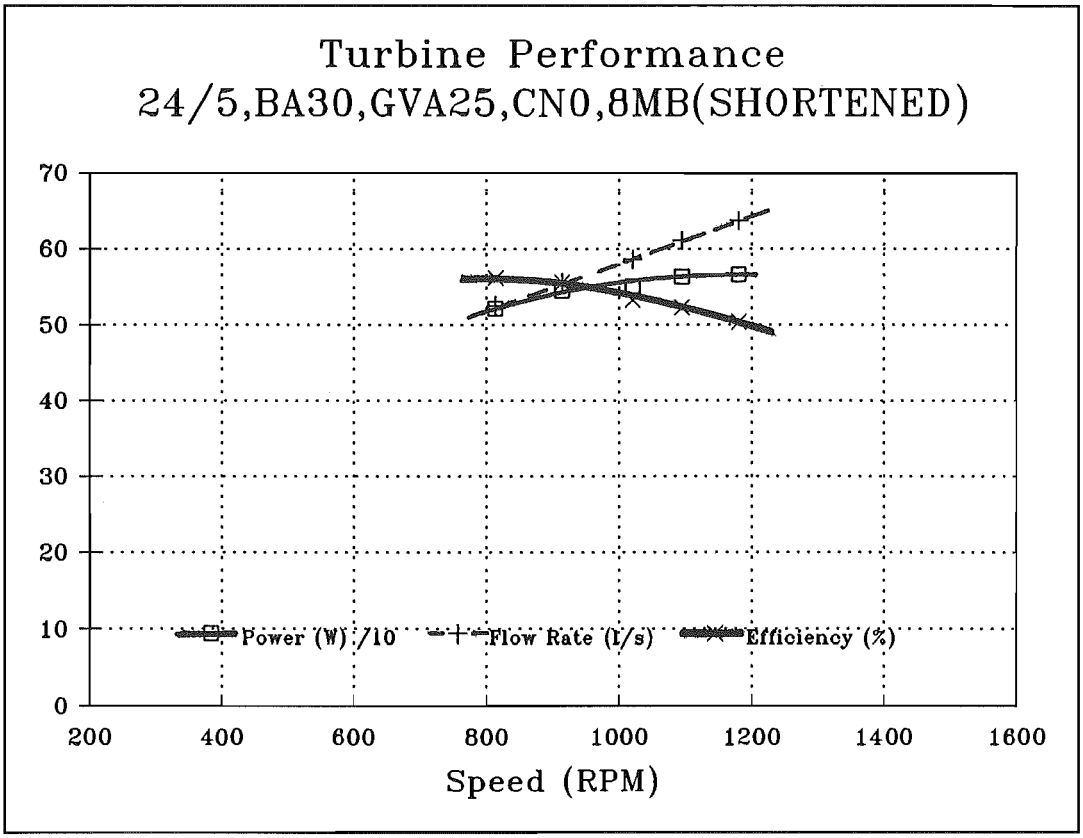

Graph W

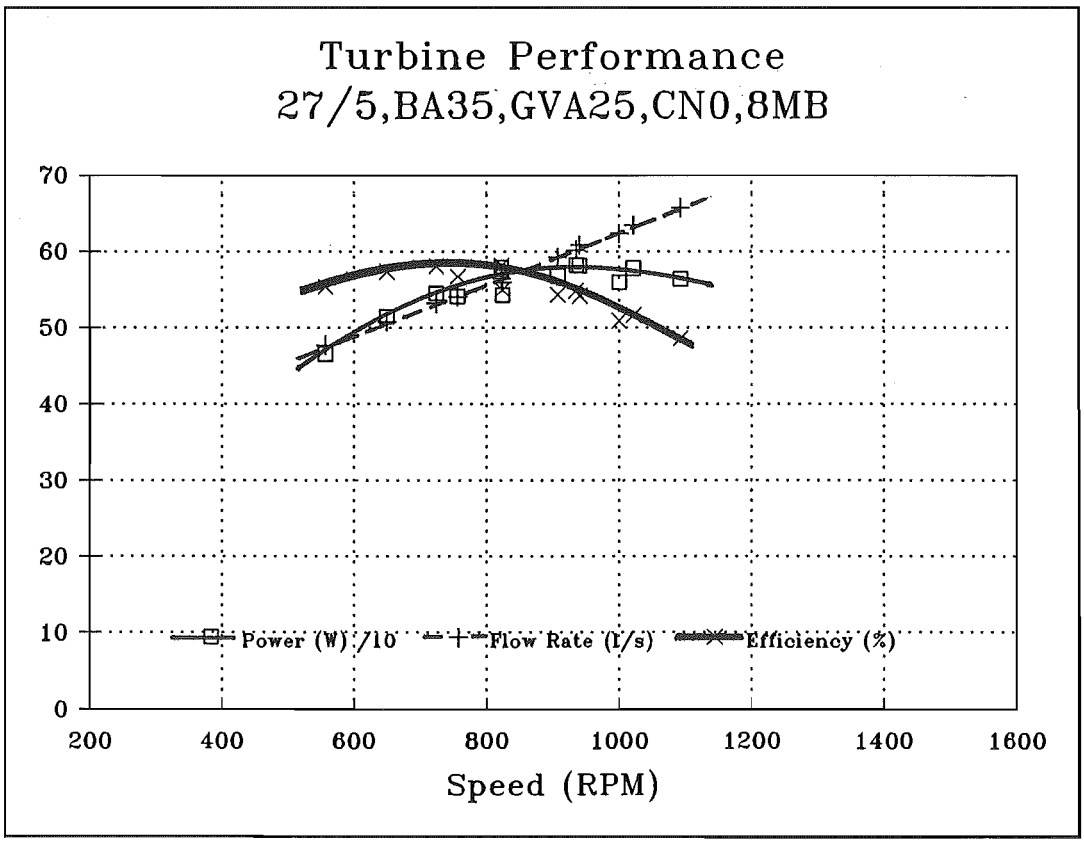

Graph X

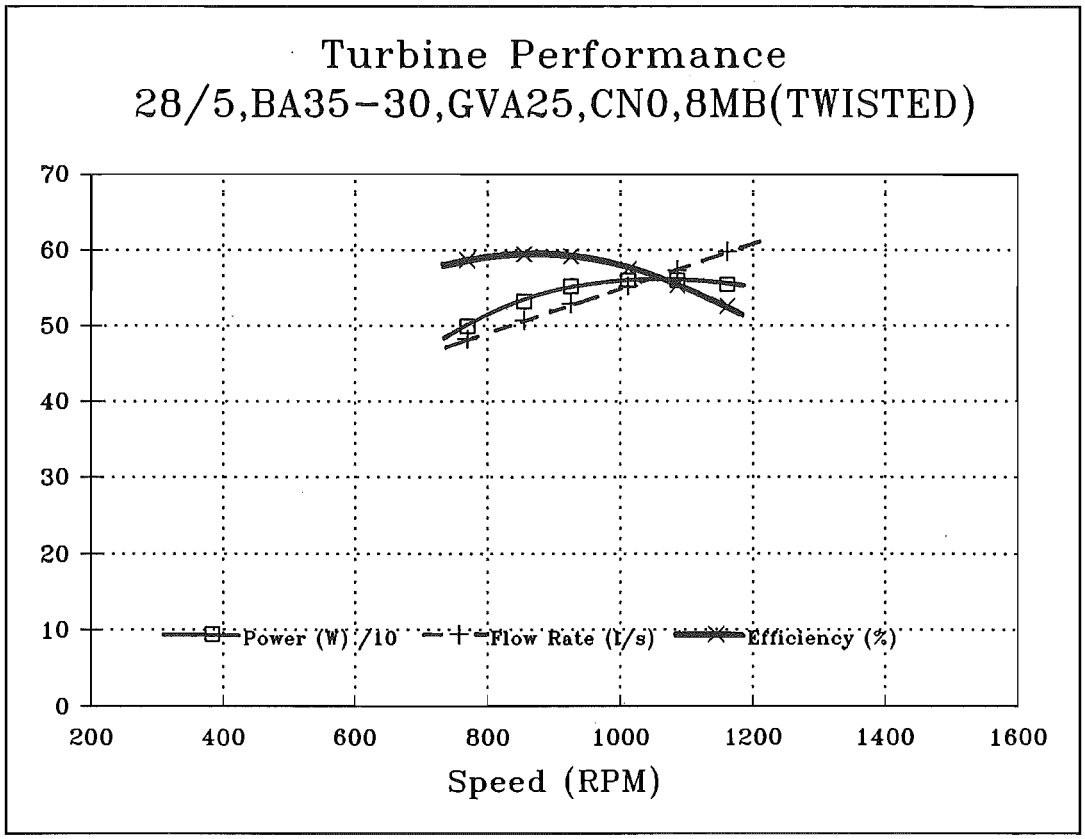

Graph Y

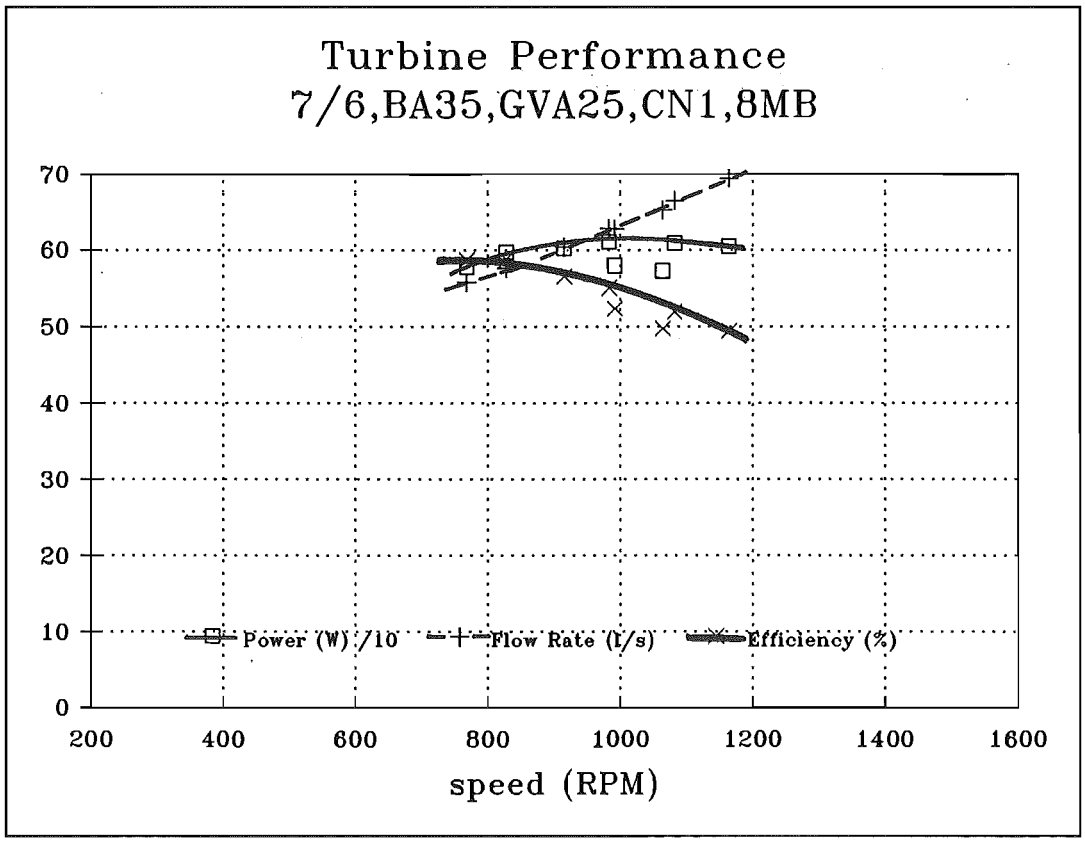

Graph Z

APPENDIX III

PROTOTYPE TURBINE DRAWINGS

WKOverall	Generall layout of turbine and generator unit.
RNNR:BLADES	Blade construction detail.
RNNR:HUB	Hub and shaft construction detail.
TRIPOD	Top plate, guide vanes, tripod support, and gearbox mount.
TTUBE	Turbine tube and toroid flanges.

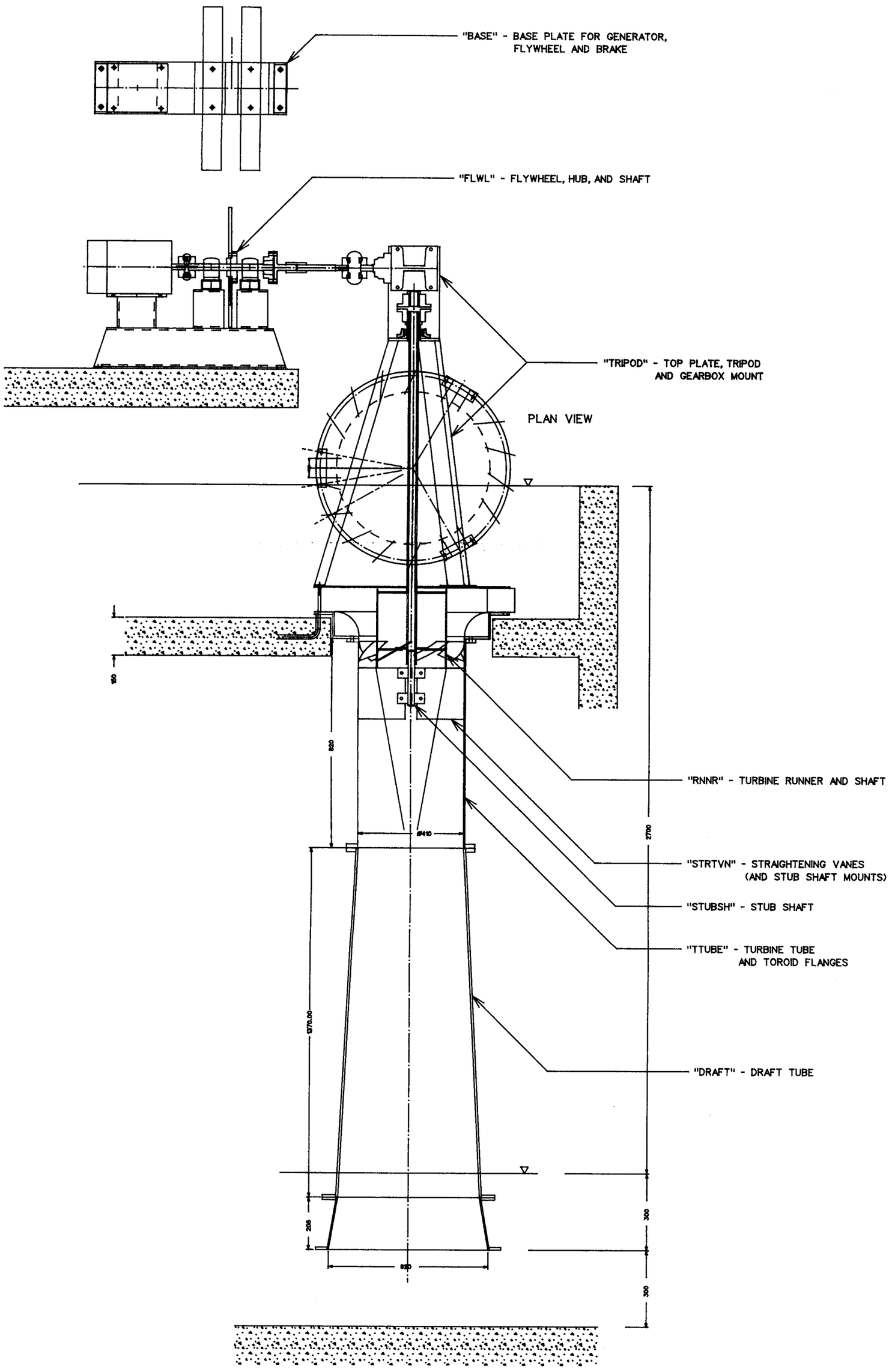

ITEM	DESCRIPTION	QNTY

SCHOOL OF ENGINEERING
MECHANICAL ENGINEERING DPT.

MICRO HYDRO PROJECT
PROTOTYPE TURBINE
GENERAL LAYOUT

DRWN: S. FAULKNER
CHKD:
DATE: 12/8/91

DRG No: WKOverall

SCALE: 1:15
A3

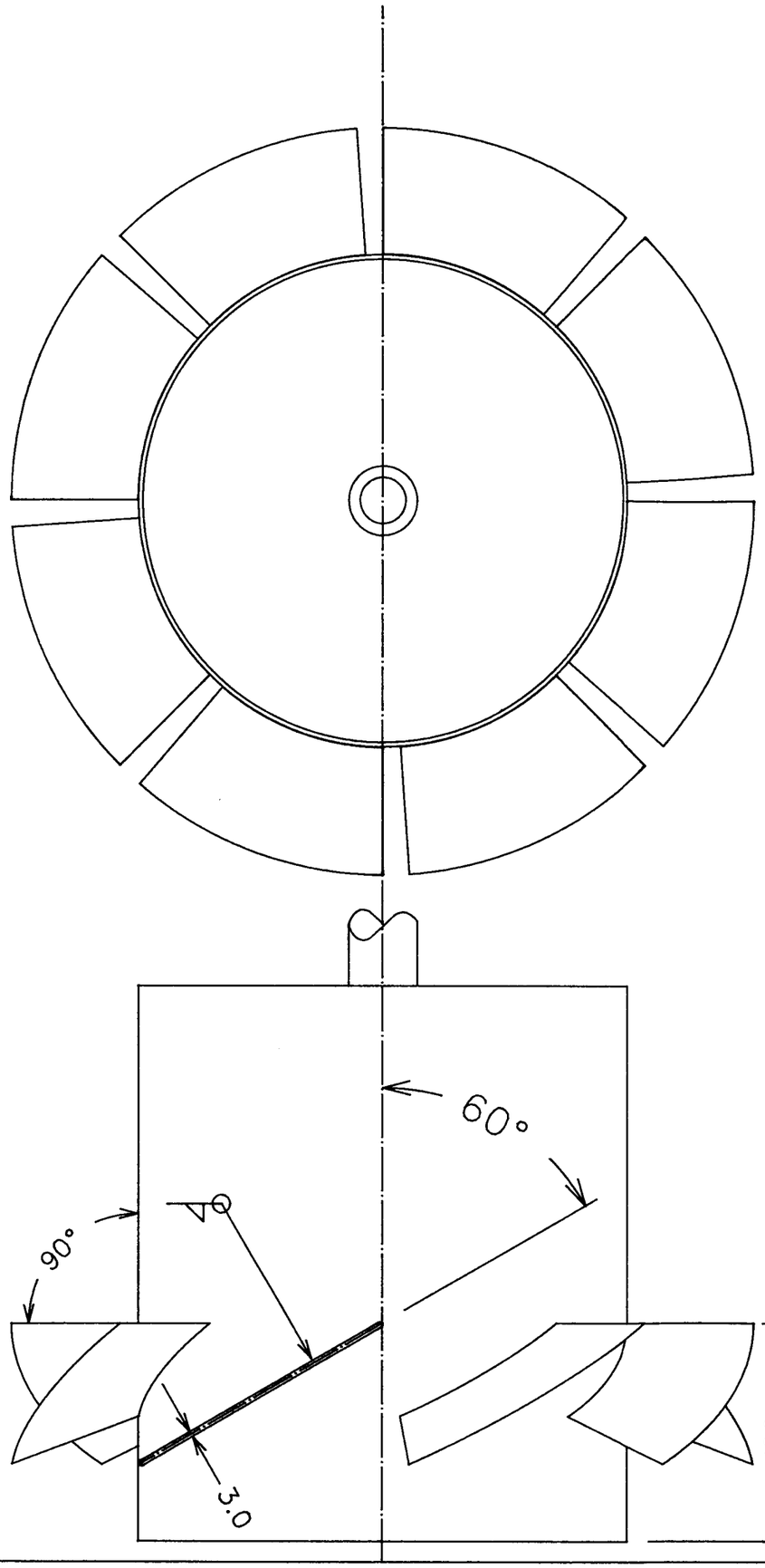

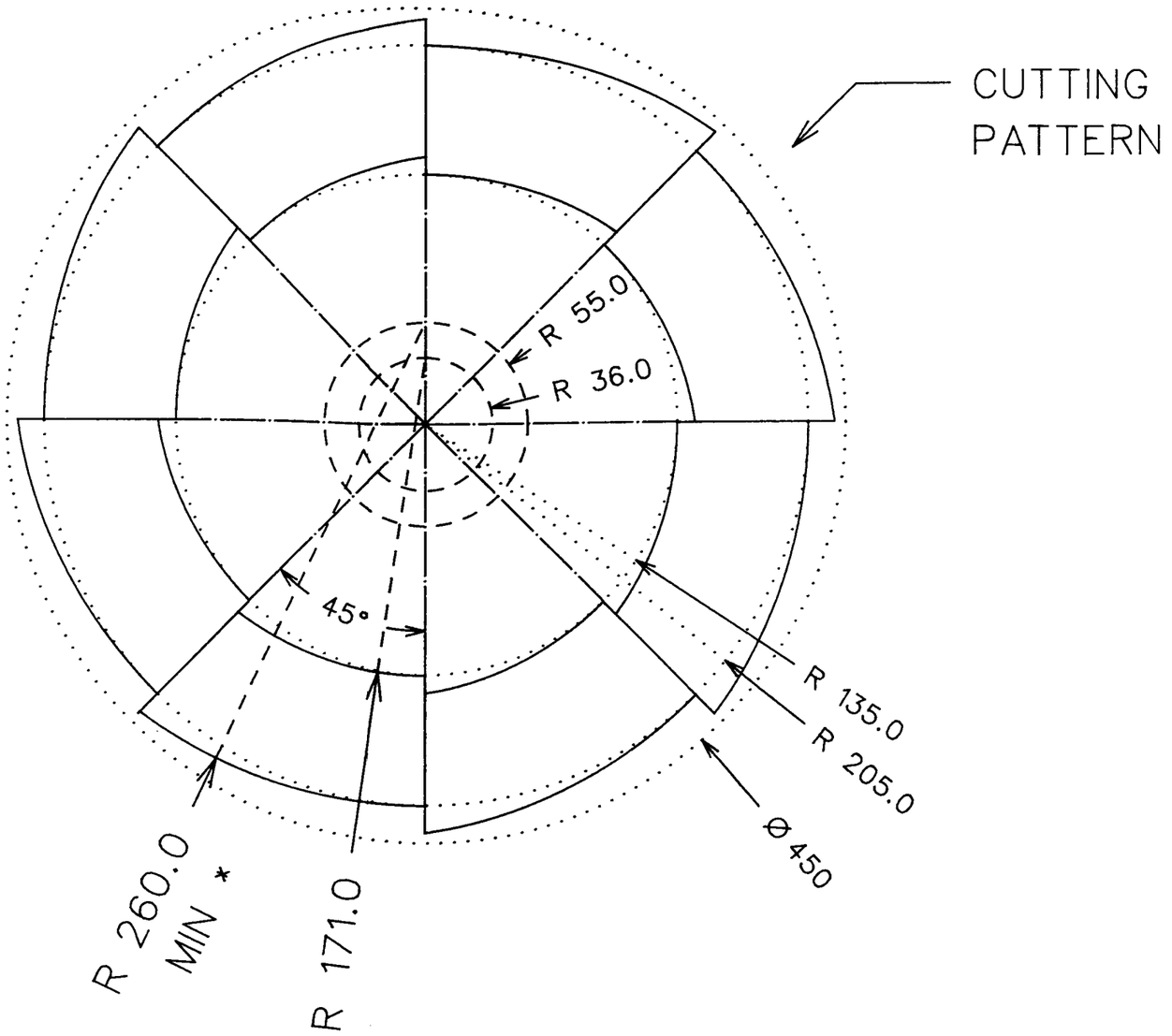

TOLERANCE 0.5mm

* OUTER DIAMETER OF BLADES GROUND AFTER WELDING TO FIT TURBINE TUBE

BLADES CUT FROM SINGLE SHEET OF 3mm STEEL PLATE (DIA 450). WELDED TO HUB

ITEM	DESCRIPTION	QUANTITY

SCHOOL OF ENGINEERING
MECHANICAL ENGINEERING DEPARTMENT

MICRO HYDRO PROJECT
TURBINE RUNNER
BLADE DETAIL

DRN: S.FAULKNER
CHKD:
DATE: 7/8/91

DRG No:
RNNR : BLADES

SCALE: 1:3.2
A3

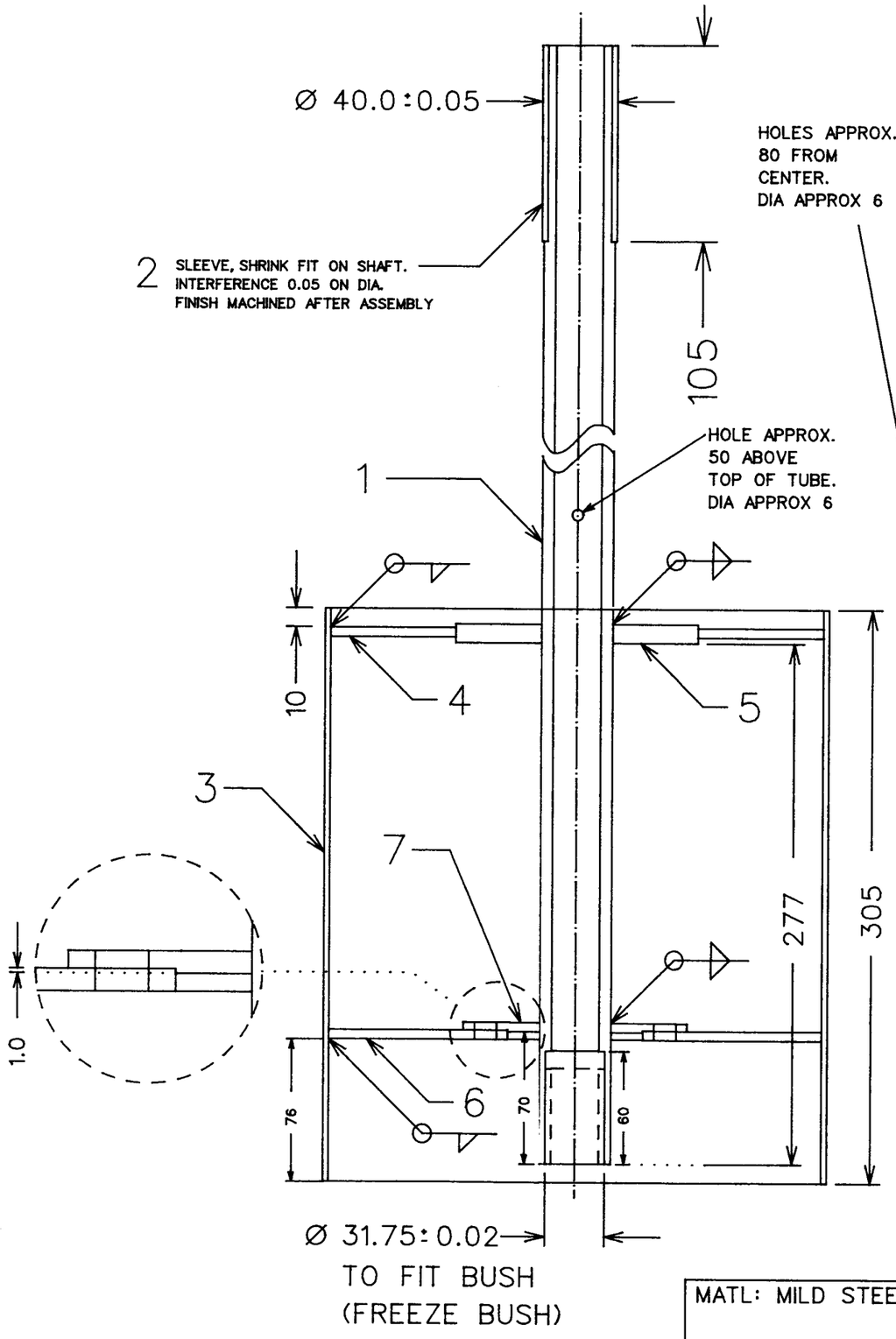

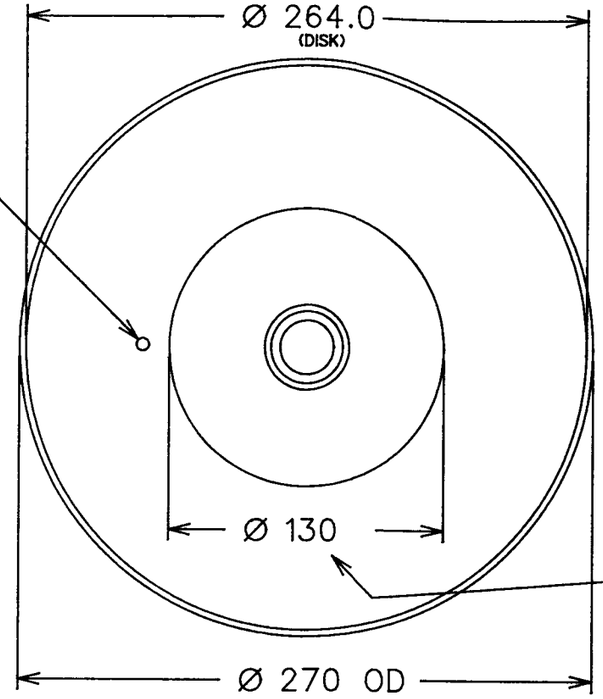

← VIEW FROM ABOVE

NOMINAL - CLEARANCE BETWEEN DISKS OF 0.2mm ON DIA. (FOR ACCURATE LOCATION)

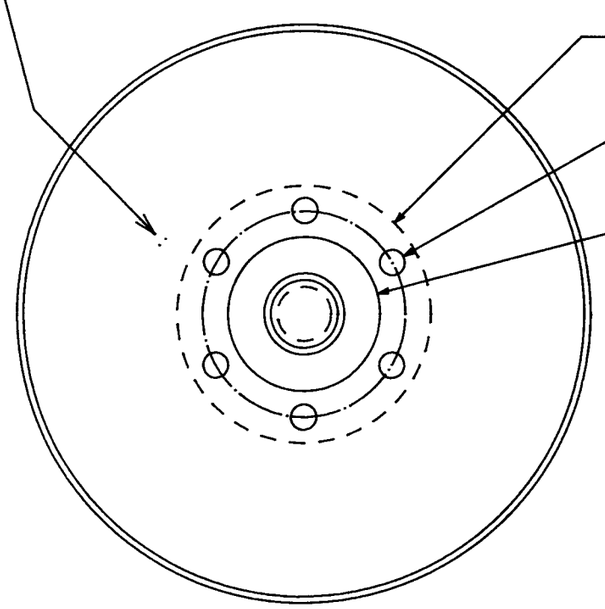

← VIEW FROM BELOW

ITEM	DESCRIPTION	QNTY
7	DISK 10mm, OD120	1
6	DISK 5mm, OD 264	1
5	DISK 10mm, OD 130 NOM.	1
4	DISK 5mm, OD 264	1
3	TUBE, ROLLED AND WELDED FROM 3mm PLATE	1
2	SLEEVE, OD 40 (FINAL), LENGTH 105	1
1	SHAFT, 38 OD BOILER TUBE LENGTH 1385 (SUPPLIED)	1

MATL: MILD STEEL

THIRD ANGLE PROJECTION | A3

TOLERANCES: 1mm

unless otherwise stated

MICRO HYDRO PROJECT
PROTOTYPE TURBINE
TURBINE RUNNER HUB DETAIL

SCALE: 1:3

SCHOOL OF ENGINEERING
MECHANICAL ENGINEERING DPT.

DRWN: S FAULKNER | DRG No:

CHKD:

DATE: 12/8/91 | RNNR : HUB

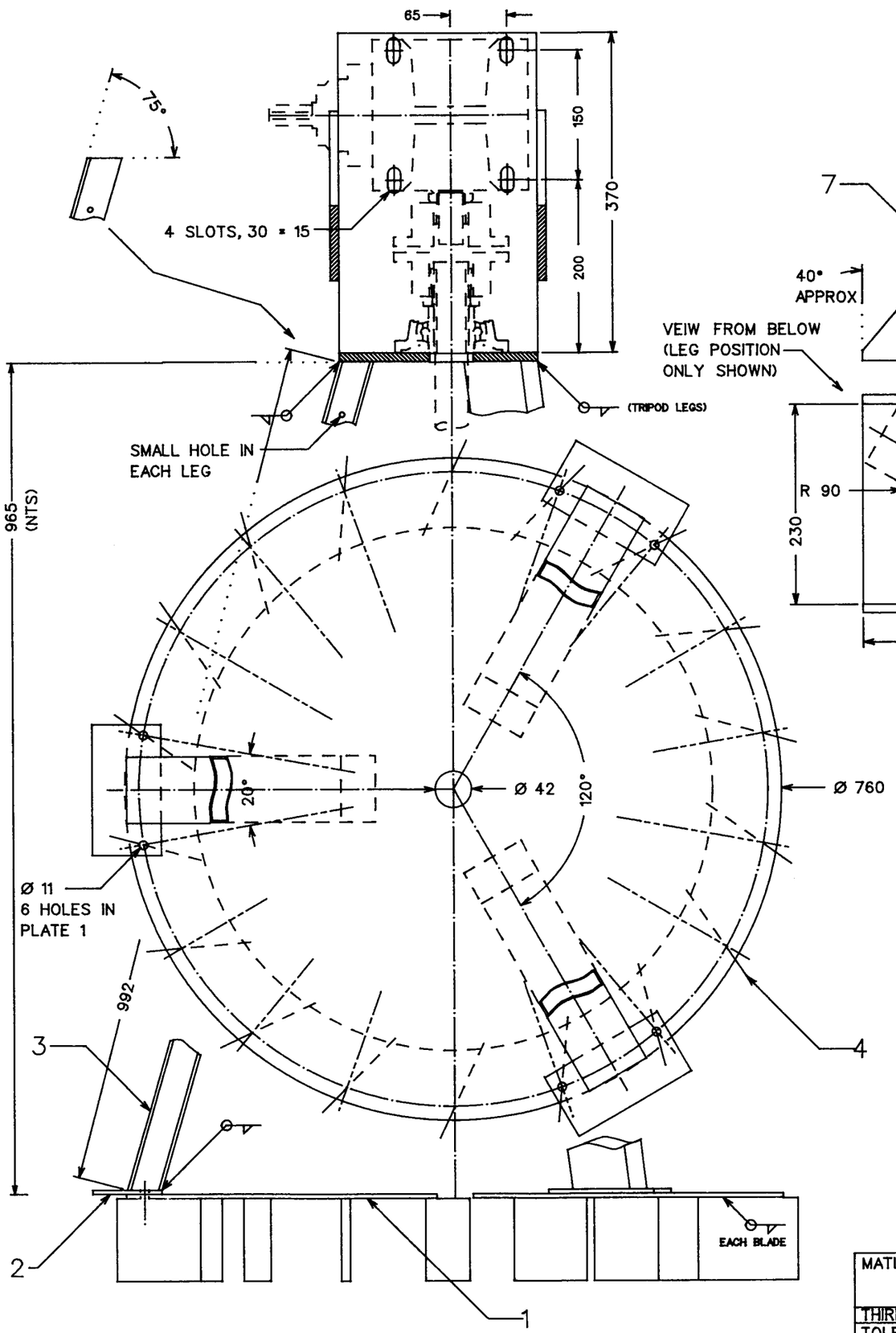

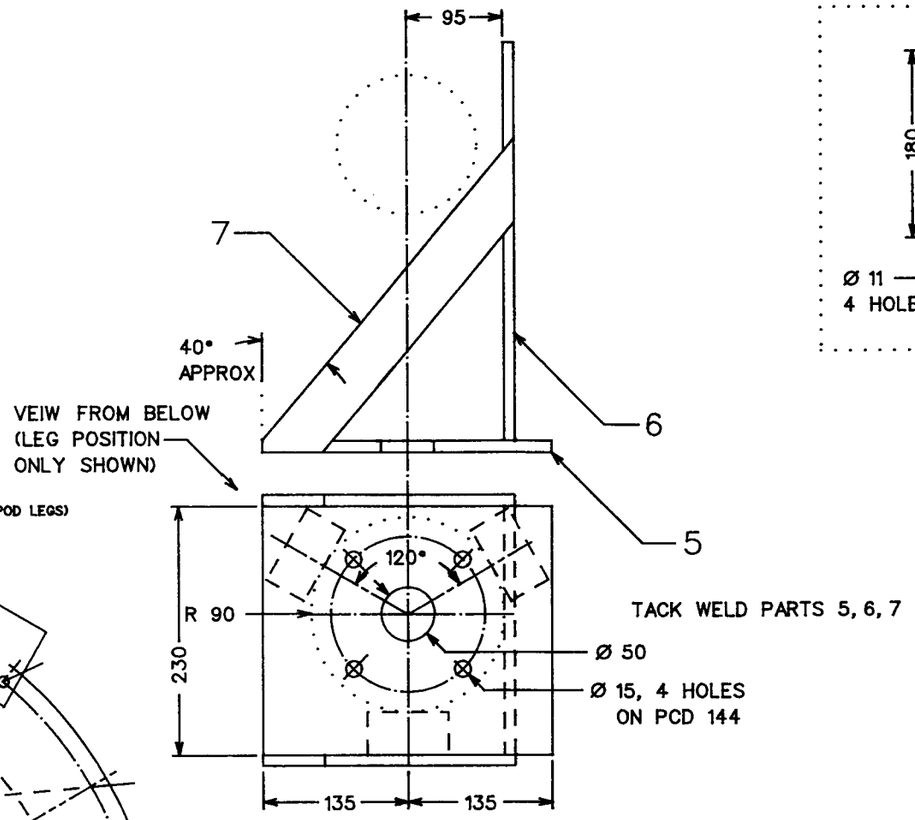

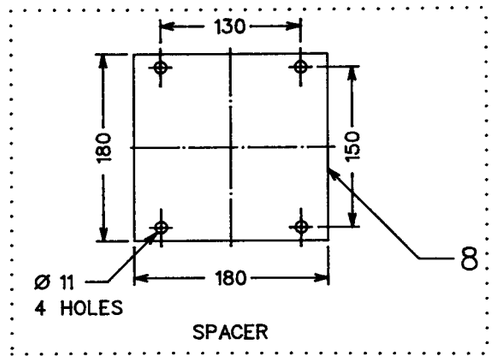

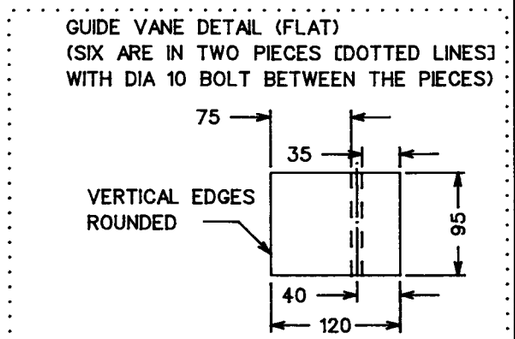

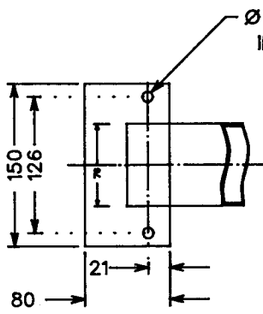

TRIPOD FOOT DETAIL

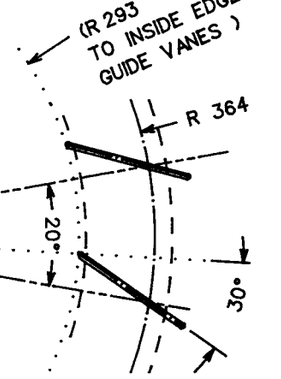

GUIDE VANE LOCATION DETAIL

NOTE:
GUIDE VANE DIRECTION AS SHOWN
ACCURACY IS MORE CRITICAL FOR THE FOLLOWING:
- BOTTOM SURFACE OF GUIDE VANES IN SAME PLANE
- PLATE 6 FLAT, AND PARALLEL TO SHAFT
  (TACK WELD SO THAT SLIGHT ADJUSTMENT CAN
  BE MADE WHEN ASSEMBLING)
- (CONCENTRICITY OF TOP RELATIVE TO BOTTOM)

ITEM	DESCRIPTION	QNTY
8	PLATE, 180 × 180 × 5 THICK	1
7	BAR, 50 × 10 × 375 LONG	2
6	PLATE, 230 × 370 × 10 THICK	1
5	PLATE, 230 × 270 × 10 THICK	1
4	PLATE, 120 × 95 × 5 THICK (SIX ARE IN TWO PIECES)	18
3	RHS 76.2 × 38.1 × 4 TOTAL LENGTH 1002 (EACH)	3
2	PLATE, 150 × 80 × 5 THICK	3
1	PLATE, DIA.760 × 5 THICK	1

MATL: MILD STEEL

THIRD ANGLE PROJECTION

TOLERANCES: +/- 1mm
HOLE LOCATION +/- 0.5mm
unless otherwise stated

MICRO HYDRO PROJECT
PROTOTYPE TURBINE
TRIPOD, TOP PLATE, AND
GEARBOX MOUNT

SCALE: 1:6 A3

SCHOOL OF ENGINEERING
MECHANICAL ENGINEERING DPT.

DRWN: S. FAULKNER
CHKD:
DATE: 20/8/91

DRG No:
TRIPOD

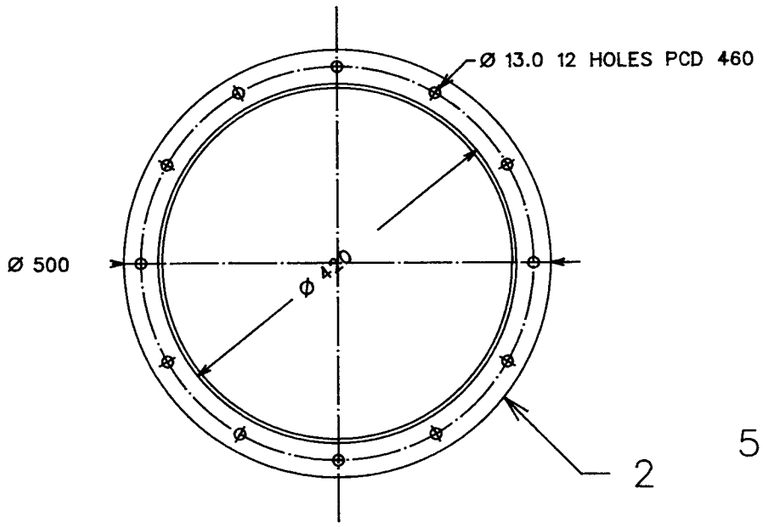

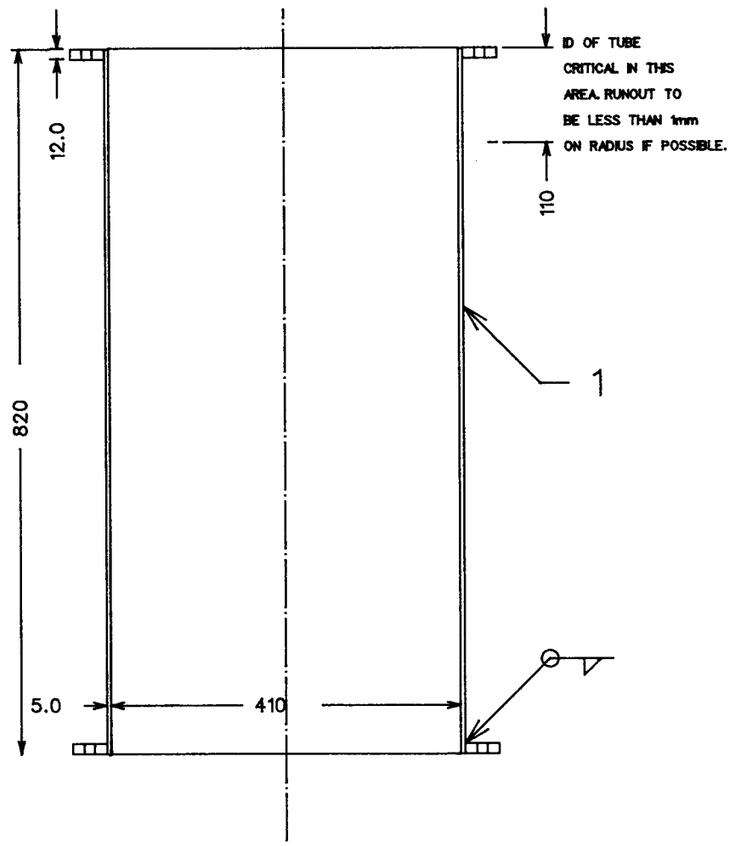

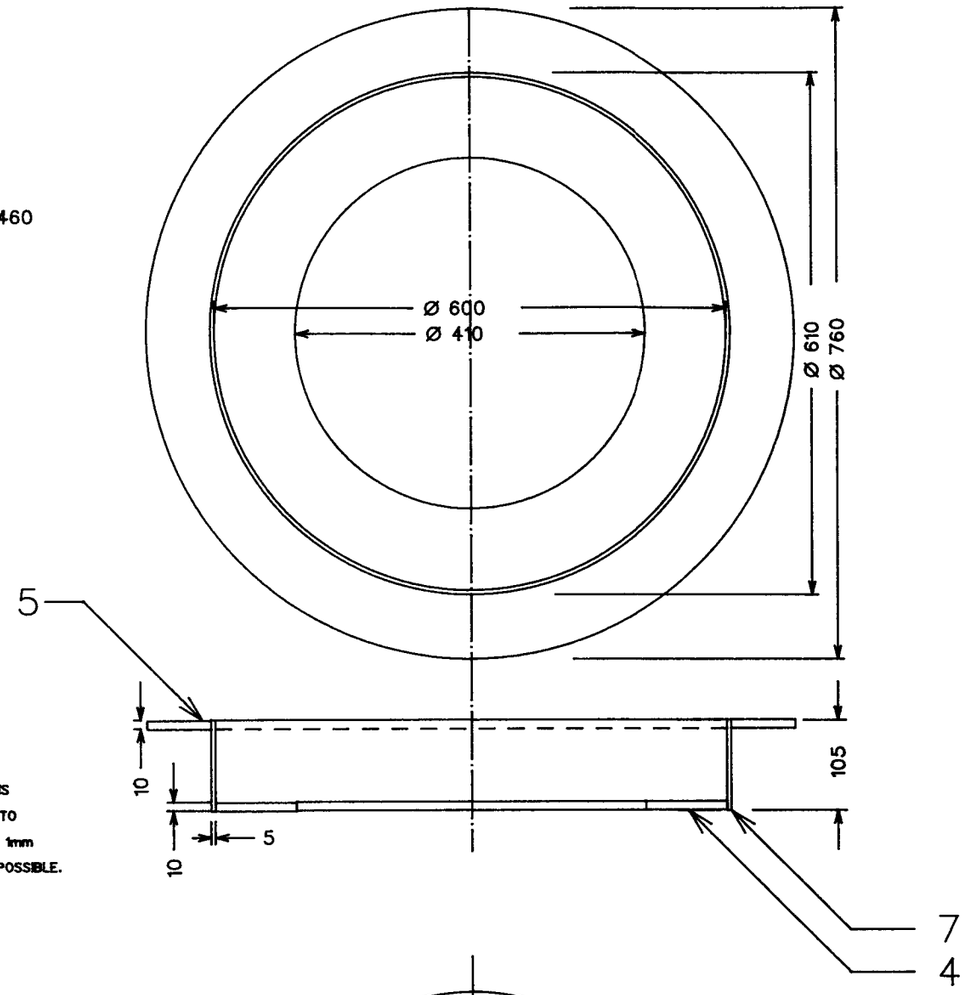

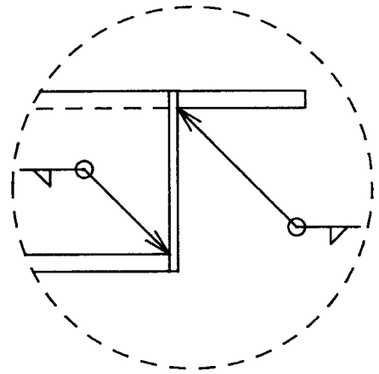

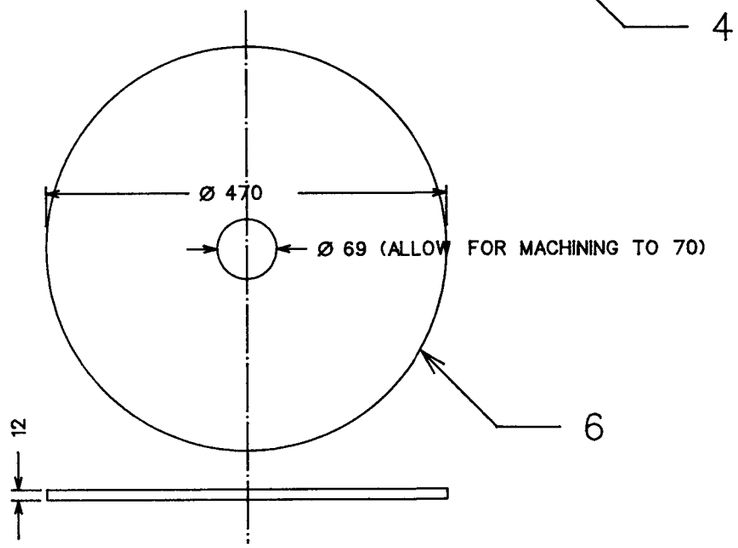

ITEM	DESCRIPTION	QNTY
7	TUBE 600 ID × 110 LENGTH × 5 THICK	1
	ROLLED AND WELDED TO 4 & 5	
6	FLWL DISK 470 OD × 69ID × 12 THICK	1
	PROFILE CUT. (NO MACHINING)	
5	FLANGE 760 OD × 610 ID × 10 THICK	1
	PROFILE CUT AND WELDED.	
4	FLANGE 600 OD × 410 ID × 10 THICK	1
	PROFILE CUT AND WELDED.	
3	FLANGE 500 OD × 430 ID × 12 THICK	1
	PROFILE CUT (NOT SHOWN)	
2	FLANGES 500 OD × 420 ID × 12 THICK	2
	WITH 12 HOLES DIA 13 ON PCD 460	
	PROFILE CUT AND WELDED TO ITEM 1	
1	TUBE 410 ID × 820 LEN × 5 THICK	1
	ROLLED AND WELDED	

MATL: MILD STEEL

THIRD ANGLE PROJECTION | A3

TOLERANCES: +/- 1mm ON FINISHED SIZES

MICRO HYDRO PROJECT
TURBINE TUBE AND FLYWHEEL DISK
TAUNTON ENGINEERING

SCALE: 1:7.5

SCHOOL OF ENGINEERING
MECHANICAL ENGINEERING DPT.

DRWN: S. FAULKNER | DRG No:
CHKD:
DATE: 6/8/91 | TTUBE